NUMERICAL INVESTIGATIONS OF MELTING OF ICE IN A BOX

BY

ABDUL MUTTALEB ALI AL-SALMAN

A Thesis Presented to the

DEANSHIP OF GRADUATE STUDIES

KING FAHD UNIVERSITY OF PETROLEUM & MINERALS

DHAHRAN, SAUDI ARABIA

In Partial Fulfillment of the
Requirements for the Degree of

MASTER OF SCIENCE

In

CHEMICAL ENGINEERING

May 2005

KING FAHD UNIVERSITY OF PETROLEUM & MINERALS
DHAHRAN 31261, SAUDI ARABIA

DEANSHIP OF GRADUATE STUDIES

This thesis, written by **ABDUL MUTTALEB ALI AL-SALMAN** under the direction of his thesis advisor and approved by his thesis committee, has been presented to and accepted by the Dean of Graduate Studies, in partial fulfillment of the requirements for the degree of

MASTER OF SCIENCE IN CHEMICAL ENGINEERING

Thesis Committee

Dr. Habib D. Zughbi
(Thesis Advisor)

Dr. Habib H. Al-Ali
(Member)

Dr. Ramazan Kahraman
(Member)

Prof. Mohamed B. Amin
(Department Chairman)

Prof. Mohammad Al-Ohali
(Dean of Graduate Studies)

١٤٢٥/٤/١٧

Date
25-5-2005

Dedicated

To my parents and to my wife, the closest person to my heart who provided me with unfailing support and encouragement throughout the period of my study.

ACKNOWLEDGEMENTS

In the name of ALLAH, the Most Beneficent, the Most Merciful

The support and the very good opportunity provided by King Fahd University of Petroleum & Minerals to enrich my knowledge are highly appreciated.

With deep sense of gratefulness, I would like to express my heartfelt thanks to my advisor Dr. Habib D. Zughbi for his invaluable guidance, help and unique supervision of the thesis work. Working with him was indeed a wonderful and learning experience, which I thoroughly enjoyed. I owe him more than I can put in black and white.

I am indebted to the thesis committee members, Dr. Habib H. Al-Ali, Dr. Ramazan Kahraman and Dr. Ashraf Hussein Fatehi for their fruitful comments and sincerest help that I derived from their immense research experience. I owe them special thanks for their comments and critical review of the thesis. I am sure without their guidance, this work would not have had taken this final shape.

I am all the more thankful to the chairman of the Chemical Engineering Department, Dr. Mohammed B. Amin for his help and cooperation. I am indebted to all Faculty members who make my stay here fruitful and enriched with all academic experience. All help from Riasat Khan, Department Secretary and office members, Tahir, Abdullah and Jerico, is truly appreciated.

Finally, I offer my sincere thanks to my father, mother, wife, brothers, and sisters for their supports and encouragements during the period of my study.

At last, but not least, I praise ALLAH, The Cherisher and Sustainer of the works, WHO gave me courage and patience to carry out this work. May HE make these efforts beneficial to the writer and all human kind. HE has the power over all thinks an all hopes are towards HIM. May the peace and blessing of ALLAH be upon, master and seal of all prophets, Muhammad and his family, and his all companions and upon whom follow them with *Ehsan* and preach their preaching till the Doomsday.

Abdul Muttaleb

Table of Contents

List of Figures

List of Tables

THESIS ABSTRACT

NAME: ABDUL MUTTALEB ALI AL-SALMAN

TITLE: SIMULATION OF ICE MELTING IN A BOX

MAJOR FILED: CHEMCIAL ENGINEERING

DATE: MAY 2005

Melting of ice in a box is numerically investigated in this study. An enthalpy based fixed grid methodology is used for the numerical solution of this natural convection-conduction controlled phase-change problem. In this approach the effects of the phase change (the latent heat evolution) are accounted for by the definition of suitable source terms in the governing equations. This makes the tracking of the moving interface not necessary. The freedom of defining these source terms allows the modeling of a variety of phase-change problems.

Melting in a small two-dimensional block was simulated using a commercial computational fluid dynamics package. The results were found to be dependent on the grid size, time step size and the difference between liquidus and solidus temperatures. For melting in a 2×2 cm block, mesh sizes varying between 40×40 and 120×120 were tested and a mesh size of 110×110 was chosen. Time step sizes varying between 30 to 1 s were tested and a time step size of 1 s was chosen. Differences between liquidus and solidus temperatures varying between 1 and 0.05 K were tested and a difference of 0.05 K was chosen. The simulation results were validated against published correlations and a good

agreement was observed. Results showed that the contribution of natural convection to melting in a block of ice heated from the top is substantially more (about eight times) than that of conduction. Results also showed that the melting rate is a function of the size and location of the heated area. The melting rate is found to be directly proportional to the size of the heating area but not in a one to one correspondence. As the size is halved, a 25% decrease in the melting rate is observed. The boundary conditions dictate the shape of the melted area. Results showed clearly that melting tends to occur away from a sub-zero wall.

Simulation of melting in a 20×20 cm was also investigated. Limited results were obtained. These results showed a reasonable qualitative agreement with experimental results. Simulation of melting in a small three dimensional model was also carried out. Due to the fine grid and the small time step needed, the computational cost of solving melting using the current method proved to be not very practical.

THESIS ABSTRACT IN ARABIC

ملخص الرسالة

الإســـــم: عبدالمطلب علي ناصر السلمان

عنوان الرسالة: بحوث رياضية لـذوبان الثلج في صندوق

الدرجـــــة: الماجستير

التخصـــص: هندسة كيميائية

التاريـــخ: مايو 2005 م

في هذه الدراسة تم بحث ذوبان الثلج في صندوق رياضياً. استخدمت طريقة بحث حرارية تعتمد على الشبكة الثابتة في الحل الرياضي لمسائل تغير حالة المادة التي يتحكم فيها الحمل و الاتصال الحراري الطبيعي. في هذا النوع من المسائل، تحسب تأثيرات تغير الحالة (تطور الحرارة الكامنة) بواسطة تعريف مصدر وحدات مناسبة في المعادلات المتحكمة. هذا يجعل تتبع السطح البيني المتحرك غير ضروري. سمحت حرية تعريف مصدر الوحدات بتشكيل مسائل مختلفة لمسائل تغير الحالة.

تم بحث الذوبان في كتلة صغيرة ثنائية الأبعاد باستخدام برنامج ديناميكي تجاري عددي للسوائل. تم انجاز اختبار شامل لتأسيس حل لا يعتمد على حجم ونوع الشبكة و لا يعتمد على سعة خطوة الوقت و لا يعتمد على الفرق بين درجات حرارة التجمد والذوبان. لقد دلت النتائج على أن مساهمة الحمل الحراري الطبيعي للذوبان في مجسم ثلج تم تسخينه من فوق هي أكثر من الاتصال الحراري. تجارب أخرى تم تنفيذها لبحث تأثيرات حجم ومكان مساحة المنطقة التي تم تسخينها والحرارة المبدأية وحرارة السطح االمسخن على سرعة الذوبان. دلت النتائج على أن درجة الذوبان

تتناسب تناسبا طرديا مع حجم السطح الساخن. علاوة على ذلك دلت النتائج على أن تغيير بسيط في حرارة الحدود قد يؤثر في عدم تماثل عملية الذوبان.

Chapter One

INTRODUCTION

1.1 Introduction:

Phase-change problems play important roles in many industrial and natural processes. Heat transfer with phase-change and more specifically melting and solidification have been the subject of intensive research in the past three decades mainly due to the significance of phase-change problems in natural and industrial processes. Examples of melting/solidification in industrial field include plastics manufacturing, purification of metals, casting of metals, latent heat of fusion in thermal energy storage, crystal growth and many other chemical processes. This study aims to investigate numerically phase change problems in bounded objects.

When a solid object is heated or a liquid is cooled at a certain boundary, if this boundary has a temperature higher than the melting point or lower than the freezing point, heat transfer will take place and result in a phase-change. A front will form between the old and the newly forming phases. The location of the front cannot be predetermined. The movement and consequently the location of the phase front are determined by the driving forces on both sides of the front.

Melting has been investigated experimentally by many researchers. Rectangular, cylindrical (in or around) and spherical enclosures have been the main geometries for

studying melting with more work done with the cylindrical and the rectangular geometries.

The majority of researchers have used a phase-change material (PCM) as a medium of their study while a few have used an ice-water system. The ice-water system is offering a bigger challenge because of the density inversion at 4 °C.

The phase-change problem of melting from a vertical wall in a rectangular enclosure has been the subject of considerable research in recent years due to its importance in current technological applications. Melting from above or below a horizontal wall was also considered by many workers. Some additional aspects such as inclination, fins and sub-cooling were also investigated. These aspects are reviewed in the next subsections.

In chapter two, the following will be reviewed:

1) Melting along a vertical wall in a rectangular enclosure
2) Melting in an inclined rectangular enclosure
3) Melting along a horizontal wall in a rectangular enclosure
4) Melting in geometries other than a rectangular enclosure
5) Experimental determination of the location of the melt-front.

1.2 Objectives:

The main objectives of this study are to:

1) Develop a 2-D model for ice melting using a CFD (FLUENT) package.

2) Study the effects of grid size, grid type, time step and turbulence model of the 2-D model if needed (depends on Rayleigh number).
3) Validate the 2-D results against some results in literature. There are plenty of experiment results available for melting/freezing along a vertical wall.
4) Develop a 3-D model for ice melting.
5) Validate the 3-D model against published results and/or experiment results obtained in the Chemical Engineering Department of KFUPM.
6) Perform parametric runs by varying the geometry.
7) Perform parametric runs by varying the heating area.
8) Perform parametric runs by varying the initial temperature of ice and heating surface.

Chapter Two

LITERATURE REVIEW

2.1 Experimental Work

2.1.1 Phase Change along a Vertical Wall in a Rectangular Enclosure

The significant influence of free convection in the melting process in rectangular cavities was clearly demonstrated by Marshall (1978); Van Buren and Viskanta (1980); Bareiss and Beer (1984); Ho and Viskanta (1984); Gau and Viskanta (1986) and Wolff and Viskanta (1987). This was also shown analytically by Gadgil & Gobin (1984); Liu *et al*. (1993) and Ho and Chu (1993).

The melting is initially controlled by conduction, but as the melt layer widens, Rayleigh number increases and a significant heat transfer occurs through convection. These experiments have shown that for the case of heating from a vertical wall, more melting took place at the top than near the bottom of the heated vertical surfaces. This change of melt shape with time provided conclusive evidence of the importance of natural convection in the melted region.

2.1.2 Melting in an Inclined Rectangular Enclosure

Melting in an inclined rectangular enclosure was investigated by Webb and Viskanta (1986) using n-octadecane. Similar to the work of Hale and Viskanta (1978), the solid-liquid interface position was recorded at pre-selected time intervals with a still

camera and the contours of the solid-liquid interface were reconstructed from the photographs. Results showed that inclination produced a strong three-dimensional vortex motion that tends to Benard convection patterns as the angle of inclination from the vertical is increased. This yielded significantly higher melting rates compared to a vertical melting case.

Inaba *et al*. (1989) found that melting front morphology closely depends on both angle of inclination and heated-wall temperature.

2.1.3 Phase Change along a Horizontal Wall in a Rectangular Enclosure

Hale and Viskanta (1980) investigated the solid-liquid interface motion during freezing and melting from above as well as below in a cell 8.9 cm high, 14.6 cm wide and 2.2 cm deep. They used a few PCM such as stearic acid, sodium phosphate and sodium sulfate. They demonstrated the significance of free convection in solid-liquid phase change heat transfer.

Brewster and Gebhart (1988) studied the effects of natural convection on freezing downward into a large scale quiescent deep layer of pure water. The coupled mechanisms of convection and freezing were shown to be very complicated due to both buoyancy force reversals and liquid super-cooling. Super-cooling is summarized by the fact that water cools down to between -5 °C to -7 °C before it freezes.

2.1.4 Melting in Geometries Other than a Rectangular Enclosure

Many experimental studies of melting and solidification in geometries other than rectangular enclosures, especially cylindrical geometries, were carried out. Webb *et al*.

(1987) investigated melting of unrestrained ice in a horizontal cylindrical capsule. Three distinct flow regimes depending on wall temperatures were identified. These temperatures were below the density inversion temperature, around the density inversion temperature and one far above it.

In addition to investigations of melting/solidification in rectangular and cylindrical geometries there have also been studies in a spherical enclosure. Experimental results were reported by Moor and Bayazitoglu (1984) and Saitoh and Moon (1993a, 1993b) (all using n-octadecane).

The effects of natural convection on solid/liquid phase change in porous media have been investigated experimentally by Weaver and Viskanta (1986) (cylindrical capsule); Beckermann and Viskanta (1988) (vertical square enclosure); Sugawara *et al.* (1988) (cooling from above in a rectangular enclosure) and Chellaiah and Viskanta (1989).

2.1.5 Experimental Determination of the Location of the Melt-Front

A major task in experimental melting research is the exact determination of the melt front. Researchers have used different techniques ranging from photographic techniques to 2-D and 3-D flow field acquisition methods.

Hale and Viskanta (1978) used photography to observe the solid-liquid interface motion during melting of a solid heated from an isothermal vertical wall. They used n-octadecane in a rectangular enclosure. The solid-liquid interface position at different times was determined directly from photographs.

Yeoh (1992), Kowalewski and Rebow (1997) and Kowalewski (1997) used a flow visualization technique for measuring temperature and velocity fields. This is primarily done using a computational analysis of the color and displacement of liquid crystal tracers and it is used to determine both the temperature and velocity fields of the flow. It combines Digital Particle Image Thermometry (DPIT) and Digital Particle Image Velocimetry (DPIV).

Diaz and Viskanta (1984) used a flow visualization technique to obtain the position of the melt front and information about flow during melting a horizontal wall in a rectangular enclosure. They used aluminum powder as a flow tracer.

Van Buren and Viskanta (1980) used interferometric measurements to obtain detailed temperature distribution and local heat transfer coefficients during melting from a vertical surface. Interferometric measurements were not possible at early times when the melt layer is not sufficiently thick to permit the passage of enough light to produce sharp interference fringes.

2.2 Numerical Work

The mathematics of freezing is complicated due to a number of factors. The problem, in general, is three-dimensional and transient in nature. There is a phase change interface which moves either into the liquid body (freezing) or into the solid body (melting) depending on the net direction of heat transfer. Heat is absorbed or liberated at the interface, the thermal properties of the two phases are different, and the position of the interface is not known *a priori.*

One boundary condition that is obtained from the energy balance at the liquid-solid interface is inherently nonlinear, Ozisik (1980), Carslaw and Jaeger (1959) and Crank (1984). The rate of travel of the interface also changes in time. Finally, the various kinds of practical boundary and initial conditions are additional factors that further complicate the mathematics. For a variety of these problems there are solutions available in the literature. The solutions in general differ according to the boundary conditions, simplifying assumptions, coordinate dimensions and solution techniques.

Numerical heat transfer is a broad and highly active research area. A recent literature survey in a series by Shih and Ohadi (1993), lists 16 subject areas with nearly 700 publications that appeared in just seven journals in the 1990-1991 period. In a similar survey, Shih *et al*. (1996) listed the same number of subject areas with over 700 publications appearing in the 1992-1993 period. Problems involving phase change and moving boundaries are dealt with in a sub-set of the literature. The first analysis of freezing-melting interfaces is widely credited to an (1891) publication by Stefan and tracking the interface is frequently referred to as the "Stefan problem".

2.2.1 Numerical Techniques for Phase Change Problems

A large amount of work dealing with numerical treatment of heat transfer associated with phase change problems has been published. The methods and techniques used are varied and numerous. Grid type and formulation of the problem will be discussed in this section.

In the finite difference literature, two alternative and popular approaches are the fixed grid and the transformed grid. In the first approach, a fixed grid is applied directly

in real space and the interface conditions are accounted for by the definition of suitable source terms in the governing equations (Voller and co-workers, 1987). In the second approach, governing equations and their boundary are cast into a generalized curvilinear coordinate system.

Fixed grids have been used to solve many problems such as convective transport solved by Salcudean and Abdullah (1988); melting of pure metal solved by Brent *et al*. (1988) and solute transport solved by Beckermann and Viskanta (1988). A comprehensive review of fixed grid methods can be found in Voller *et al*. (1990).

There are two alternative versions of the governing equations. The first is based on primitive variable with the energy expressed in terms of enthalpy. The second is a stream function-vorticity formulation with a temperature energy equation.

In this proposal and for the numerical work which will follow, fixed grids technique and primitive variables will be used as this will make it feasible to go to full three-dimensional model and it is expected that this approach will be adequate to solve the phase change problem of concern.

In summary, phase change problems have been widely investigated experimentally and to a lesser extent numerically. However, there is still a need to investigate the effects of natural convection on the melting in a box when heated from above.

2.3 Numerical Techniques

2.3.1 Fixed Grid Technique

In the fixed grid phase-change approach, the heat and mass conditions on the moving interface are incorporated into the governing equations via the definition of suitable volume source terms.

In this approach a fixed grid is applied directly in real space and the interface conditions are accounted for by the definition of suitable source terms in the governing equations. The freedom of defining the source terms allows the modeling of a variety of phase-change problems.

Fixed-grid techniques have also been developed for dealing with conduction and convection-controlled phase-change problems. When accounting for heat flow in the phase-change region, the fixed-grid method employed is the so-called enthalpy method.

In the enthalpy approach, the heat flow at the interface is accounted for by specifying a volume source term to track the latent heat content of a computational cell or on the introduction of an enhanced heat

The essential feature of the resulting numerical implementation is the “smear” out the interface phenomena over an element of the numerical discretization and thereby remove the need to know the exact location of the liquid-solid interface.

In summary, in a fixed grid technique (i) the enthalpy of each grid cell is calculated, (ii) the enthalpies of liquid phase and solid phase are know, and (iii) the amounts of liquid and solid in each cell can be found.

Chapter Three

MATHEMATICAL FORMULATION

3.1 Primitive Variables Formulation

In this formulation the dependent variables are the velocities and the pressure, which require a system of three partial differential equations which are the continuity and motion in two dimensions. The solution of these equations leads to considerable difficulty owing to the non-linearity, especially when coupled equations for energy and possibly turbulence have to be solved simultaneously. One method of tracking the solid liquid interface is to use a method called the marker and cell (MAC) method and was developed at Los Alamos Laboratories by Harlow and Welch (1965) and Hirt *el al.* (1975 and 1981). As the name implies, this method involves placing marker particles on the interface and then moving these markers by using interpolations of the local fluid velocities.

The Navier-Stokes equations cannot be solved in the primitive variable form by using the "control volume method". The technique TEACH (Teaching Elliptic Axi-symmetric Characteristics Heuristically) and follow up codes have been developed at the Imperial College of Science and Technology in the UK, Gosman and Ideriah, (1976) and Patankar (1980).

These days, most solutions use the Semi Implicit Pressure Linked Equations (SIMPLE) algorithm that developed by Patankar (1980) or a version of it such as SIMPLER or SIMPLEST.

3.2 Solution Using a CFD Package (FLUENT)

In the case of using a computational fluid dynamics package, the full set of mass, momentum and energy equations are solved for the liquid phase in two- or three-dimensions. The change of phase is determined by a heat balance and the interface is tracked by determining the volume fraction of each of the two phases (solid and liquid) in each cell of the computational domain. The accuracy of the interface tracking is expected to be enhanced by the proper choice of the size of the grid cells and the size of the time steps.

3.3 Mathematical Formulation

The governing equations for a phase change problem are the mass, momentum and energy equations. The model is made complete with an equation resulting from an energy balance at the interface and an equation showing density variations with temperature.

3.4 General Formulation For a Two-Dimensional Example

Consider a Newtonian incompressible fluid in the laminar flow regime. Heat and momentum transfer phenomena are described as follows:

(a) Conservation of mass (equation of continuity) can be represented as follows:

$$\frac{\partial \rho}{\partial t} + \rho \frac{\partial}{\partial x}(\upsilon_x) + \rho \frac{\partial}{\partial y}(\upsilon_y) = 0 \qquad (3.1)$$

where υ_x and υ_y are velocities in x- and y-directions respectively.

(b) The conservation of momentum (equations of motion) becomes:

X-direction

$$\rho\left(\frac{\partial \upsilon_x}{\partial t} + \upsilon_x \frac{\partial \upsilon_x}{\partial x} + \upsilon_y \frac{\partial \upsilon_x}{\partial y}\right) = \mu\left[\left(\frac{\partial^2 \upsilon_x}{\partial x^2} + \frac{\partial^2 \upsilon_x}{\partial y^2}\right) + \frac{1}{3}\frac{\partial}{\partial x}\left(\frac{\partial \upsilon_x}{\partial x} + \frac{\partial \upsilon_y}{\partial y}\right)\right]$$

$$- \frac{\partial p}{\partial x} + S_x \qquad (3.2)$$

Y-direction

$$\rho\left(\frac{\partial \upsilon_y}{\partial t} + \upsilon_x \frac{\partial \upsilon_y}{\partial x} + \upsilon_y \frac{\partial \upsilon_y}{\partial y}\right) = \mu\left[\left(\frac{\partial^2 \upsilon_y}{\partial x^2} + \frac{\partial^2 \upsilon_y}{\partial y^2}\right) + \frac{1}{3}\frac{\partial}{\partial y}\left(\frac{\partial \upsilon_x}{\partial x} + \frac{\partial \upsilon_y}{\partial y}\right)\right]$$

$$+ \rho g - \frac{\partial p}{\partial y} + S_y + S_b \qquad (3.3)$$

where P is pressure, ρ is density, μ is viscosity, S_x, S_y and S_b are source terms which need to be defined.

(c) Conservation of Heat:

A suitable conservation of heat equation can be written in terms of enthalpy $h = CpT$ (i.e. the product of specific heat and temperature) as in Patankar (1980):

$$\rho\frac{\partial h}{\partial t} + div(\rho \mathbf{u} h) - div(\alpha\ grad\ h) + S_h = 0 \tag{3.4}$$

where α is the thermal diffusivity and S_h is a source term. In a phase change problem the source term S_h will depend on the nature of the latent heat evolution and will require careful definition.

3.5 A Three-Dimensional General Formulation in Primitive Variables

The governing equations can be represented as follows:

Conservation of mass (equation of continuity)

$$\frac{\partial \rho}{\partial t} + \rho \left(\frac{\partial \upsilon_x}{\partial x} + \frac{\partial \upsilon_y}{\partial y} + \frac{\partial \upsilon_z}{\partial z} \right) = 0 \tag{3.5}$$

where υ_x, υ_y, and υ_z are velocities in x-,y- and z-directions respectively

Conservation of momentum (equation of motion) - X

$$\rho\left(\frac{\partial \upsilon_x}{\partial t} + \upsilon_x \frac{\partial \upsilon_x}{\partial x} + \upsilon_y \frac{\partial \upsilon_x}{\partial y} + \upsilon_z \frac{\partial \upsilon_x}{\partial z} \right) = \mu\left[\left(\frac{\partial^2 \upsilon_x}{\partial x^2} + \frac{\partial^2 \upsilon_x}{\partial y^2} + \frac{\partial^2 \upsilon_x}{\partial z^2} \right) \right.$$

$$\left. + \frac{1}{3}\frac{\partial}{\partial x}\left(\frac{\partial \upsilon_x}{\partial x} + \frac{\partial \upsilon_y}{\partial y} + \frac{\partial \upsilon_z}{\partial z} \right) \right] - \frac{\partial p}{\partial x} + S_x \tag{3.6}$$

where P is pressure, ρ is density, μ is viscosity and S_x is the source term.

Conservation of momentum (equation of motion) - Y

$$\rho\left(\frac{\partial \upsilon_y}{\partial t} + \upsilon_x \frac{\partial \upsilon_y}{\partial x} + \upsilon_y \frac{\partial \upsilon_y}{\partial y} + \upsilon_z \frac{\partial \upsilon_y}{\partial z} \right) = \mu\left[\left(\frac{\partial^2 \upsilon_y}{\partial x^2} + \frac{\partial^2 \upsilon_y}{\partial y^2} + \frac{\partial^2 \upsilon_y}{\partial z^2} \right) \right.$$

$$\left. + \frac{1}{3}\frac{\partial}{\partial y}\left(\frac{\partial \upsilon_x}{\partial x} + \frac{\partial \upsilon_y}{\partial y} + \frac{\partial \upsilon_z}{\partial z} \right) \right] - \frac{\partial p}{\partial y} + S_y \tag{3.7}$$

where S_y is the source term.

Conservation of momentum (equation of motion) - Z

$$\rho\left(\frac{\partial \upsilon_z}{\partial t}+\upsilon_x\frac{\partial \upsilon_z}{\partial x}+\upsilon_y\frac{\partial \upsilon_z}{\partial y}+\upsilon_z\frac{\partial \upsilon_z}{\partial z}\right)=\mu\left[\left(\frac{\partial^2 \upsilon_z}{\partial x^2}+\frac{\partial^2 \upsilon_z}{\partial y^2}+\frac{\partial^2 \upsilon_z}{\partial z^2}\right)\right.$$

$$\left.+\frac{1}{3}\frac{\partial}{\partial z}\left(\frac{\partial \upsilon_x}{\partial x}+\frac{\partial \upsilon_y}{\partial y}+\frac{\partial \upsilon_z}{\partial z}\right)\right]+\rho g-\frac{\partial P}{\partial z}+S_z+S_b \qquad (3.8)$$

where g is the acceleration due to gravity and S_z and S_b are the source terms.

Conservation of energy

$$\rho C_p\left(\frac{\partial T}{\partial t}+\upsilon_x\frac{\partial T}{\partial x}+\upsilon_y\frac{\partial T}{\partial y}+\upsilon_z\frac{\partial T}{\partial z}\right)=$$

$$k\left(\frac{\partial^2 T}{\partial x^2}+\frac{\partial^2 T}{\partial y^2}+\frac{\partial^2 T}{\partial z^2}\right)+2\mu\left[\left(\frac{\partial \upsilon_x}{\partial x}\right)^2+\left(\frac{\partial \upsilon_y}{\partial y}\right)^2+\left(\frac{\partial \upsilon_z}{\partial z}\right)^2\right]$$

$$+\mu\left[\left(\frac{\partial \upsilon_x}{\partial y}+\frac{\partial \upsilon_y}{\partial x}\right)^2+\left(\frac{\partial \upsilon_x}{\partial z}+\frac{\partial \upsilon_z}{\partial x}\right)^2+\left(\frac{\partial \upsilon_y}{\partial z}+\frac{\partial \upsilon_z}{\partial y}\right)^2\right]+S_h \qquad (3.9)$$

where T is the temperature, Cp is the heat capacity and S_h is the source term.

Energy balance at the interface for multidimensional cartesian coordinate system:

$$\rho_S L\frac{\partial s}{\partial t}=\left[1+\left(\frac{\partial s}{\partial x}\right)^2+\left(\frac{\partial s}{\partial y}\right)^2\right]\left[k_S\left(\frac{\partial T_S}{\partial z}\right)_S-k_l\left(\frac{\partial T_l}{\partial z}\right)_l\right] \qquad (3.10)$$

Where S is the thickness of the melt layer, ρ_S is the solid density, T_S is the solidus temperature, T_l is the liquidus temperature.

Density variation with temperature is governed by the following equation:

$$\rho = \rho_{T_{ref}} - \rho_{T_{ref}} \beta_{T_{ref}} \left(T - T_{ref} \right) \tag{3.11}$$

3.6 Tracking the Interface

Tracking the moving interface is a major task of the numerical method. In 2-D and 3-D, it involves a great deal of bookkeeping, i.e. if temperature based governing heat transfer equations are used, difficulties may arise. The main reason for this is that in the vicinity of the phase change, conditions on temperature, velocity and heat removal have to be accounted for.

There are methods that make the tracking of the interface not necessary. These methods use fixed grids and enthalpy formulation. Their main feature is to account for the latent heat evolution by defining suitable source terms in the governing equations. Here, the melting is assumed to occur over a narrow temperature range. This is more true for alloy compared to a pure component. The temperature range could be made very small i.e. 0.01 ^{o}C or even less. Material in this temperature range is assumed to behave like a mushy (porous medium or solid/liquid) material.

At the solid-liquid interface, or in the case of a non-isothermal phase change in the mushy region, the velocities in the x and y directions (for a 2-D case) go to zero. Therefore, to apply the momentum equations in a solid/liquid phase change, this behavior must be taken into account.

There are a number of alternative methods by which the behavior of the velocities in the vicinity of the phase change can be modeled, these methods are:

(a) Switch-off techniques

(b) Darcy source

(c) Variable viscosity

These ways of handling the source terms in the governing equations will be discussed in more details in the next section.

3.7 Source Terms

3.7.1 Momentum Source Terms - Switch-off Techniques

A straight forward approach of modeling the velocity change is to overwrite the velocity solution in the solid to be zero (Voller *et al.* 1987). The problem is in identifying the solid and liquid regions. Predicted values of the latent heat contribution can be used. Let ΔH_r be the representative latent heat of an element of the numerical discretization. The velocity components associated with the element can be set to zero if $\Delta H_r \leq A$, where $0<A<L$. If A=L, the velocity is switched off in an element just as the phase change commences in that element. If A = 0, the velocity is not switched off until the element has completed the phase change.

3.7.2 Momentum Source Terms - Darcy Source

S_x and S_y source terms are used to modify the momentum equations in the mushy region (Voller and Prakash 1987 and Voller et al. 1987):

$$S_x = -A\upsilon_x$$
$$S_y = -A\upsilon_y \tag{3.12}$$

A increases from zero to a large value as the local solid fraction F_s increases from its liquid value of zero to its solid value of 1. If the solid fraction, F_s, is equal to 0 then $S_x = S_y = 0$ and the momentum equations are in terms of actual liquid velocities.

In the mushy region, the value of A increases such that the values of the sources begin to dominate the transient, convective and diffusive terms. The momentum equations approximate the Darcy law where

$$\mathbf{u} = -(K/\mu)grad\ P \tag{3.13}$$

where the permeability, K, is a function of the porosity λ (=1-solid fraction).

When an element of the numerical discretization is changing phase its latent heat will be $0<\Delta H_r<L$. The value of ΔH_r indicates the amount of solid in the element. A possible model would be that of a porous medium with the liquid fraction flowing through a solid matrix. This is physically significant in a mushy phase change. For isothermal change A is selected by experience. For mushy problems a Carman-Koseny equation can be used as basis:

$$A = -C(1-\lambda^2)/(\lambda^3 + q) \tag{3.14}$$

C depends on morphology of system (e.g. 1600), q is a small number to avoid division by 0 (e.g. 0.001).

3.7.3 Momentum Source Terms -Variable Viscosity

Another technique is to have a variable viscosity (Voller *et al.* 1987). The viscosity is taken to be a function of enthalpy (more convenient than temperature) such that in the mushy region it rises to a large value. This has the effect of inhibiting the velocity so that any predicted velocities in the solid region are negligible. If viscosity is a function of enthalpy, isothermal and mushy problems can be handled (if a function of temperature then mushy problems only can be handled). A suitable function is :

$$\mu = \mu_l + B[L-\Delta H_r] \tag{3.15}$$

where μ_l is the liquid viscosity, B is a large value and L is the latent heat of fusion.

When a numerical element is all liquid $\Delta H_r = L$ and $\mu=\mu_l$. When a part of the element changes phase ΔH_r becomes less than L and μ will increase. For a solid, $\Delta H_r = 0$ and $\mu = \mu_l + BL$

3.7.4 The Buoyancy Source Term

S_b is a buoyancy term used to induce natural convection (Voller and Prakash, 1987). ***Boussinesq*** approximation is assumed, i.e. density is constant in all terms except a gravity source term:

$$S_b = \rho g \beta (h - h_{ref}) / c \tag{3.16}$$

where β is a thermal expansion coefficient and h_{ref} is a reference value of sensible heat.

3.7.5 The Latent Heat Source Term

The essential feature of the current enthalpy method for convection/diffusion phase change problems is the latent heat source term in the above equation. In a system which is undergoing a change of phase under heat transfer the total enthalpy is often expressed as:

$$H = h + \Delta H \tag{3.17}$$

The sum of sensible enthalpy h and latent heat ΔH.

The latent heat contribution is some function of temperature:

$$\Delta H = F(T) \tag{3.18}$$

The form of this function, F, will depend on the problem. Examples include:

(i) Binary alloy solidification/melting:

$$F(T) = \begin{cases} L, & T > T_L \\ L(1 - F_s), & T_L > T > T_S \\ 0, & T < T_S \end{cases} \tag{3.19}$$

where F_s is the solid fraction, which may be a non-linear function of temperature, L is the latent heat of fusion and T_L and T_S are the liquidus and solidus temperatures, respectively.

(ii) Isothermal solidification/melting:

$$F(T) = \begin{cases} L, & T > 0 \\ 0, & T < 0 \end{cases} \tag{3.20}$$

In this case the latent heat of evolution is released at a single temperature T_m, which has the value 0 in the previous equation for convenience. Using the definition of enthalpy provided earlier, the heat transfer equation for a region undergoing a phase change is developed. The form of S_h derived by this equation is cast into the form of the conservation of heat equation.

$$S_h = \rho \frac{\partial \Delta H}{\partial t} \tag{3.21}$$

that is the rate of change of volumetric latent heat.

3.8 Implementation

The previous discussion is general in nature. It can be implemented using any reasonable numerical technique such as control volume (CV). The latent heat content of each CV needs to be updated after each iteration. Voller *et al.* (1983) have developed a reliable method to update the latent heat content.

A CFD package such as FLUENT can be used to implement the conservation equations. Here, the CFD package utilizes a finite domain method which is fully implicit in time and uses upwind differencing in space. The finite domain discretization follows the same notations given by Patankar (1980), uses the energy equation as an example and refers to the grid arrangement shown in Figure 1 below. This can be written as:

$$a_P h_P = a_H h_H + a_L h_L + a_N h_N + a_S h_S + a_P^{\circ} h_P^{\circ} + b \tag{3.22}$$

where the subscripts indicate the appropriate nodal values, the *a's* are coefficients which depend on the diffusion and convective fluxes in to p^{th} control volume, $a_P{}^{\circ} = \rho\delta z\delta y/\delta t$ and $(\,)^{\circ}$ represents evaluation at previous time step. The parameter *b* incorporates a discretized form of the source term S_h.

The discretized form of the momentum equations is similar to the above equation, but the grid is staggered (see the dashed control volumes in Figure 1). A staggered grid makes the accounting for the pressure more accurate, Patankar (1980).

The Fluent code uses an algorithm similar to the SIMPLE algorithm presented by Patankar (1980).

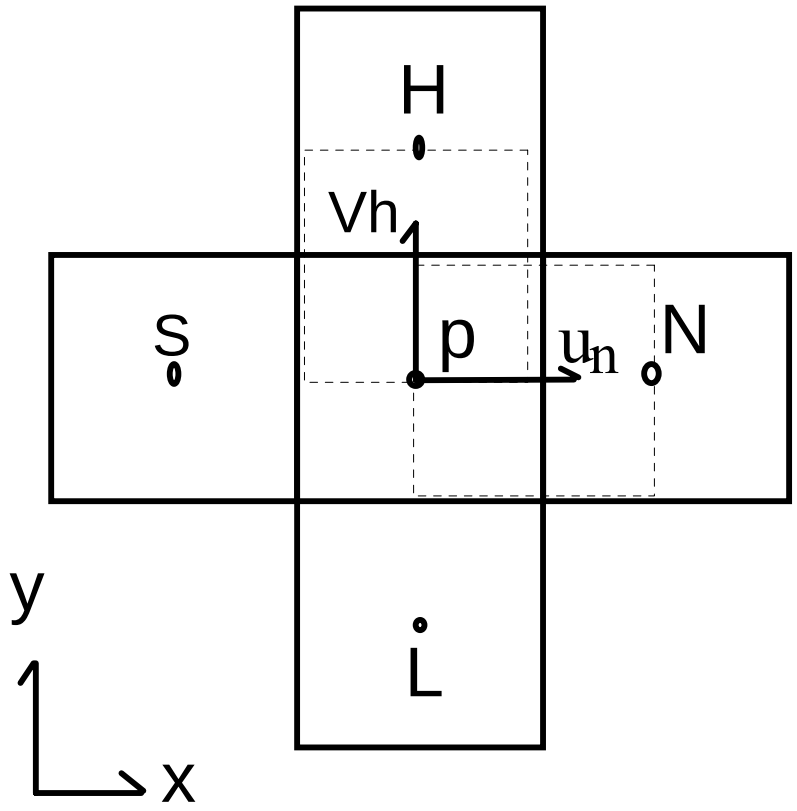

Figure 3.1: An example of a staggered grid caption.

Chapter Four

MELTING IN A TWO-DIMENSIONAL ICE BOX

4.1 Introduction

To implement the previously discussed case numerically, a fixed-grid technique is used. A commercial general purpose three-dimensional CFD package (FLUENT) is utilized. The package implements the lumped heat capacity approach discussed in the previous chapter.

The competing effects of positive and negative buoyancy forces and interacting layers of hot and cold liquid create interesting flow patterns that are difficult to model. To obtain a clear idea of the melting process and how it is affected by natural convection, a base case is first presented.

A two dimensional model is considered first. A thorough testing of the solution dependence on grid size, grid type, time step size and the difference between liquidus and solidus temperatures was carried out. The model is then used to carry out some parametric runs.

4.2 Melting in 2 by 2 cm Two-Dimensional Box

As a test case, a two-dimensional 2x2 cm box filled with a frozen substance was chosen. A numerical model of this box was constructed. Since the geometry is a regular

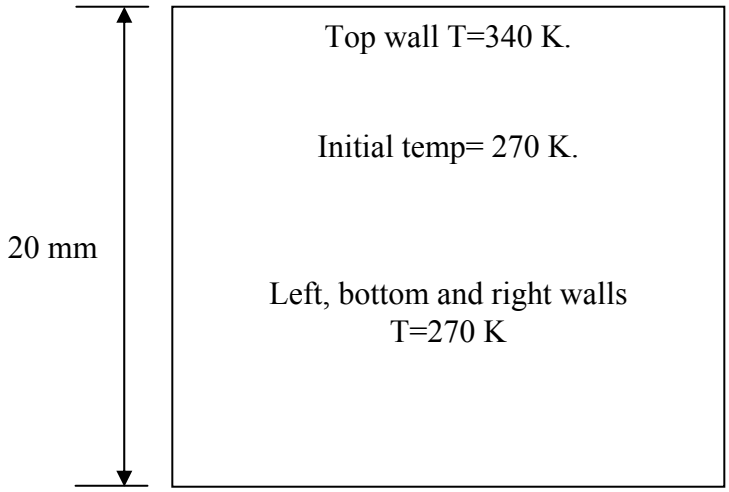

Figure 4.1 A schematic diagram of the two-dimensional box

square, a structured mesh is used. A schematic diagram of the test case is shown in Figure 4.1

The box is a 2 cm a side square, initially filled with a frozen material at 270 K. The top wall is kept at a constant temperature of 340 K while the remaining left, bottom and right walls are kept at 270 K. Zughbi *et al*. (1998) reported a somewhat similar experimental set-up, where frozen material (ice) was melted in a box by heating the top surface. The ice box was immersed in an ice bath so that the side and bottom walls were kept at a temperature close to the freezing temperature of water. However, a part of the top surface only was heated.

In this case, the latent heat of solid/liquid material was set at 333 kJ/kg while the solidus and liquidus temperatures were set at 273 K and 274 K respectively. This is a large difference for a pure component such as ice. It will be refined later on. The physical properties of the substance used initially are close but not the same as those of

water. In a later section, runs with water and its properties will be reported. The physical properties used in sections 4.2-4.6 are shown in Table 4.1.

A 40 by 40 mesh was used to discretize the geometry using a Quad type mesh. This is a rectangular mesh. This means that a total of 1600 cells were needed. A time step size of 30 seconds was used and the effects of turbulence were neglected. The time is measured from the start of turning on the heating system.

Figure 4.2 shows the velocity vectors at times of 10, 20, 30 40, 50 and 60 minutes. This figure shows how the flow pattern due to natural convection develops with time and with the increase in the thickness of the melt layer. These flow patterns did not show any

Table 4.1: Properties of frozen material

Density of solid state (kg/m3) @ 270 K	990
@ 273 K	995
Density of liquid state (kg/m3) @ 274 K	999
@ 277 K	1000
@ 293 K	998
@ 313 K	997
@ 353 K	992
Heating Capacity, Cp (J/kg-K)	4174
Thermal Conductivity (W/m-K)	0.621
Viscosity (kg/m-s)	0.00553
Heat of melting (J/kg)	333793
Molecular Weight (kg/kmole)	18

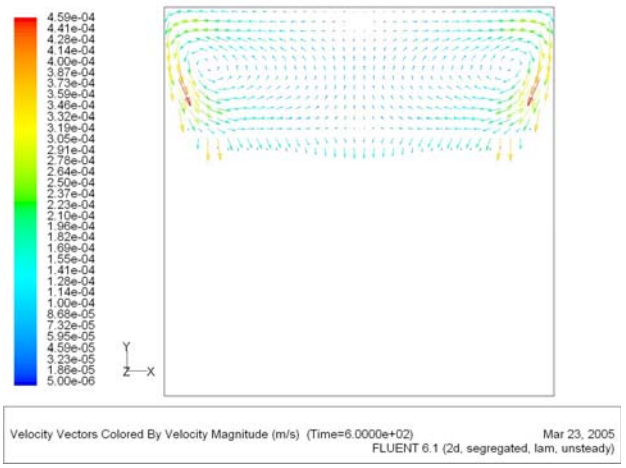

t=10 min.

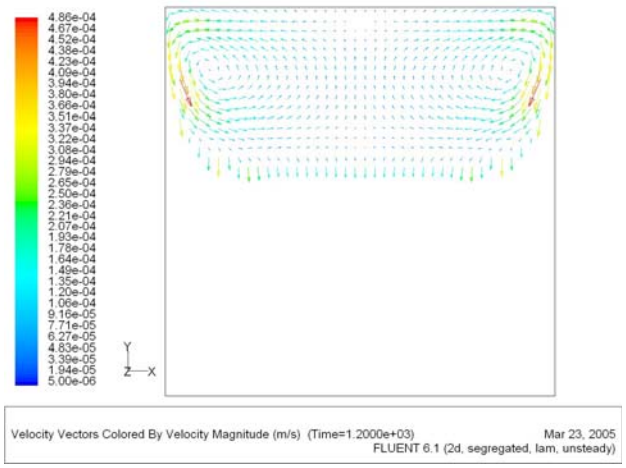

t=20 min.

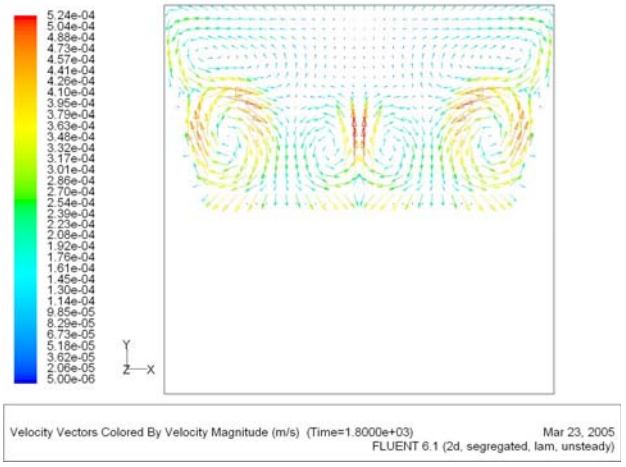

t=30 min.

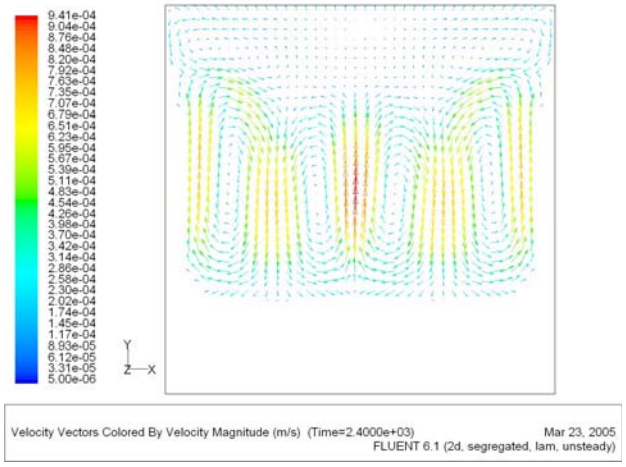

t=40 min.

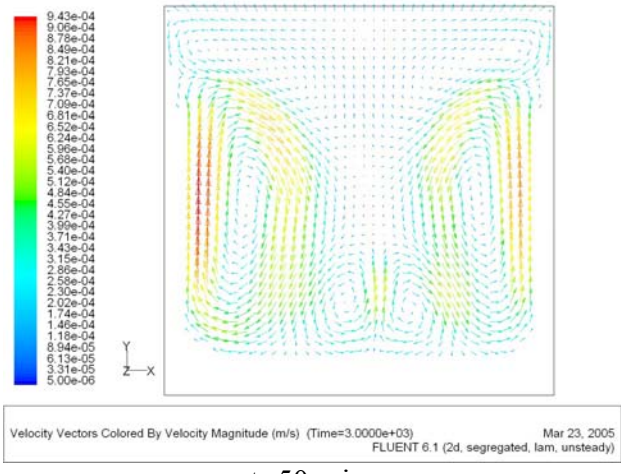

t=50 min.

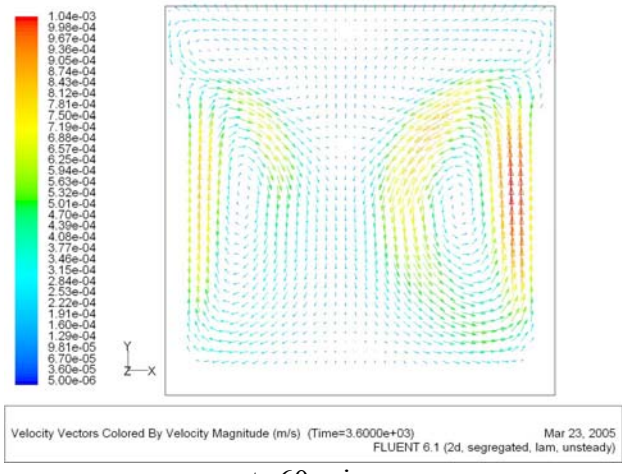

t=60 min.

Figure 4.2 Velocity vectors at different times for a 2x2 cm ice box of 40x40 mesh size. A time step size of 30 second is used.

further significant change after the 30 minutes mark. It is clear from this figure that six main circulations can be seen from the velocity vectors in Figure 4.2. There is one clockwise circulation pocket near the left wall in the lower part of the melt area, followed by a counter-clockwise, a clockwise and finally a counter-clockwise circulation pattern. Near the top left hand corner, there is a counter-clockwise circulation while near the top right hand corner there is a clockwise circulation pattern. As time advances these circulation patterns got elongated, but no significant change in the flow patterns was observed. The velocities in the melt layer are in the range of a one mm/sec. This agrees with values reported in the literature for similar cases (Kowaleswski and Rebow, 1998). The hot liquid is transported from the top to the bottom of the box through the center of the ice. The two top circulation patterns move the hot water from the top of the box downwards along the left and right walls. The four central and lower patterns contribute significantly to the melting rate by enhancing heat transfer through natural convection.

Figure 4.3 shows the melt front in the box at the same time intervals shown in Figure 4.2, i.e. at 10, 20, 30, 40, 50, and 60 minutes. The depth of the melt region can be seen clearly. The interface thickness is a few millimeters. This is a function of the grid size and the difference between the liquidus and solidus temperatures. The thin un-melted layer at the side and bottom boundaries is a result of setting these walls at a temperature below the melting temperature, i.e. 270 K. This layer is likely to stay as long as the boundaries are kept at 270 K.

Figure 4.4 shows a plot of melt thickness in mm versus the time of heating. The change in the rate of melting is clear. A steep rate is observed in the first 7 minutes,

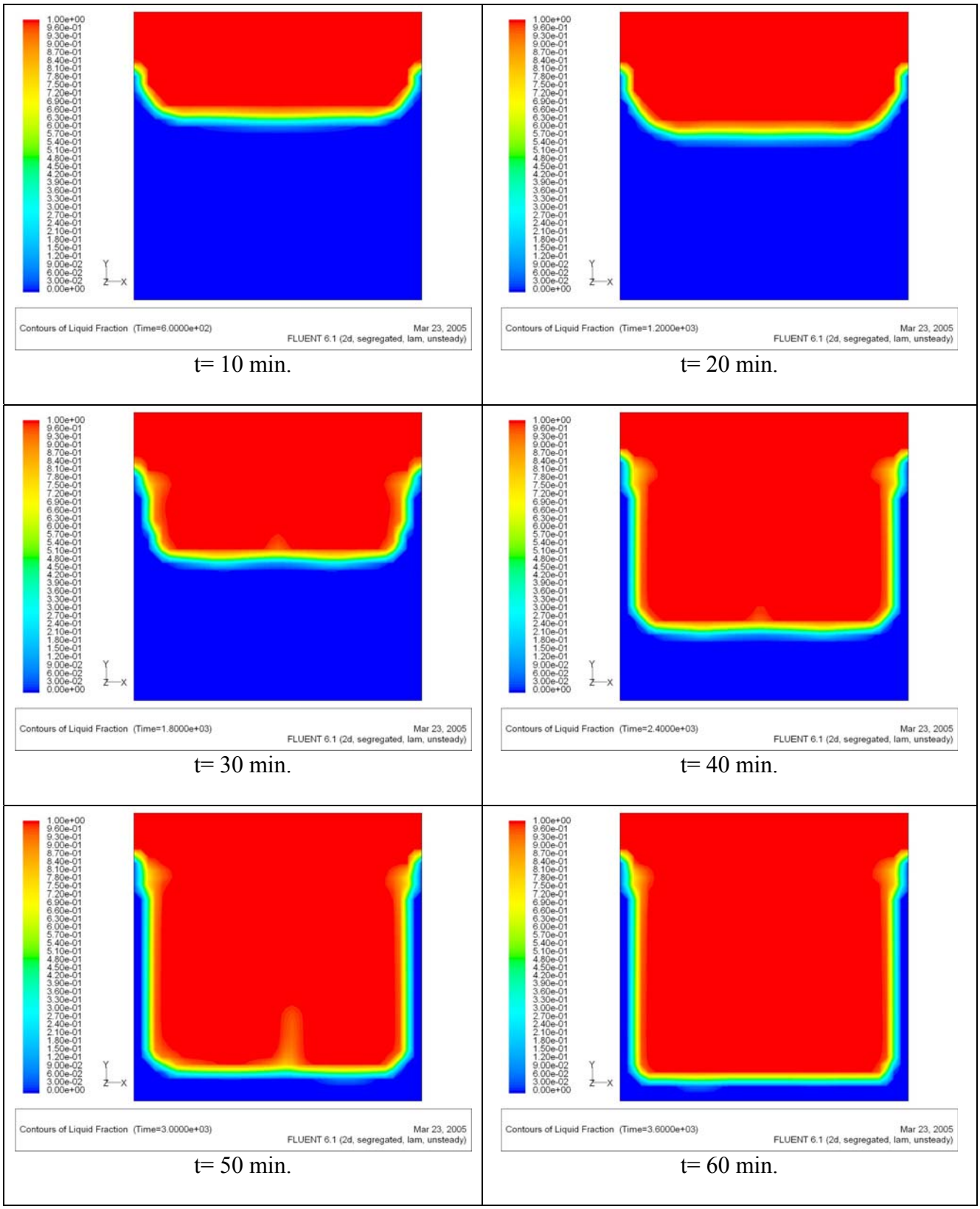

Figure 4.3 Liquid volume fractions at different times for a 2x2 cm ice box of 40x40 mesh size. A time step size of 30 second is used.

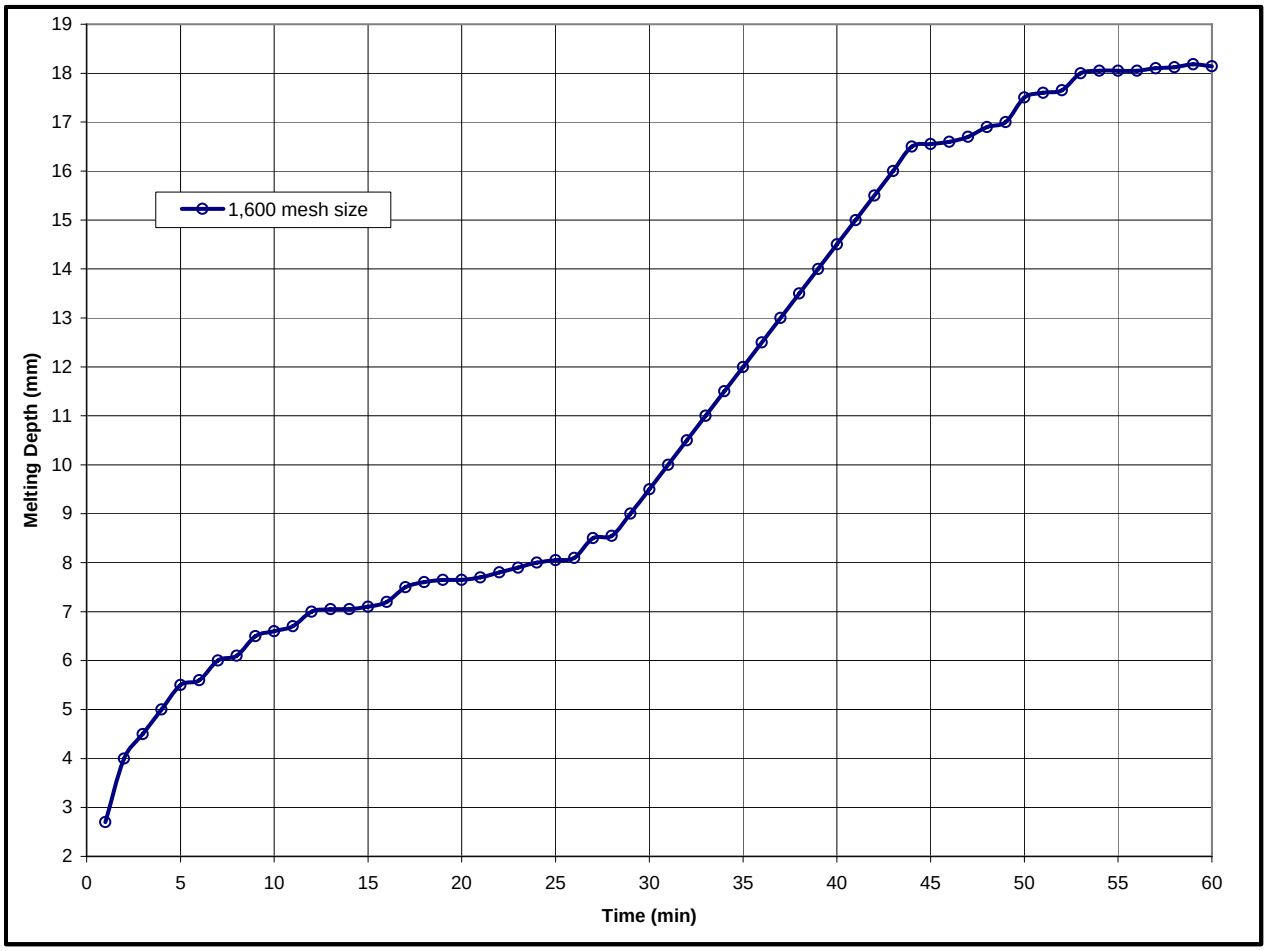

Figure 4.4: The melting rate versus time for a 2x2 cm ice block of 40x40 mesh size. The time step size is 30 seconds.

followed by a plateau where the melting rate is sharply reduced, then followed by a region of higher melting rate but lower than that of the first 7 minutes. At a time of about 45 minutes, the melting rate hits a plateau again and is sharply reduced in value. These melting rates in cm/minute are summarized in Table 4.2

4.3 Solution Independence of the Grid Size

The independence of any CFD solution of the grid size has to be established before the results can be considered as credible. A number of grid sizes was considered, and the melt thickness versus time was compared. In addition to the 40× 40 mesh, meshes of 80×80, 90×90, 100×100, and 110×110 were considered. This means a total number of 1600, 6400, 8100, 10,000 and 12,100 cells respectively is used. The size of each grid cell is 0.05, 0.025, 0.02222, 0.02, 0.01818 cm.

Figure 4.5 shows a plot of the melt thickness versus time for all five mesh sizes. It is clear that for mesh sizes 80×80 and finer the long plateau following the steep melting rate has disappeared. This is more in line with expectations as the long plateau cannot be explained. However the slowing in the melting rate can be easily explained. As the melt

Table 4.2 The melting rate for a 2x2 cm ice block at 10, 20, 40 and 50 min

Time (minutes)	Melt Thickness (cm)	Melting Rate cm/min.
10	0.670	0.067
20	0.775	0.0388
40	1.45	0.0363
50	1.75	0.035

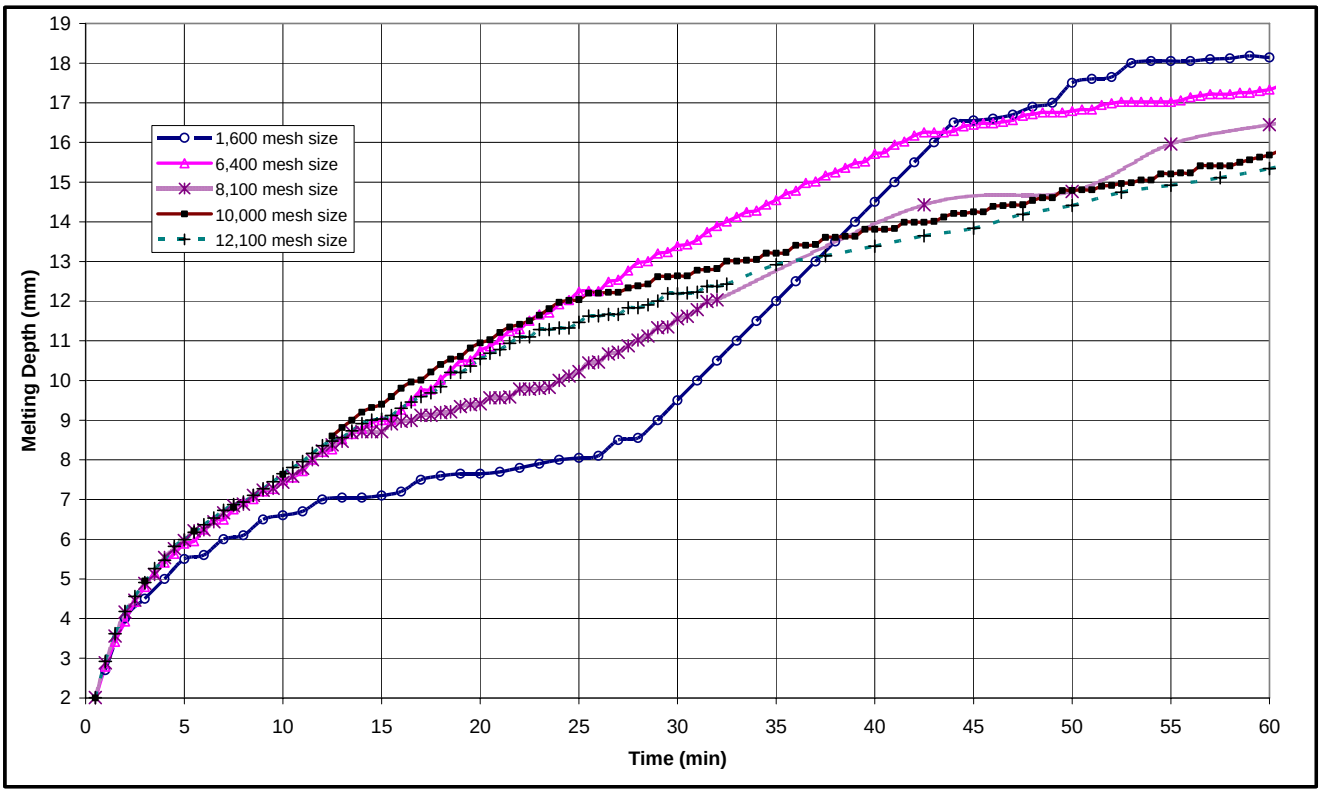

Figure 4.5: The melting rate versus time for a 2x2 cm ice block with different mesh sizes (Quad type). A time step size of 30 seconds is used.

thickness increases the resistance to conduction heat transfer increases, while no significant change is noticed in the contribution of the natural convection. For mesh sizes 80×80 and finer, the melting rate over the first 14 minutes is almost identical. This is mainly because in this region the conduction heat transfer was still playing a major role of the solution. The plots of the melt thickness versus time for the 100×100 and 110×110 are very close. The difference over 60 minutes is less than 0.5 mm which means an error of about 3% error. Therefore a mesh size of 110×110 is chosen. In a later section a mesh size of 120×120 will be tested and compared with 110×110 mesh size to confirm the selection of 110×110 mesh size. This will be done after examining the solution independence of solidus and liquidus temperatures and applying the actual physical properties of water and ice.

Figure 4.6 shows the velocity vectors for each of the mesh sizes at time equals to 20 and 60 minutes. The patterns for mesh sizes of 80 x 80 and finer are very similar. To investigate the similarities between the solutions of various mesh sizes further, a line was defined across the melted region at a time equal to 30 minutes and at y = 1.0 cm. A plot of velocity along this line for all mesh sizes is shown in Figure 4.7. The proximity of the solutions for mesh sizes 100 × 100 and 110 × 110 is further strengthened.

4.4 Solution Independence of the Grid Type

For a rectangular geometry, such as the two dimensional ice box considered in this chapter, a structured (Quad) mesh is first used because the grid can perfectly fit the

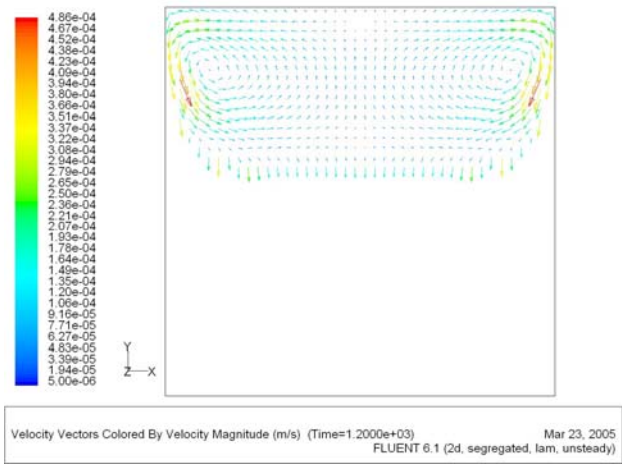

t=20 min., 40 x 40 mesh

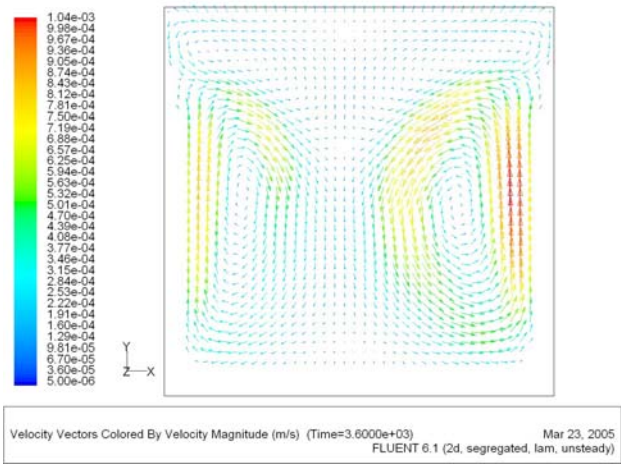

t=60 min., 40 x 40 mesh

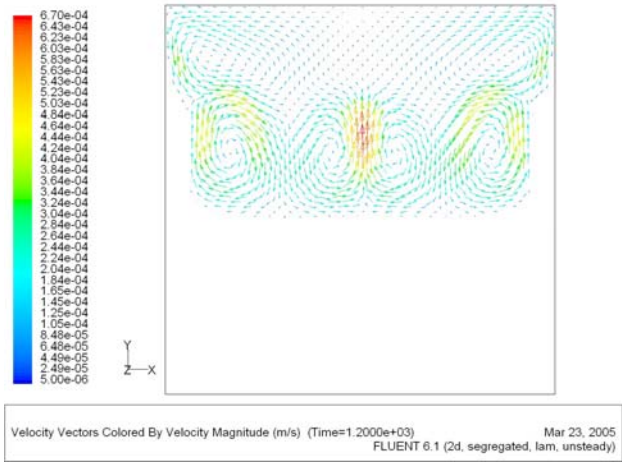

t=20 min., 80 x 80 mesh

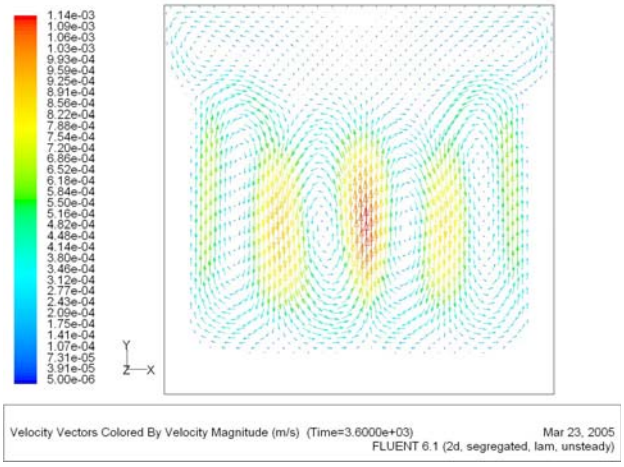

t=60 min., 80 x 80 mesh

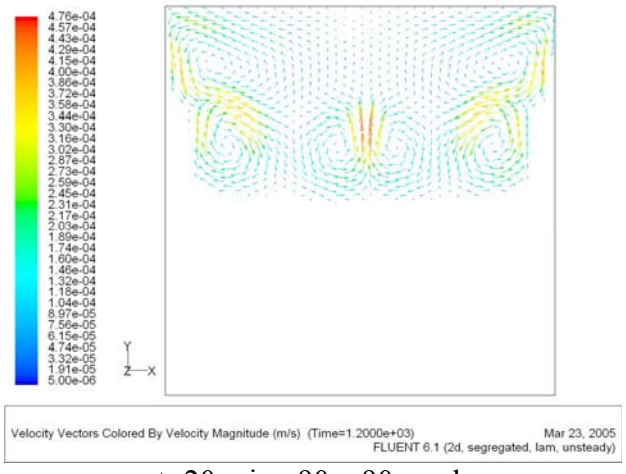

t=20 min., 90 x 90 mesh

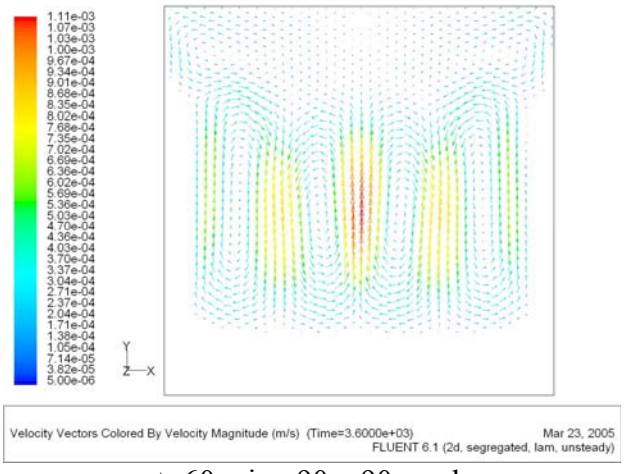

t=60 min., 90 x 90 mesh

Figure 4.6a: Velocity vectors for 40x40, 80x80 and 90x90 mesh sizes. The time step size is 30 seconds.

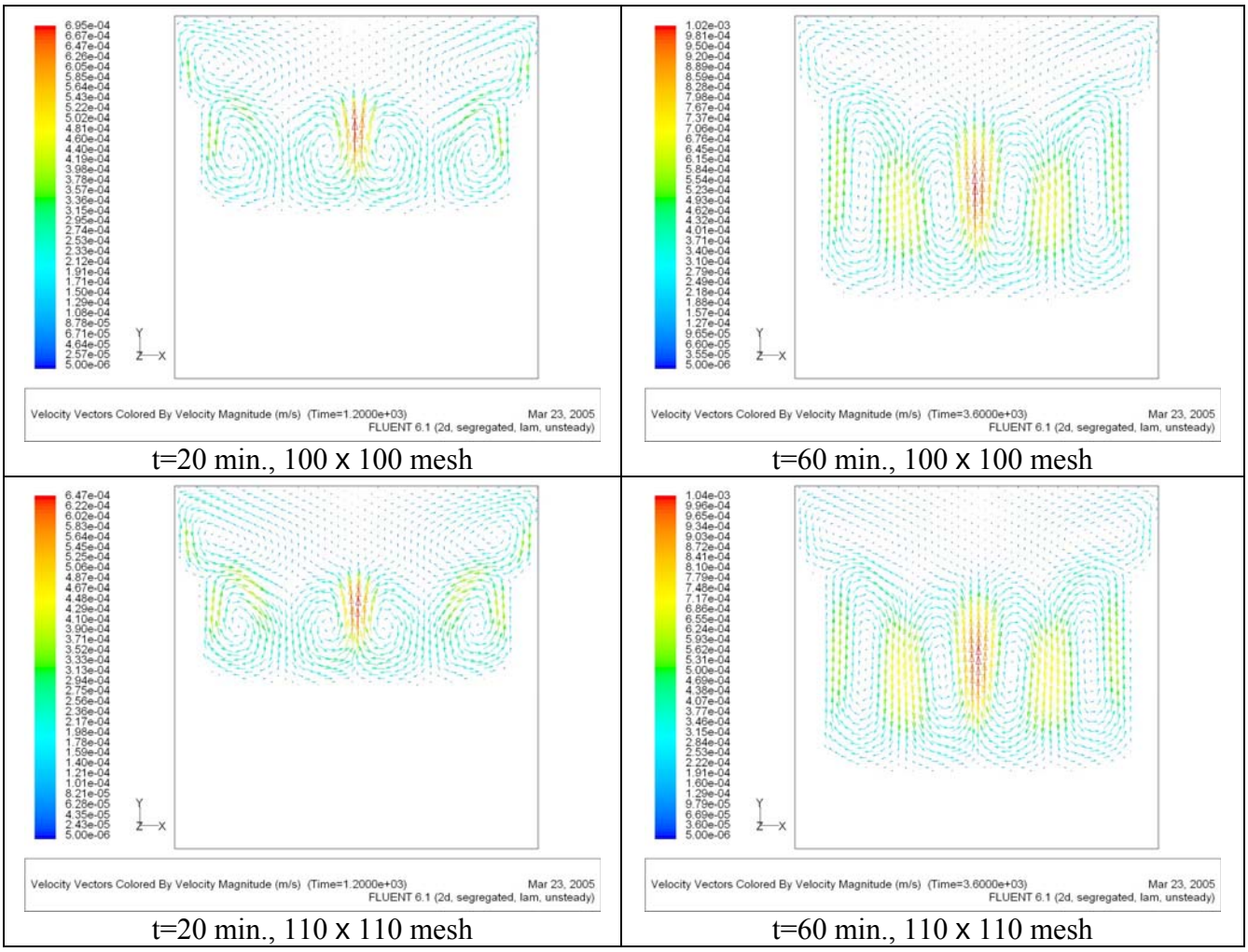

t=20 min., 100 x 100 mesh | t=60 min., 100 x 100 mesh

t=20 min., 110 x 110 mesh | t=60 min., 110 x 110 mesh

Figure 4.6b: Velocity vectors for 100x100 and 110x110 mesh sizes. The time step size is 30 seconds.

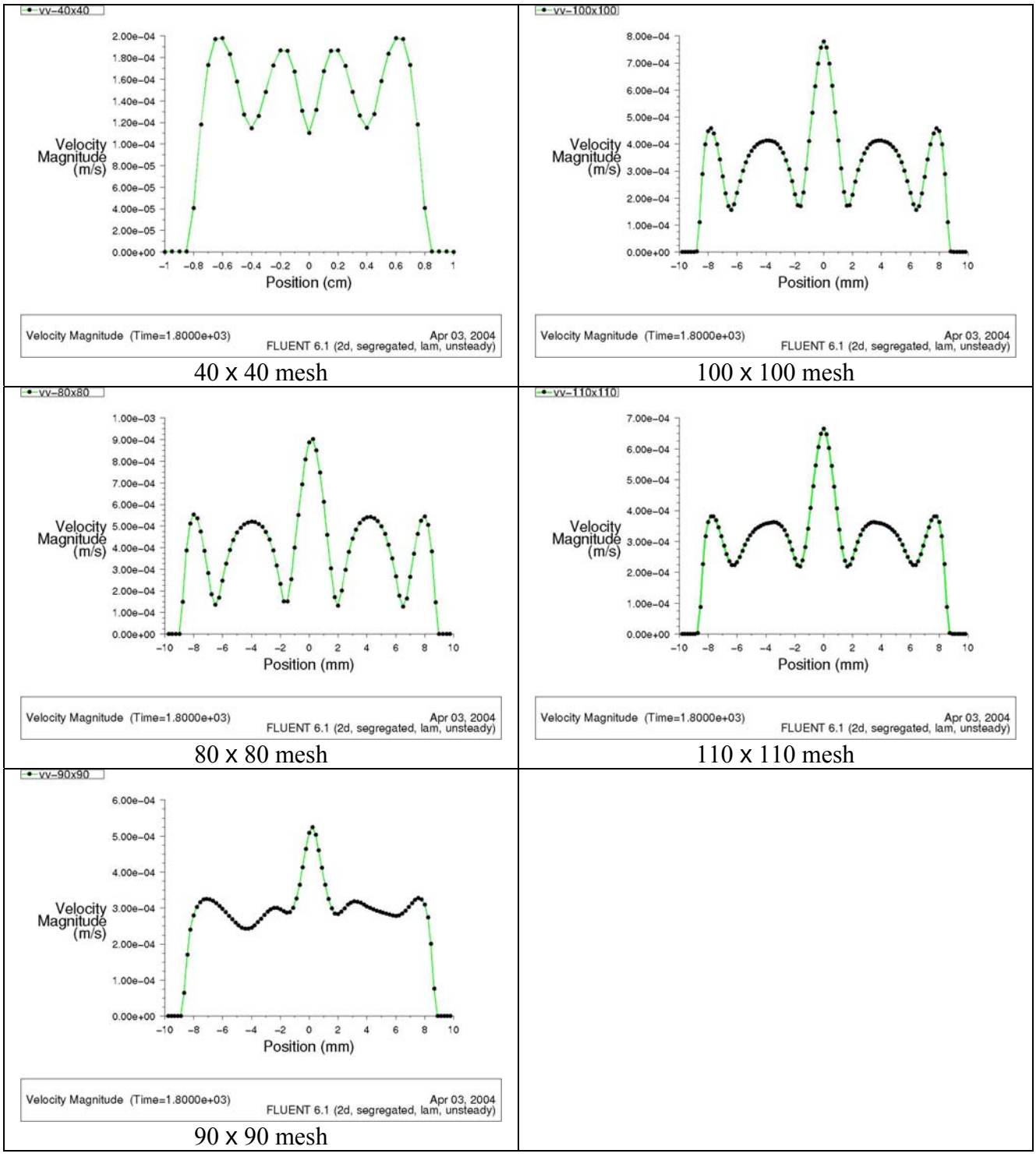

Figure 4.7: Velocity magnitudes at y = 1 and t = 30 min. for 2x2 cm ice box and mesh sizes of 40x40, 80x80, 90x90, 100x100 and 110x110. The time step size is 30 seconds.

domain and the grid maintains its orthogonality. However, because of the curved melt front, convergence at the cells forming the melt interface may become difficult. An unstructured (triangular) mesh can usually better handle un-orthogonal meshes. An unstructured mesh of 110 nodes specified per edge (the same number as for the quad mesh) is constructed. The total number of cells needed to mesh the box is 27200 cells compared to 12,100 cells needed when using quadrilateral mesh.

Figure 4.8 shows the structured (Quad) and the unstructured (Tri) 110×110 meshes. The increase in the number of mesh cells in the case of unstructured is clear.

Figure 4.9 shows the melting thickness versus time for the Quad and Tri 110×110 meshes. A small difference up to a time of 60 minutes was observed. This difference is about 1.8 mm of melt thickness which is about 12% error. To further compare the results of Quad and Tri meshes, Figure 4.10 compares the velocity along a central line at y = 1.0 cm for both mesh types. The magnitude of the velocity in both cases is similar for time greater than 20 minutes. Consequently, Quad meshes are used in this study due to savings in computational time and also due to the fact that a Tri mesh did not result in significantly different results. The velocity profiles in figure 4.10 are also similar.

4.5 Solution Independence of the Size of the Time Step

Following the establishment of the independence of the solution of the grid size and type, it is important to examine the dependence of the solution on the size of the time step. Runs with time step sizes of 30, 15, 5, 2 and 1 seconds for the Quad mesh and with

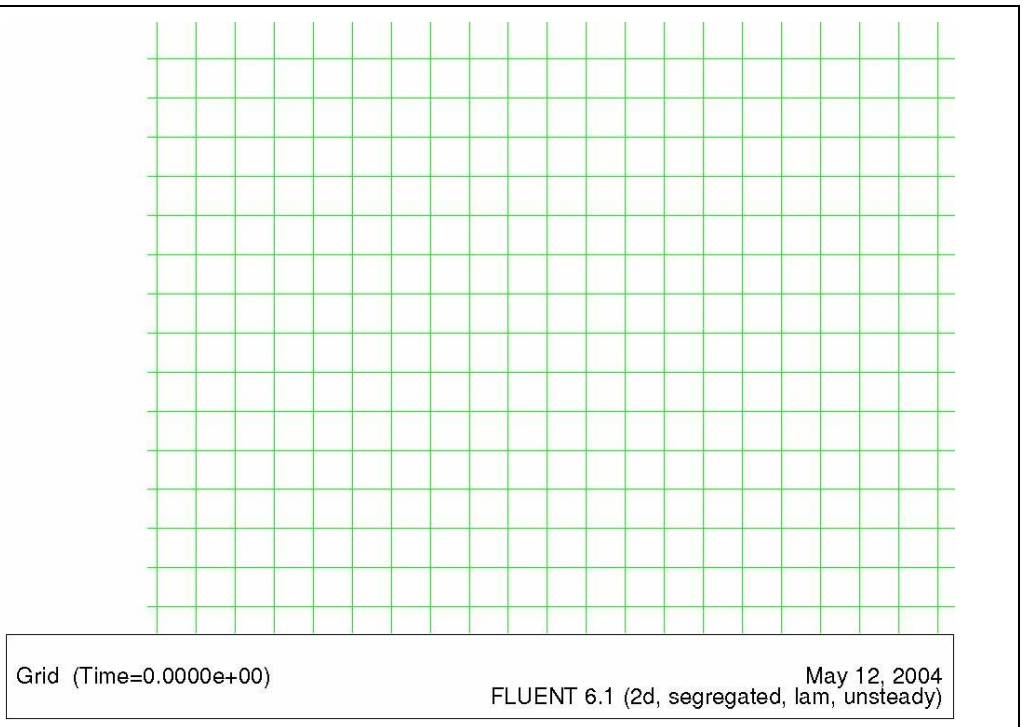

Structured grid (Quad type)

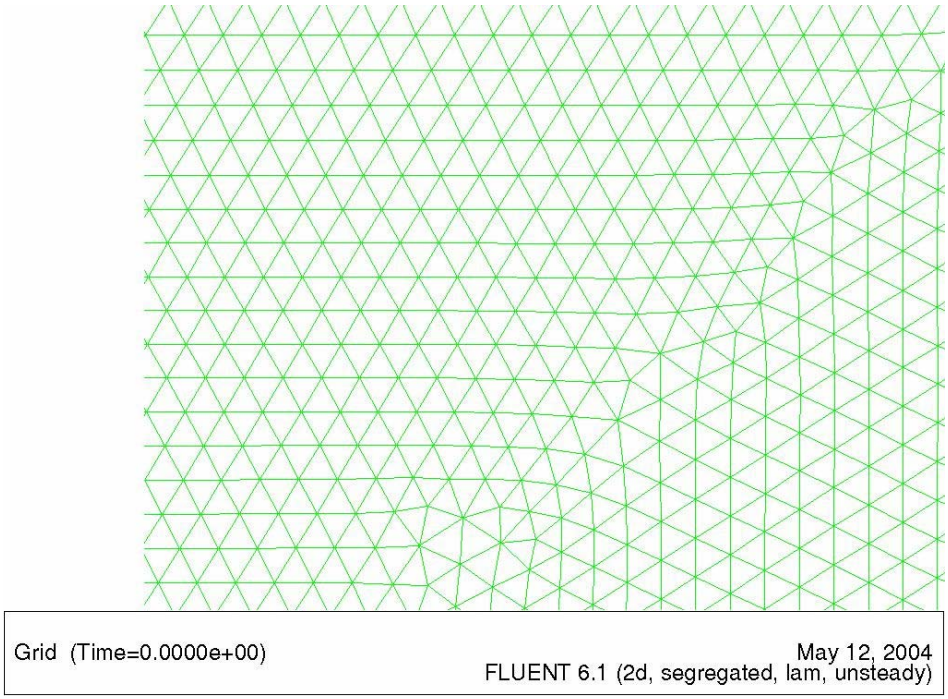

Unstructured grid (Tri type)

Figure 4.8: Structured (Quad) and unstructured (Tri) Grids for the 110x110 mesh.

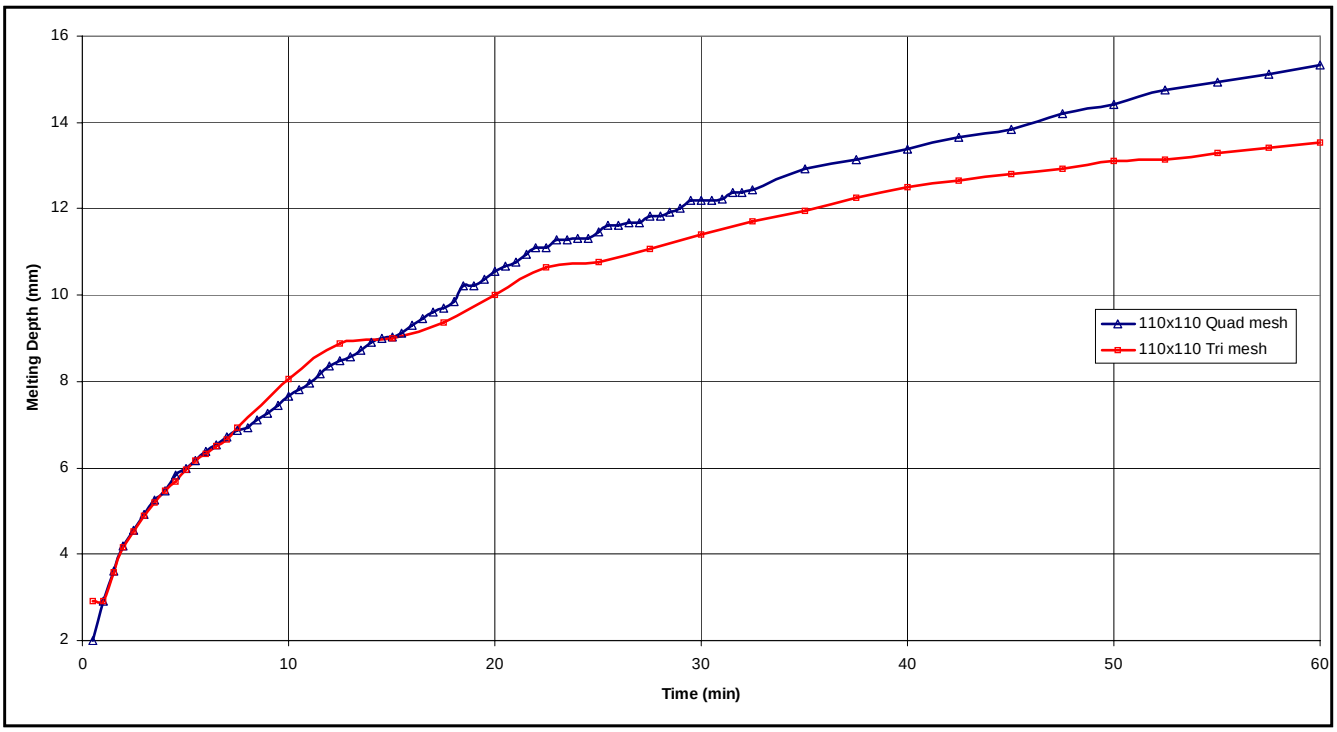

Figure 4.9: The melting depth versus time for 2x2 cm ice box with 110x110 mesh size for structured (Quad) and unstructured (Tri) grids. A time step size of 30 seconds was used.

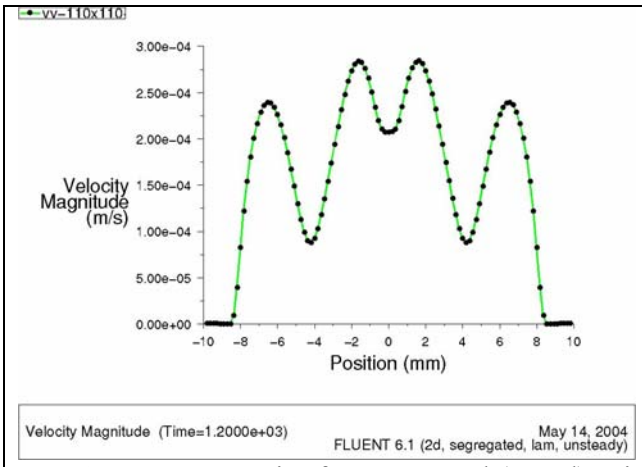

y=1 cm & t=20 min. for structured (Quad) grid

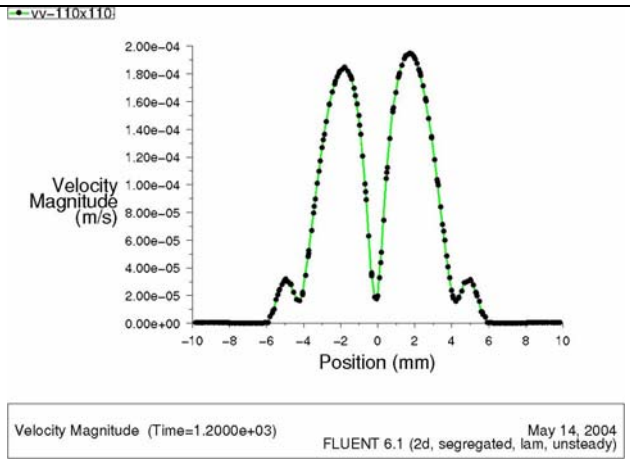

y=1 cm & t=20 min. for unstructured (Tri) grid

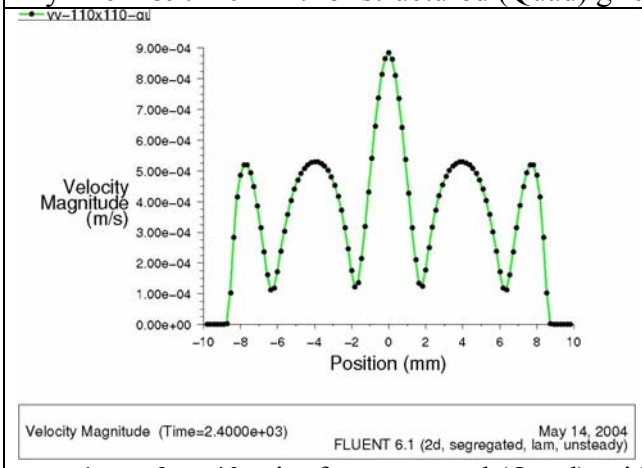

y=1 cm & t=40 min. for structured (Quad) grid

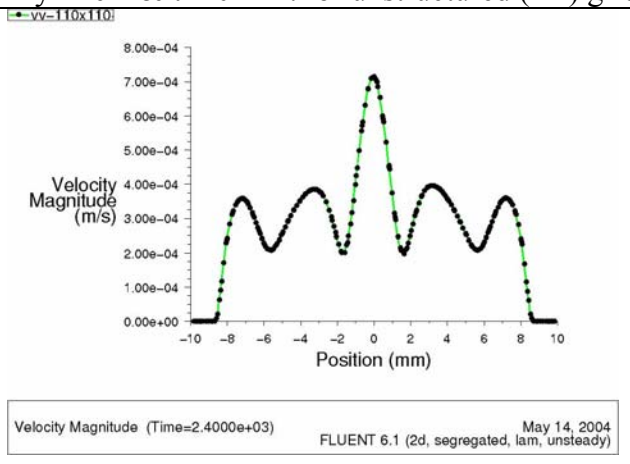

y=1 cm & t=40 min. for unstructured (Tri) grid

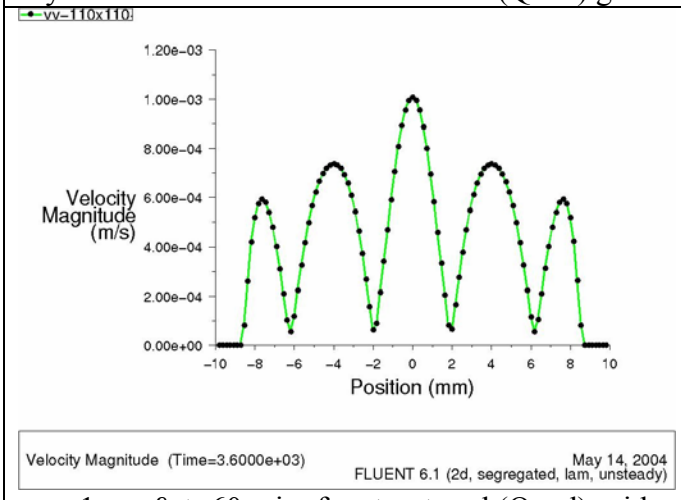

y=1 cm & t=60 min. for structured (Quad) grid

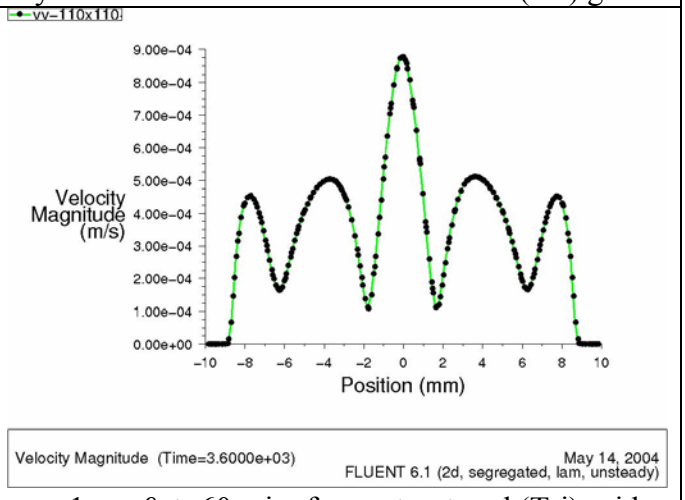

y=1 cm & t=60 min. for unstructured (Tri) grid

Figure 4.10: Velocity magnitude for a 2x2 cm ice box and for a mesh size of 110x110 for a structured (Quad) and an unstructured (Tri) grids for different melting time. The size of time step used is 30 seconds.

sizes of 30, 5, 2 and 1 seconds for the Tri mesh were attempted. The plots of melt thickness versus time for a case of 110 × 110 mesh and each of the above time step sizes are shown in Figure 4.11. The melting rate over the first 15 minutes is controlled mainly by conduction and was found to be independent of the time step size. However, the melting rate was found to increase as the size of the time step is decreased. For the Quad mesh the results of 1 and 2 seconds are quite close. The overall melting rate for Quad and Tri meshes is found to be quite similar. However, using one (1.0) second for Tri mesh the melting rate was found to be higher (by about 1.0 mm) than that for Quad mesh at the 45 minutes mark.

4.6 Solution Dependence on the Difference Between the Liquidus and Solidus Temperatures

The lumped heat capacity method used in this study is best suited for melting or solidification of alloys that melt over a small range of temperatures rather than at one sharp temperature. However, it can produce good approximations for melting of pure components if melting is restricted to a narrow range of temperature. For the previous runs a solidus temperature of 273 K and a liquidus temperature of 274 K were assumed. In this section, the effects of narrowing down the difference between the solidus and liquidus temperatures on the solution are investigated. The solidus and liquidus temperatures considered are shown in Table 4.3.

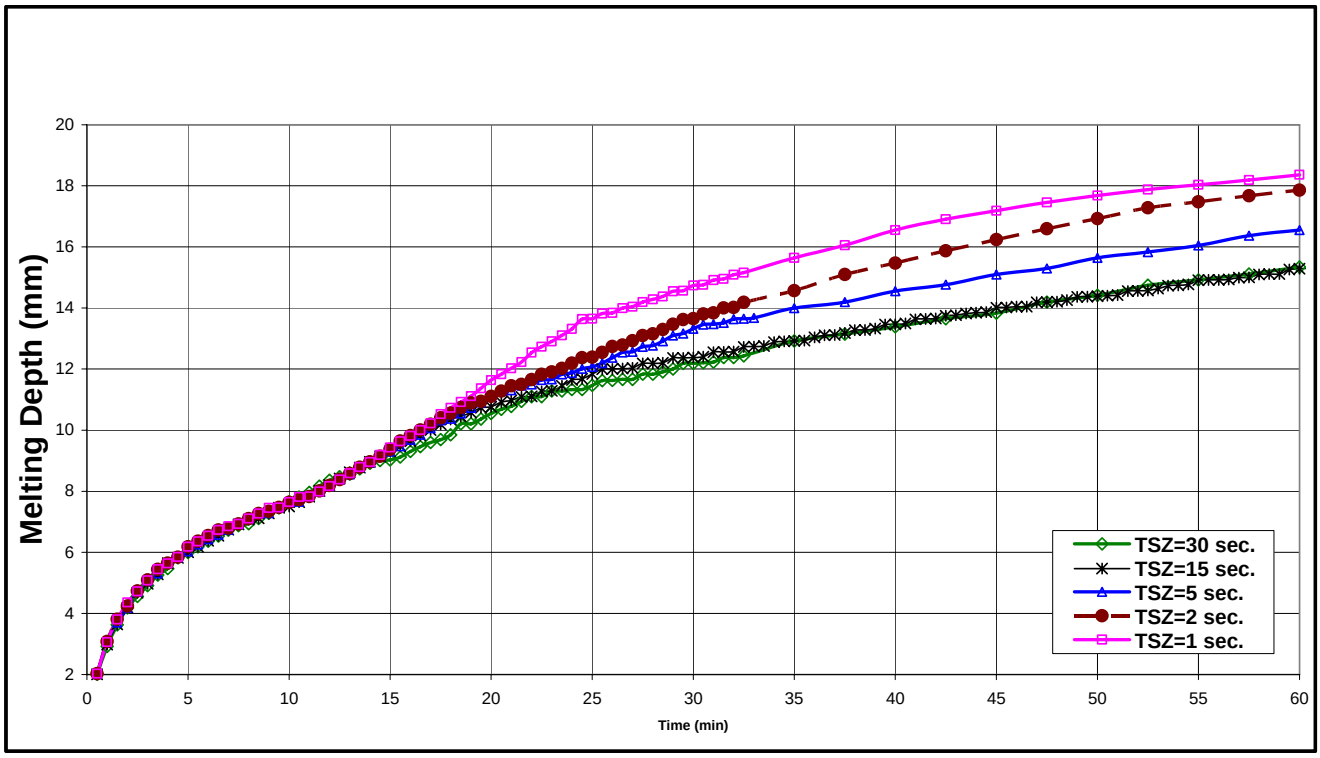

(a)

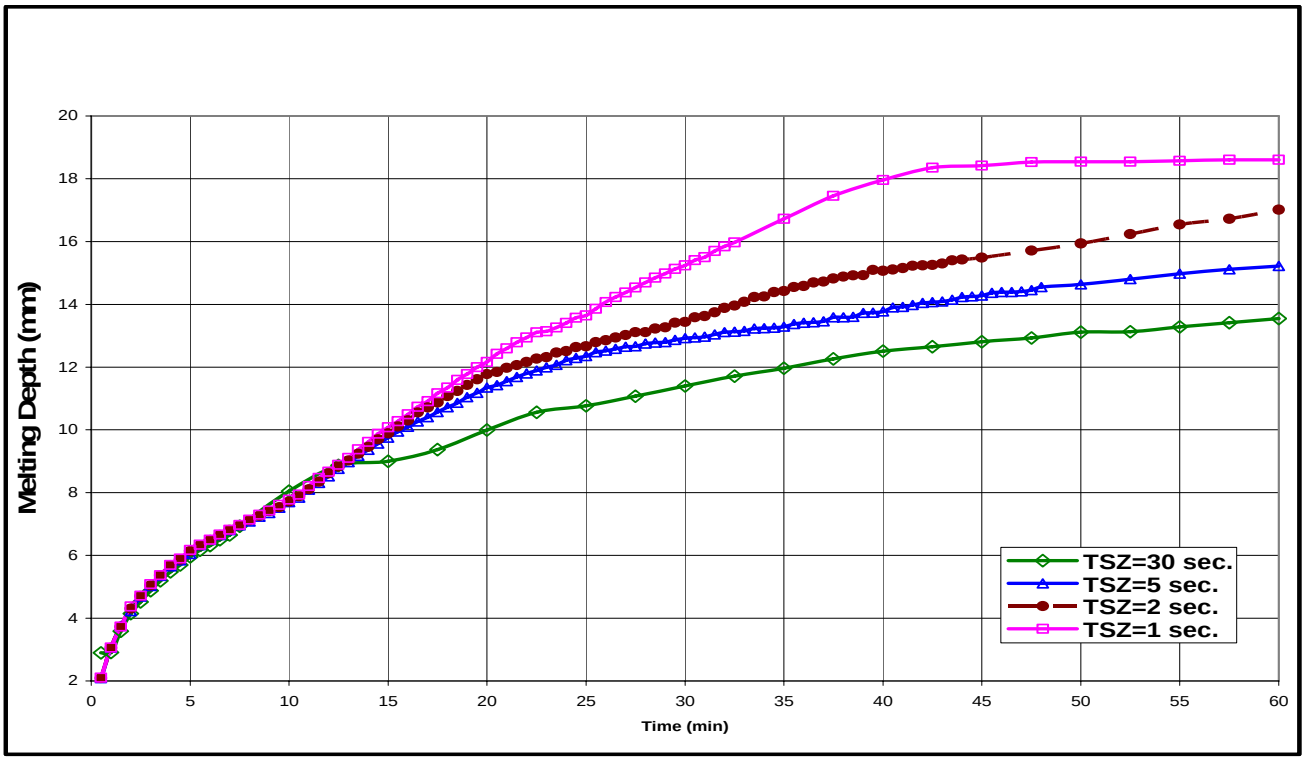

(b)

Figure 4.11 Plots of melt thickness versus time for a case of 110x110 for various time step sizes and for (a) Quad mesh and (b) Tri mesh.

Table 4.3: Solidus and liquidus temperatures considered in this study

Run	Solidus Temperature K	Liquidus Temperature K	Tl-Ts ^{o}C
1	273	274	1.00
2	273	273.15	0.15
3	273.05	273.15	0.10

Figure 4.12 shows plots of the melt thickness versus time for a case of 110 × 110 mesh and the ranges of liquidus and solidus temperatures shown in Table 4.3. The melting rate over the first 12 minutes is controlled mainly by conduction and was found to be independent of the difference between liquidus and solidus temperatures. However, the melting rate was found to decrease as the difference between liquidus and solidus temperatures is decreased. The melting rates for liquidus and solidus temperatures difference of 0.15 and 0.1 K are found to be quite similar up to a time of 35 minutes. However, a difference of about 2 mm of melt thickness is found after 60 minutes of melting. This is equivalent to about 12% error.

A run with a difference of 0.05 K between the solidus and liquidus temperatures (T_s=273.1 K and T_l=273.15 K) was attempted. However, the results were not consistent with other results and consequently it will not be reported.

4.7 Melting of Ice in a 2×2 cm Enclosure

In the previous sections, the melting of a substance with physical properties close to but not quite the same as those of water was examined. In this section the melting of ice is examined and the physical properties used are as shown in Table 4.4:

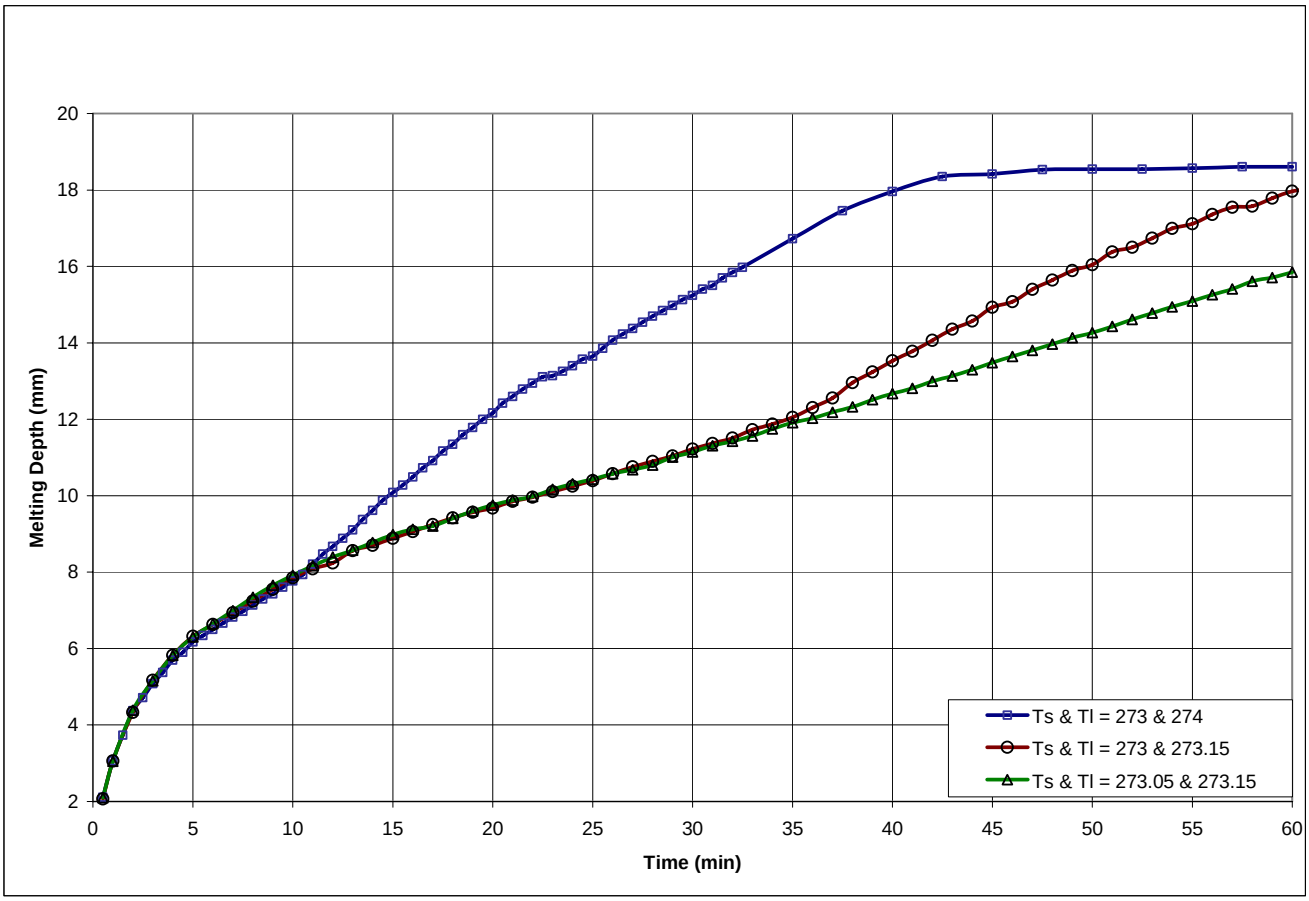

Figure 4.12 Plots of melt thickness versus time for various ranges of liquidus and solidus temperature110x110 Tri mesh. The time step sized used is 1 second.

Table 4.4: Physical properties of ice and water

Density of solid state (kg/m3) @ 273.1 K	990.0
Density of liquid state (kg/m3) @ 273.15 K	999.3
@ 277 K	999.9
@ 293 K	998.2
@ 313 K	992
@ 333 K	983.2
@ 353 K	971.8
Heating Capacity, Cp (J/kg-K)	4174
Thermal Conductivity (W/m-K)	0.621
Viscosity (kg/m-s)	0.00553
Heat of melting (J/kg)	333793
Molecular Weight (kg/kmole)	18

Figure 4.13 shows the melting rate of ice versus time in a 2x2 cm block using a mesh of 110x110. An unstructured Tri mesh is used and a time step size of 1 second is also used. A solidus temperature of 273.1 and 273.05 K and a liquidus temperature of 273.15 K are considered. This represents a difference of 0.1 and 0.05 K. The melting rate is slower than before due to the change in the physical properties. However, it shows a similar trend to that in previous section, namely a steep melting rate in the first minutes then a gradual slowing down in the melting rate.

Figure 4.14 shows the velocity vectors at 10, 20, 40, 60, 80 and 100 minutes. The flow patterns due to natural convection are similar to those shown in the previous section. Figure 4.15 shows the melting front at the same time intervals as above. The shape and size of the melt zone are also similar to those shown in the previous sections.

4.8 Confirmation of Grid Size Independency

In section 4.3, the solution was tested for the dependency on grid size and a mesh size of 110x110 was selected for further simulations. This was done before carrying out the test of the solution independence of the solidus and liquidus temperatures and before utilizing the actual physical properties of water and ice.

A case with 120x120 mesh size was tested after applying the actual physical properties of water and ice and after identifying the independence of the solution of the solidus and liquidus temperatures. Figure 4.16 shows a comparison of melting rate for 110x110 and 120x120 mesh sizes. It is clear that both melting rate curves are almost identical. This confirms the selection of 110x110 mesh size.

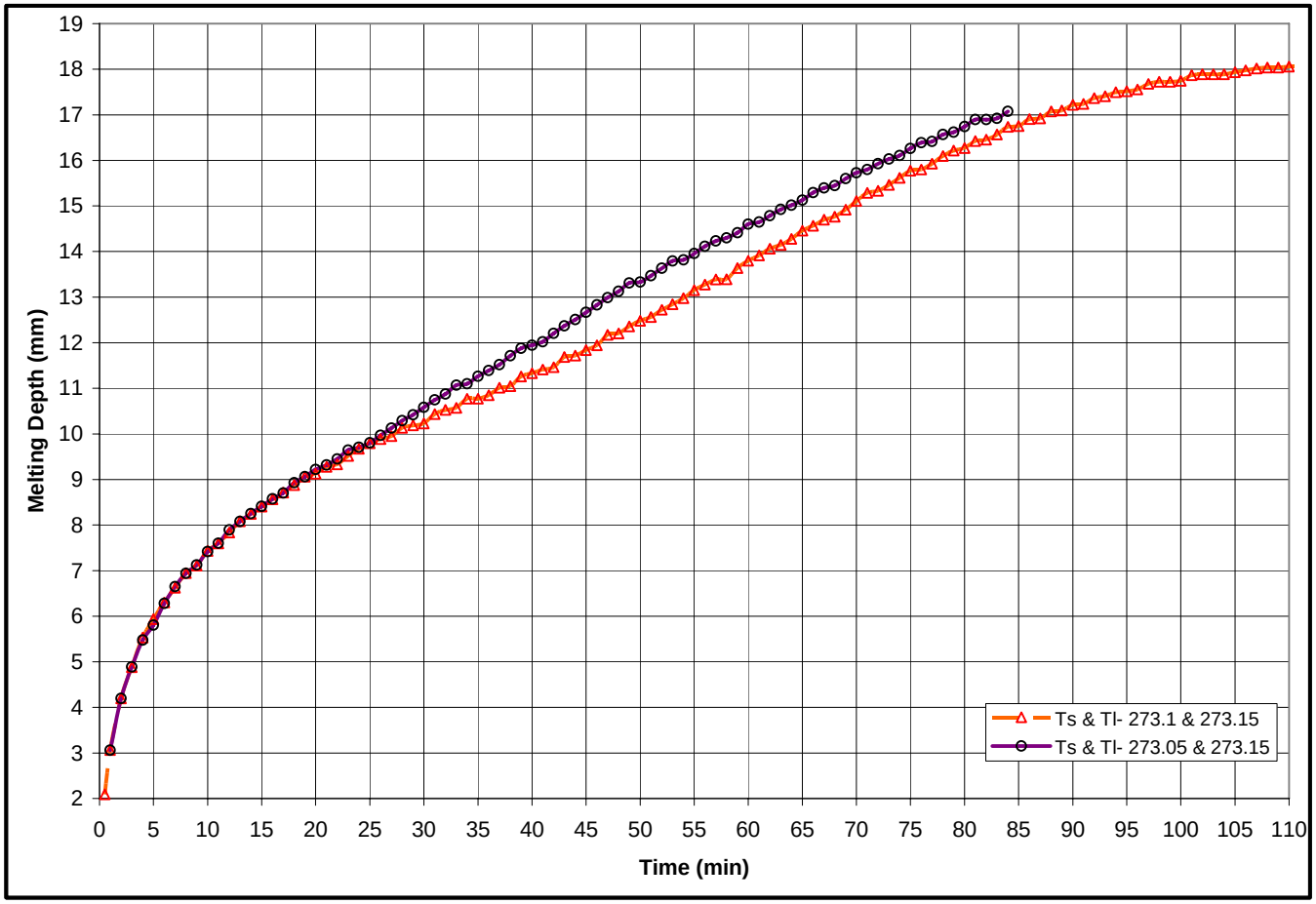

Figure 4.13: Melting rate of ice versus time in a 2x2 cm using a mesh of 110x110. An unstructured (Tri) grid and a time step size of 1.0 second are used.

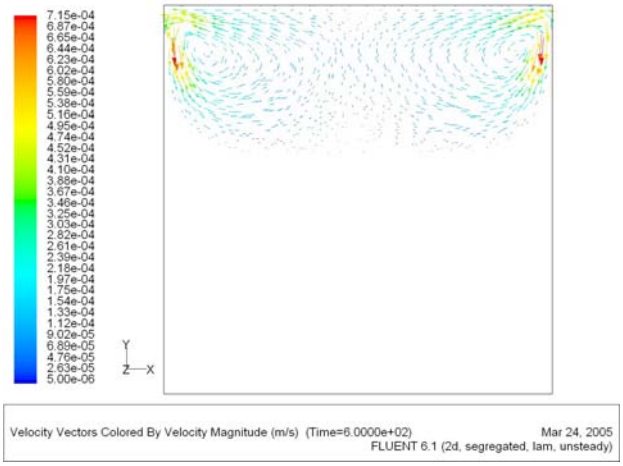

t= 10 min

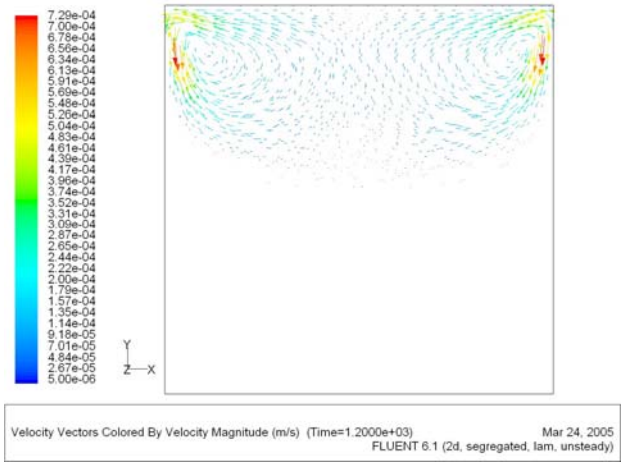

t= 20 min

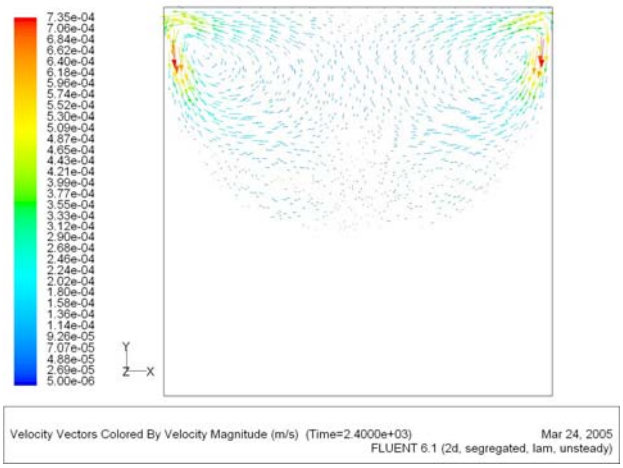

t= 40 min

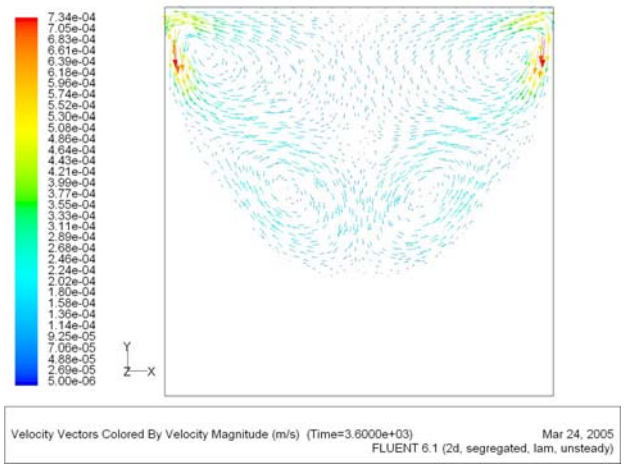

t= 60 min

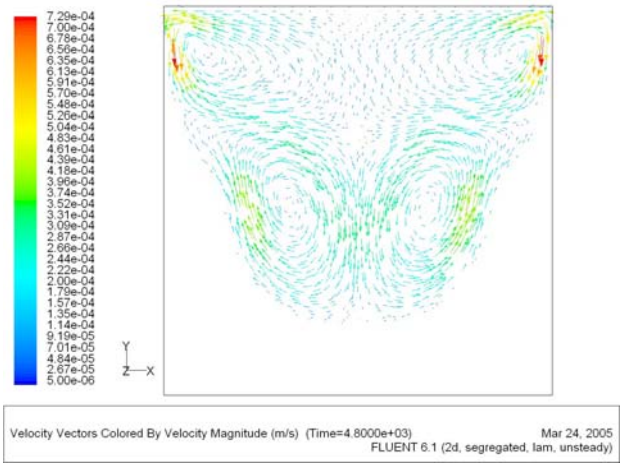

t= 80 min

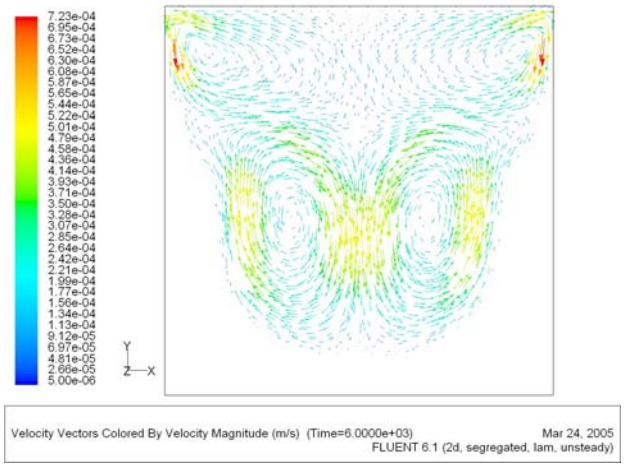

t= 100 min

Figure 4.14: Velocity vectors at different times for 2x2 cm ice box of 110x110 mesh size. An unstructured (Tri) grid type and a time step size of 1.0 second are used. Ts = 273.1K and Tl = 273.15K.

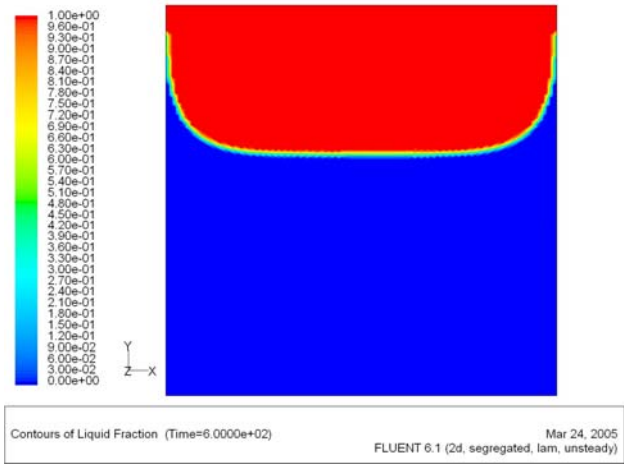

t= 10 min

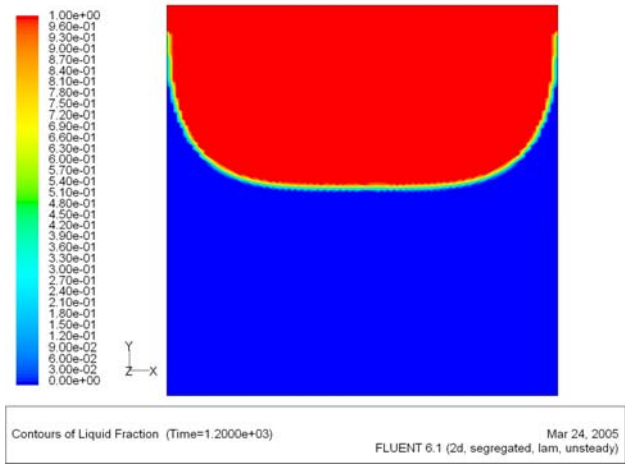

t= 20 min.

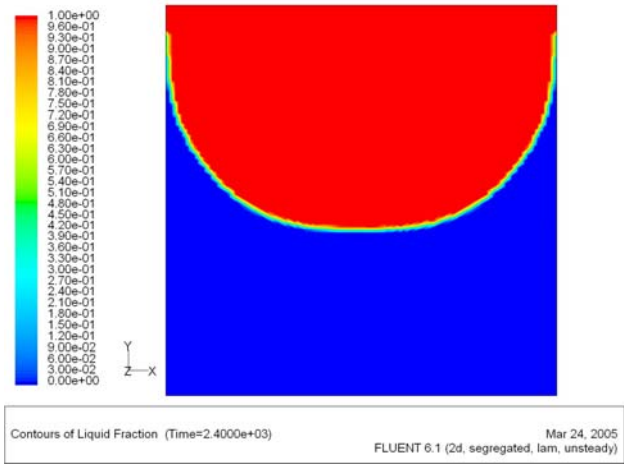

t= 40 min.

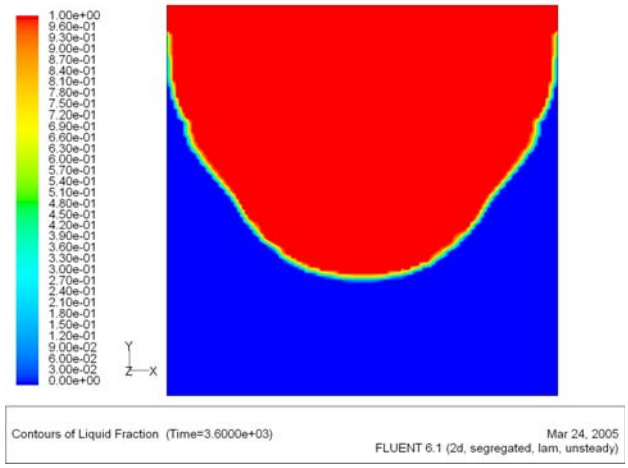

t= 60 min.

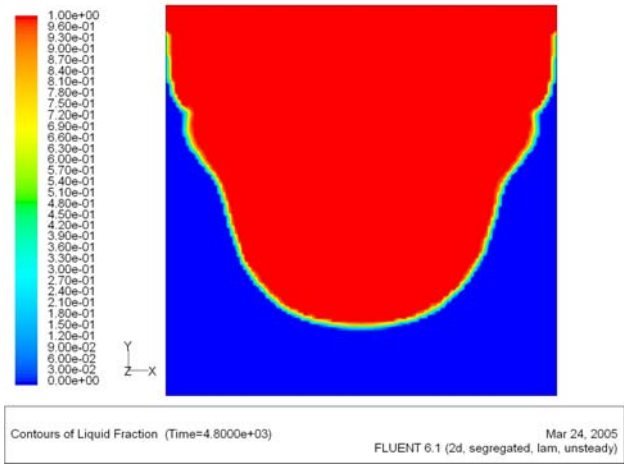

t= 80 min.

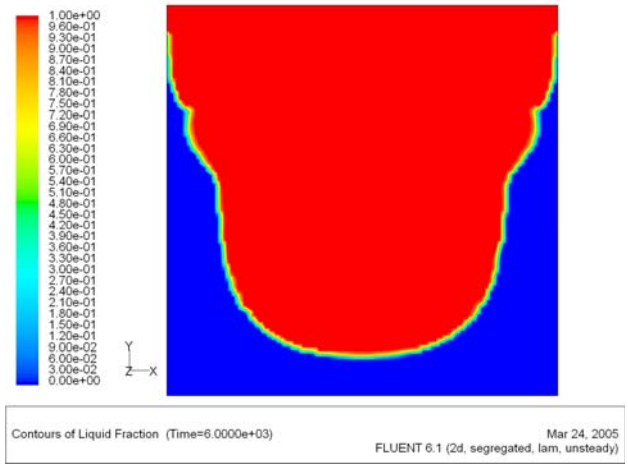

t= 100 min.

Figure 4.15: The melting front at different times for 2x2 cm ice box of 110x110 mesh size. An unstructured (Tri) grid type and a time step size of 1.0 second are used. Ts = 273.1K and Tl = 273.15K.

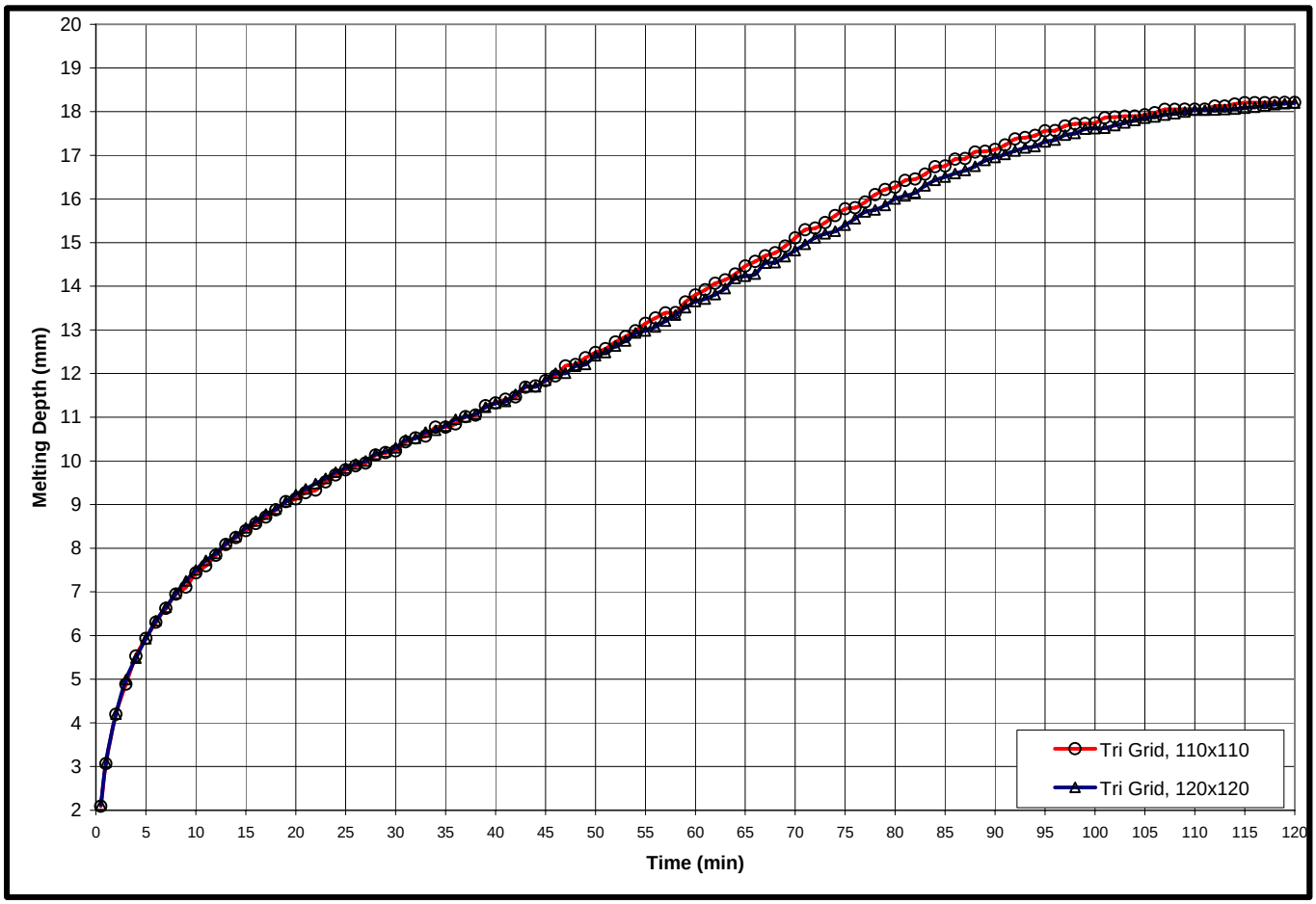

Figure 4.16: Comparison of melting rates for 2x2 ice block with 110x110 and 120x120 meshes.

4.9 Effects of Natural Convection on Melting

One objective of this study is to investigate the effect natural convection has on the melting rate of a pure component. In the previous sections melting with natural convection was considered. In this section, melting of a 2×2 cm ice block due to conduction only is considered, i.e. the effects of natural convection are neglected. This is also done numerically by solving only the energy equation and neglecting the solution of the Navier-Stokes equations.

Figure 4.17 shows a comparison of the melting rate of a 2x2 cm ice block with and without the effects of natural convection. Natural convection reduced the melting time for 1.5 cm of the block from 8 hours to about 1 hour. It is also noticed that in the initial melting period, the melting rates with and without natural convection were close to each other. Natural convection started to have an impact on the melting process 15 minutes following the onset of the melting process.

4.10 Dependence of Natural Convection on Rayleigh Number

The effects of natural convection increases as the value of Rayleigh number, *Ra*, increases. Rayleigh number is defined as:

$$Ra = GrPr \tag{4.1}$$

where *Gr* is Grashoff number and *Pr* is Prandtl number. Grashoff numbers is defined as:

$$Gr_x = \frac{g\beta(T_w - T_\infty)x^3}{\nu^2} \tag{4.2}$$

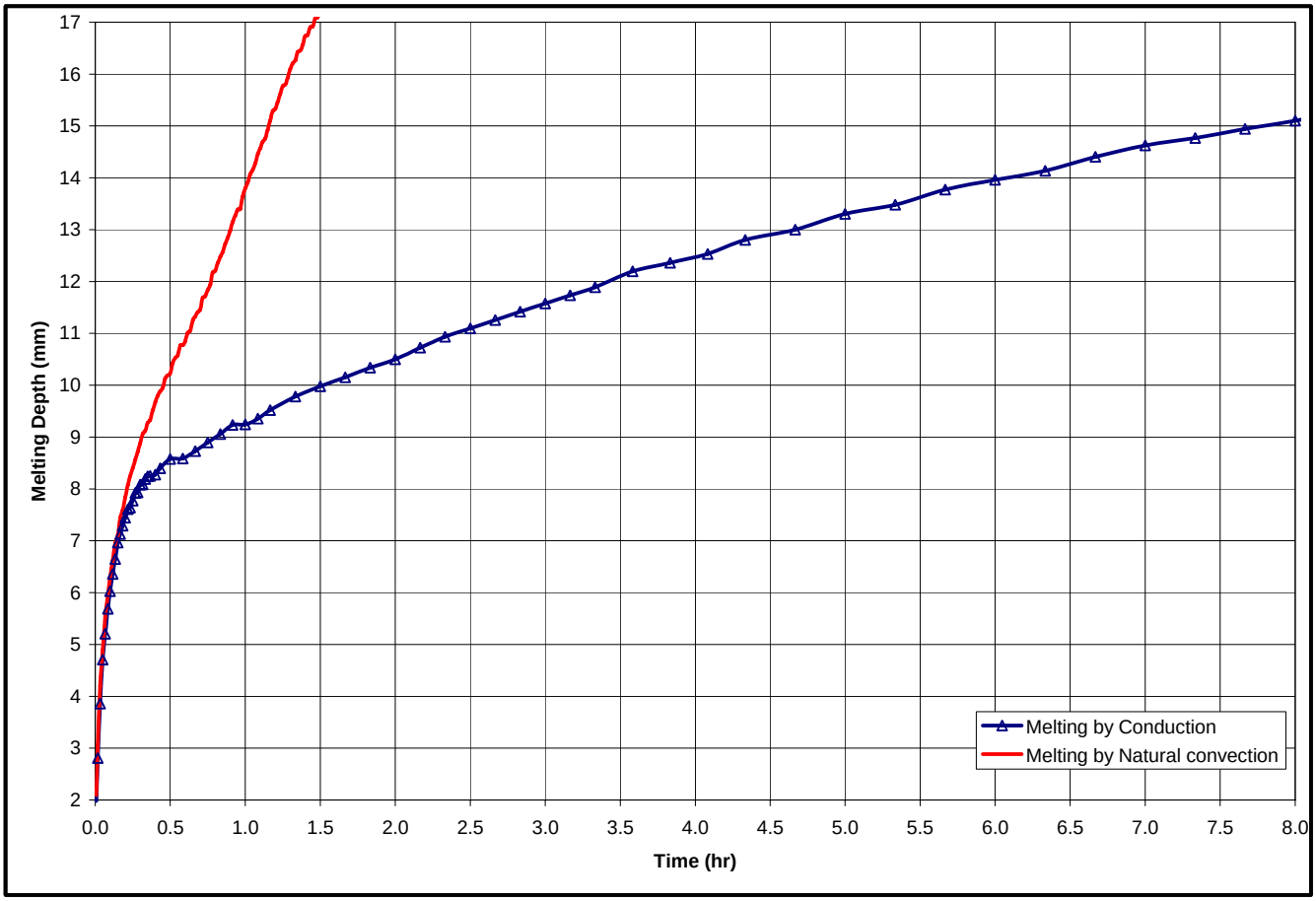

Figure 4.17: A comparison of the melting rate of a 2x2 cm ice block with and without the effects of natural convection.

where g is the gravitational acceleration, T_w and T_∞ are the temperatures at the hot wall and from away from it (at x). x is a characteristic length which varies with the system considered and ν is the kinematic viscosity of the fluid.

Prandtl number is defined as:

$$Pr = \frac{Cp\,\mu}{k} \tag{4.3}$$

where C_p is the heat capacity, μ is the dynamic viscosity and k is the thermal conductivity.

The average natural convection heat transfer coefficient can be represented in the following form:

$$Nu_f = \frac{hd}{k} = C\,(Gr_f\ \mathrm{Pr}_f)^m \tag{4.4}$$

where f refers to the film temperature and $T_f=(T_\infty + T_w)/2$, C and m are constants which vary according to the circumstances of the problem at hand, e.g. they differ for different cases such as convection in an enclosure or from a hot place facing downwards, etc.

Natural convection in an enclosure is very minute for very low Grashoff numbers and the heat transfer occurs mainly by conduction across the fluid layer. As the Grashoff number is increased, different flow regimes are encountered with a progressively increasing heat transfer. It is generally accepted that for *Ra* below 1000, the effects of natural convection is negligible.

For the 2×2 cm ice block, *Ra* ranges from 1.33×10^2 for a melt layer of 1 mm to 7.76×10^5 for a melt layer of 18 mm. According to the above criteria, *Ra* will reach 1000 when the melt depth is about 2.0 mm. The negligible or little effect of natural convection is confirmed by looking at Figure 4.17. It can be seen that the melting rates with and without the effect of natural convection are identical until the melting thickness reaches 7.0 mm. This corresponds to a *Ra* of 4.5×10^4. This means that the effects of natural convection become significant a short time before *Ra* reached the above value.

For natural convection, it is generally accepted that turbulence effects are not important for $Ra < 10^8$. Consequently and based on the above values of *Ra*, it can be concluded that the effects of turbulence on melting in a 2x2 cm enclosure can be neglected. This means there is no need to include any turbulence model in simulating melting in a 2x2 cm box.

CHAPTER FIVE

VALIDATION

5.1 Introduction

The enthalpy based method was used in the previous chapter to develop a two-dimensional CFD model to simulate melting of ice in a block. A significant effort was made to establish the independence of solution of the grid size, grid type and size of the time step. In general, the grid size for which independence was established was rather fine, namely, a 110x110 mesh for a 2x2 cm block. For a regular quad mesh, that meant 12100 cells. However, if an irregular Tri mesh is used, the total number of cells used which meant 27200 cells.

In this chapter the numerical results are compared against some results obtained using some correlations and against some experimental data. The aim is mainly to validate the numerical model.

5.2 Validation of the Model against Solomon's Correlation

Alexiades and Solomon [1983] presented a comprehensive review of mathematical modeling of melting and freezing processes. A simple approximation with a relative error below 10% for finding the melt time for a rectangular body under imposed temperature was suggested by Solomon [1979]. For a rectangle, of dimensions a by b, initially solid at

T_m, if a constant temperature $T_l > T_m$ is imposed on all sides, its melt time according to Solomon [1979] is approximated by:

$$t_{melt} = \begin{cases} \dfrac{a^2\left[1+0.25St_L\right]}{8\alpha_L\, St_L} & if \quad \dfrac{a}{b} < \dfrac{2\left[1+0.42\,St_L\right]}{\pi\left[1+0.25StL\right]} \\ \dfrac{ab\left[1+0.42St_L\right]}{4\pi\alpha_L\, St_L} & if \quad \dfrac{a}{b} > \dfrac{2\left[1+0.42\,St_L\right]}{\pi\left[1+0.25StL\right]} \end{cases}$$

where a is the rectangle width, b is the rectangle height, the Stefan number for liquid $St_L = c_L(T_L-T_m)/L$, c_L is the specific heat of the liquid, T_L is the liquidus temperature, T_m is the initial solid temperature, the thermal diffusivity, α, is $k/\rho c$, k is the thermal conductivity, ρ is the density and c is the specific heat.

Applying the above correlation for a 2cm by 2 cm block of almost pure ice, initially at 270 K and at time equal to zero, all four walls are set at a temperature of 283 K. Using an average value of heat capacity, c_L, of 4204 J/kg.K, an average value of density of 998.75 kg/m3, latent heat value of 337000 J/kg and a thermal conductivity value of 0.5575 W/m.K, the melt time for this block using the Solomon's correlation is found to be 1578.9 seconds or 26.3 minutes. When the same case is simulated using the current model, the whole block was melted at 25.5 minutes, which is within 3.0 % of the value found using Solomon's correlation.

The above 2cm by 2 cm block of ice was melted with the four boundary conditions set at the specified hot temperature. The velocity fields at certain time intervals are shown in Figure 5.1. The velocity fields show clearly how the effect of natural convection on the

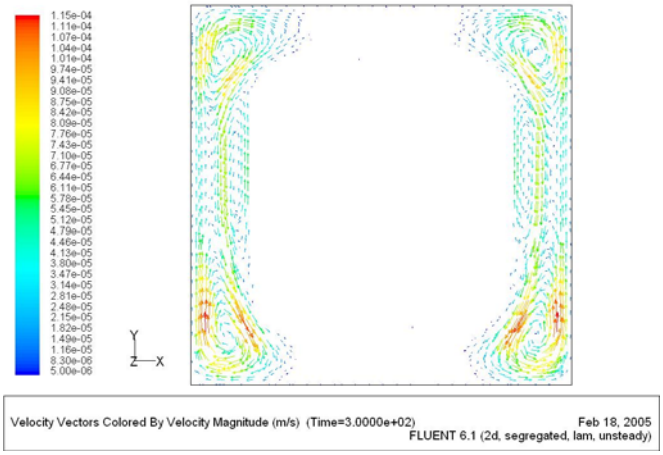

t=5 min

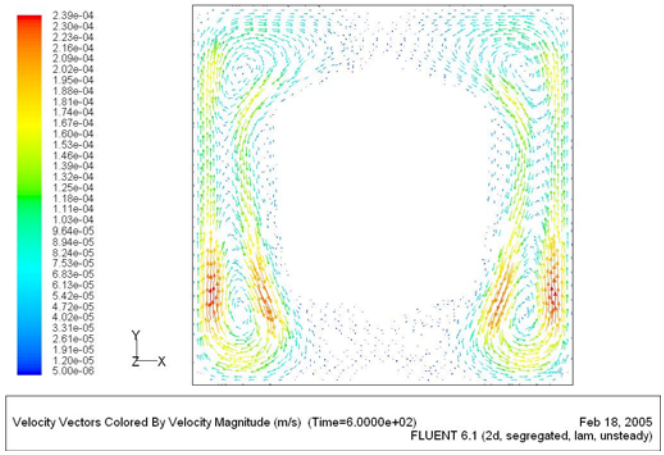

t=10 min

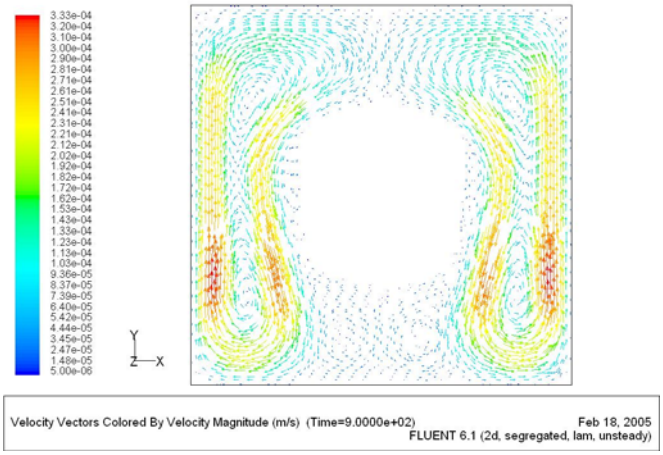

t=15 min

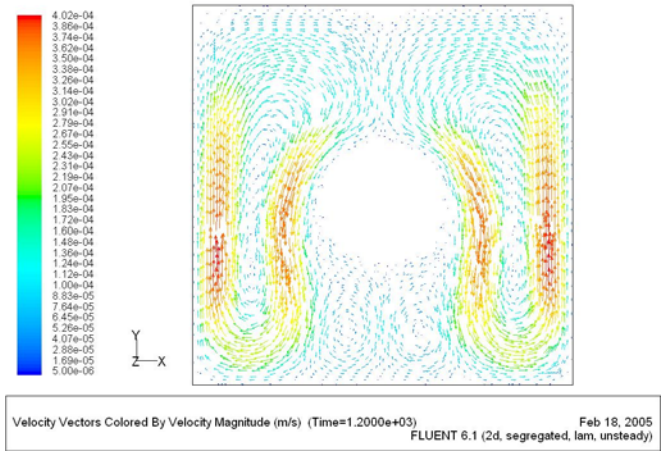

t=20 min

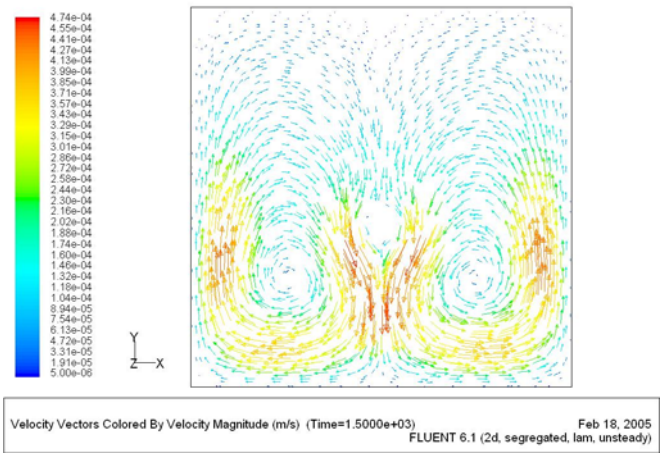

t=25 min

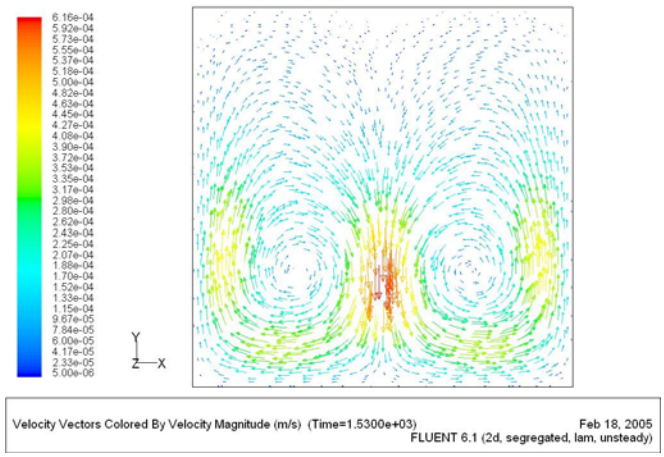

t=25.5 min

Figure 5.1: Velocity vectors at different times for 2x2 cm ice box of 110x110 mesh size. An unstructured (Tri) grid type and a time step size of 1.0 second are used. All walls have the same temperature of 283 K.

melting process progresses. At time lower than 5 minutes, natural convection is mainly from the left and right sides and very little is observed at the top melt layer. As time progresses and the thickness of the top melt layer increases, the natural convection contributes to melting from all sides, especially around the time interval of 15 to 20 minutes. Figure 5.2 shows the melting front at different times for same case.

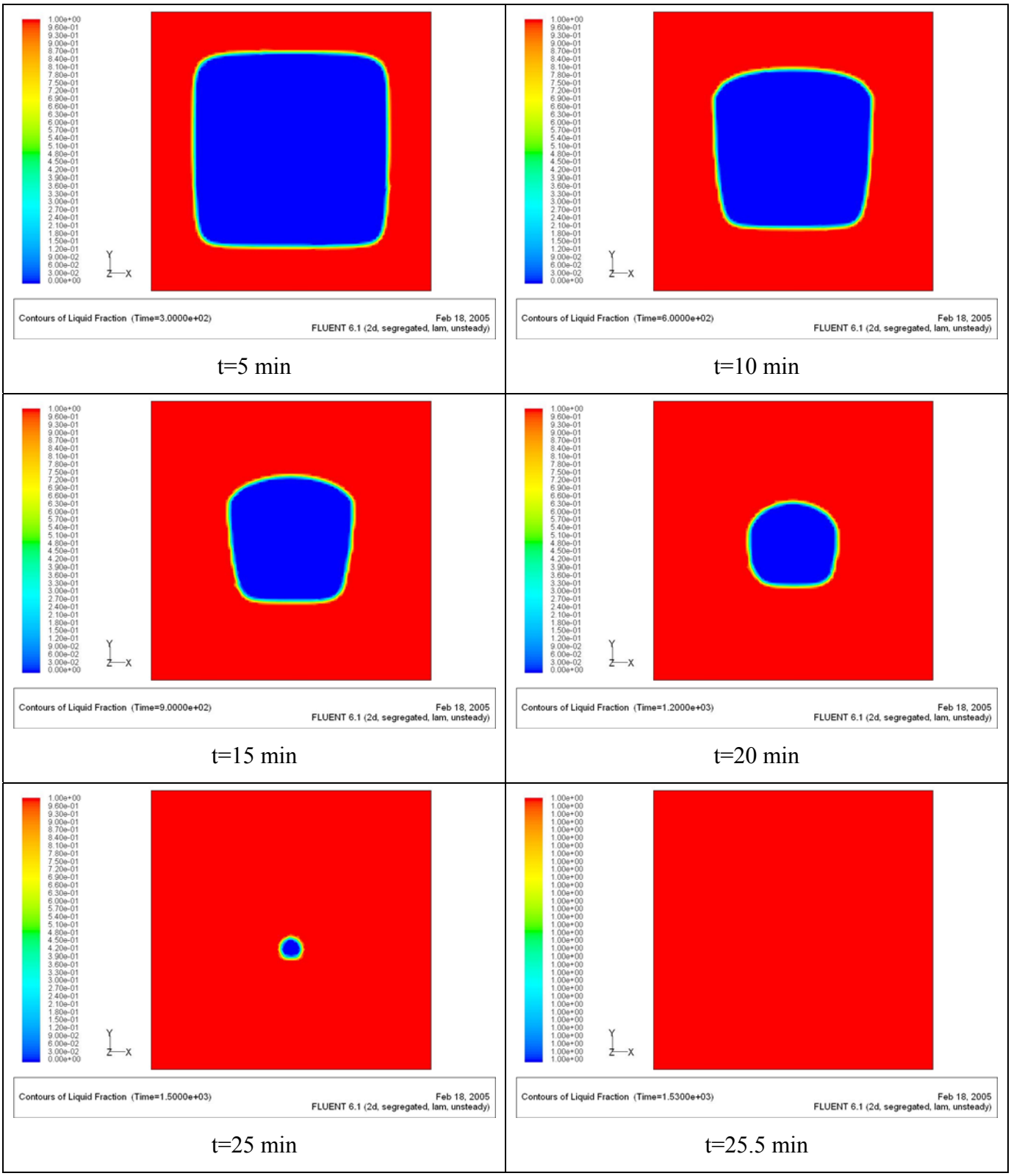

Figure 5.2: Melting front at different times for 2x2 cm ice box of 110x110 mesh size. An unstructured (Tri) grid type and a time step size of 1.0 second are used. All walls have the same temperature of 283K.

5.3 Melting in a Three Dimensional Block

The above melting model was applied to melting in a three dimensional block of ice, 2×2×2 cm. A structured quad mesh of 110×110×110 is used. This means the total number of cells used is 1,331,000 cells. The time step size used was also 1 second. These figures are similar to those used for the two dimensional model. At such a high number of cells, the convergence is very slow. The model took a long time to converge. It was run for a total of 420 seconds.

The run was terminated at this early time, simply because, a conclusion that the current solution method is limited by the large number of cells needed to capture the details even for such a small three dimensional block.

Figure 5.3 shows the three dimensional melting front for melting in this three dimensional block over the first 7 minutes. The front shows that it is symmetric, and as expected, the thickness of the front is highest right at the center of the block which is away from the cold boundary conditions.

Figure 5.4 shows the melting front in a central plane for the same three dimensional ice box. It shows the progression of the melt front with time up to 7 minutes of melting. The same conclusion can be drawn from this figure, which is that melting is fastest in the center away from the sub zero boundary conditions.

Figure 5.5 shows velocity vectors at the same time interval show in the previous figures. The frames are shown in three dimensions. Similar but two dimensional velocity

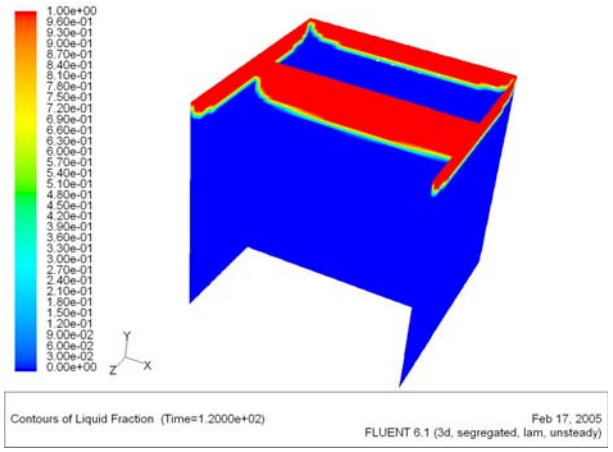

t=2 min

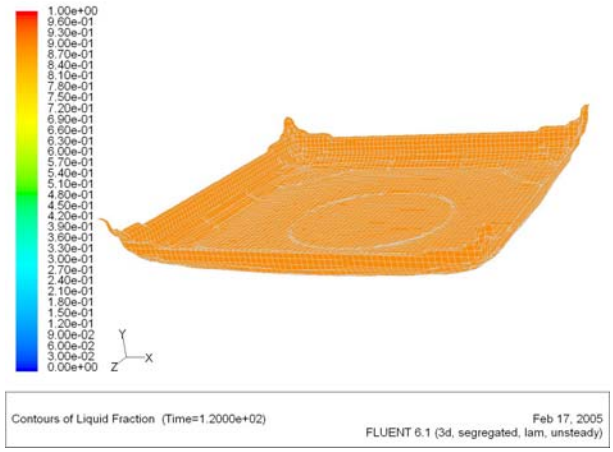

t=2 min

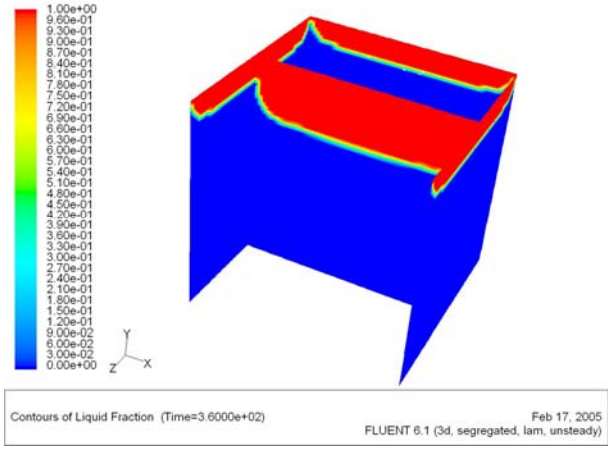

t=4 min

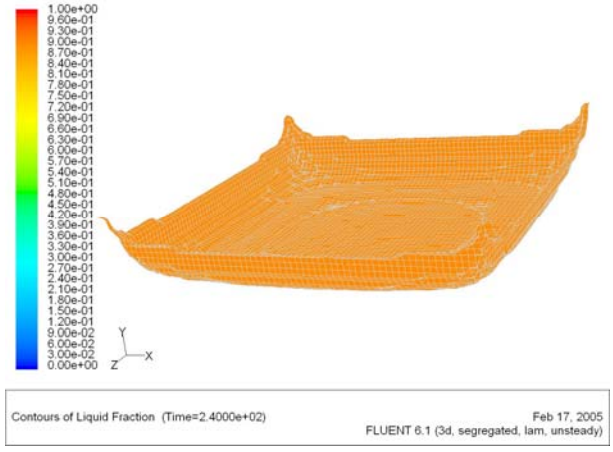

t=4 min

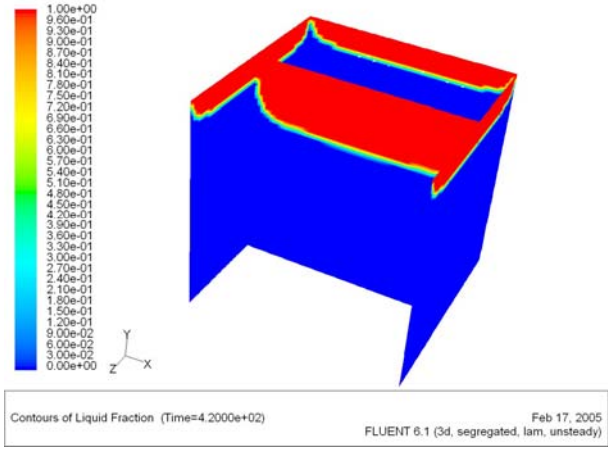

t=7 min

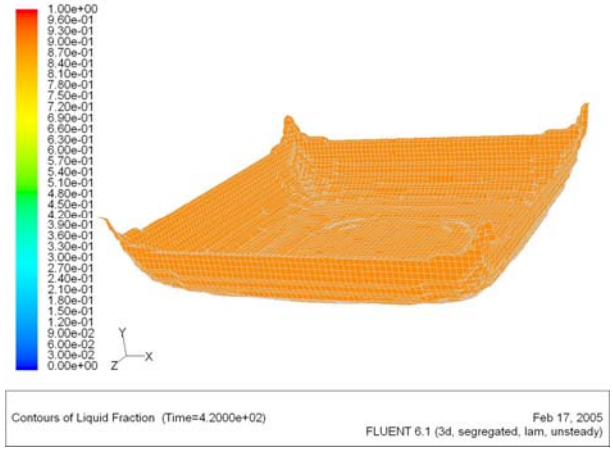

t=7 min

Figure 5.3: Three dimensional melting front at different times for 2x2x 2 cm ice box of 110x110x110 mesh. A structured (Quad) grid type and a time step size of 1.0 second are used.

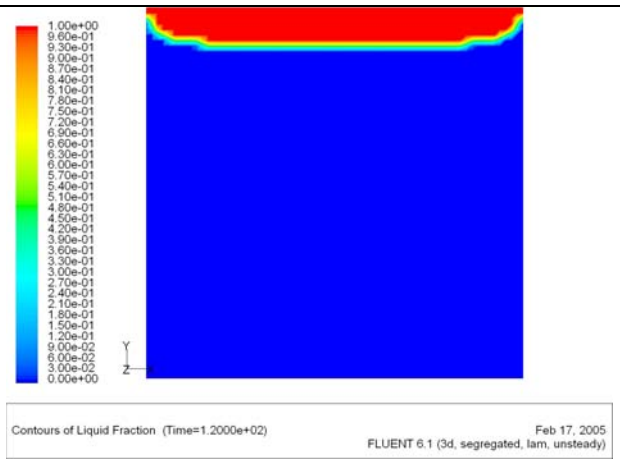

z=0 and t= 2 min.

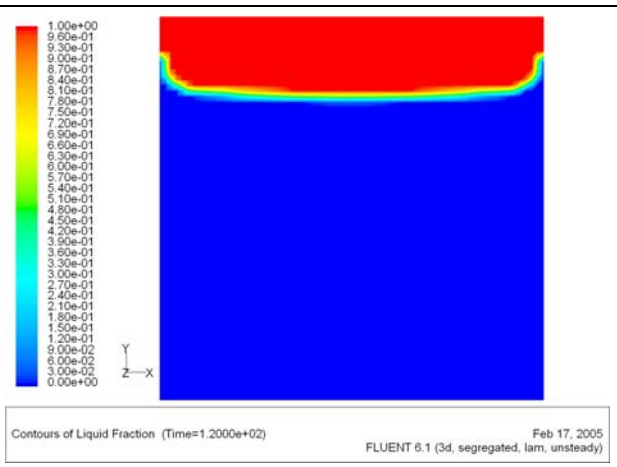

z=1 and t= 2 min.

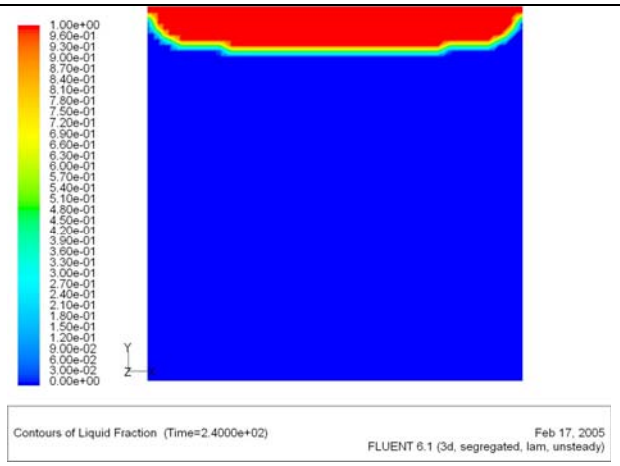

z=0 and t= 4 min.

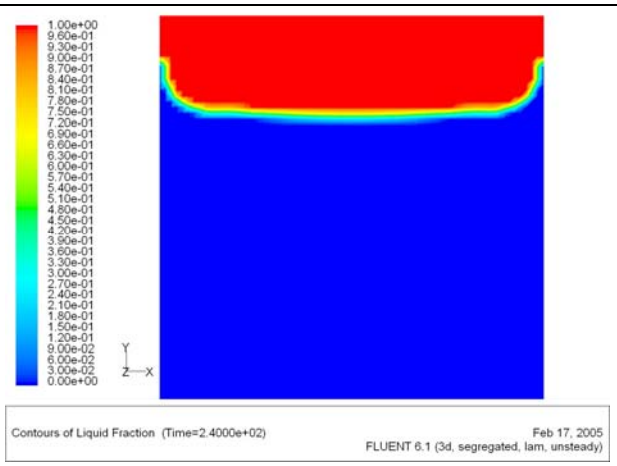

z=1 and t= 4 min.

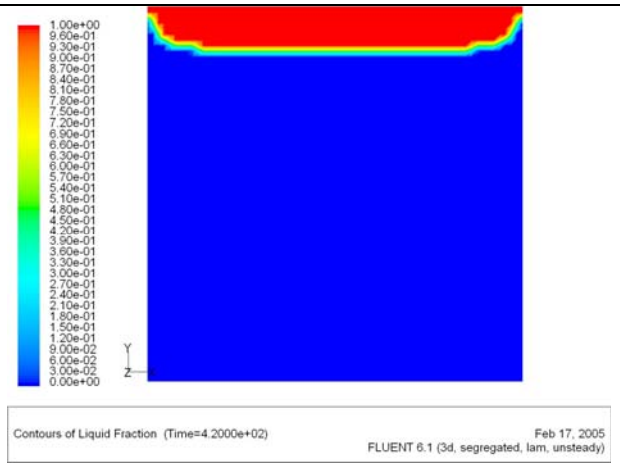

z=0 and t= 7 min.

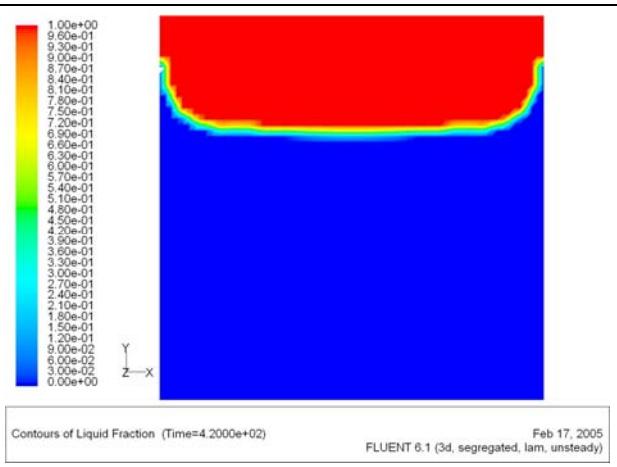

z=1 and t= 7 min.

Figure 5.4: Melting front in a central plane at different times for a 2x2x2 cm ice box of 110x110x110 mesh. A structured (Quad) grid type and a time step size of 1.0 second are used.

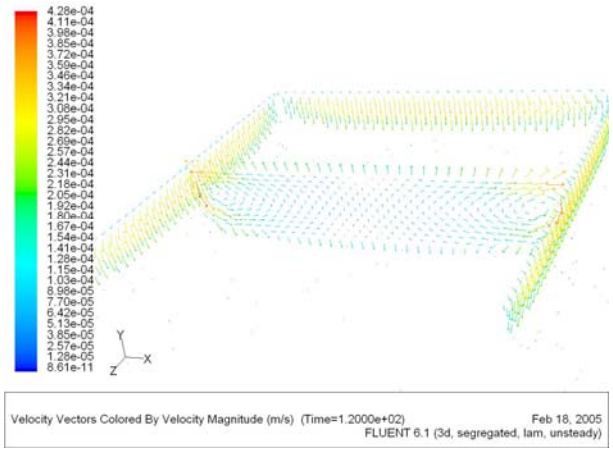

t=2 min

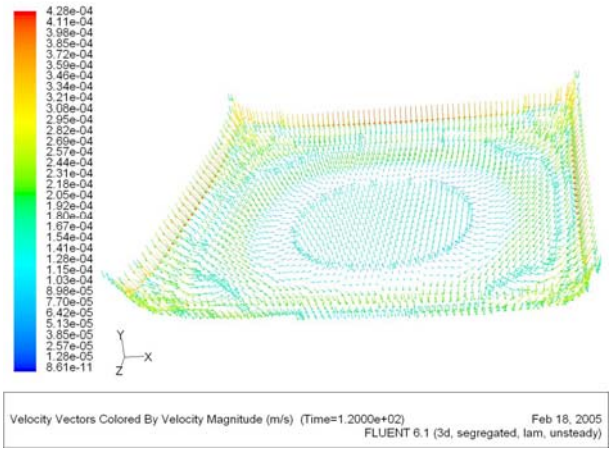

t=2 min

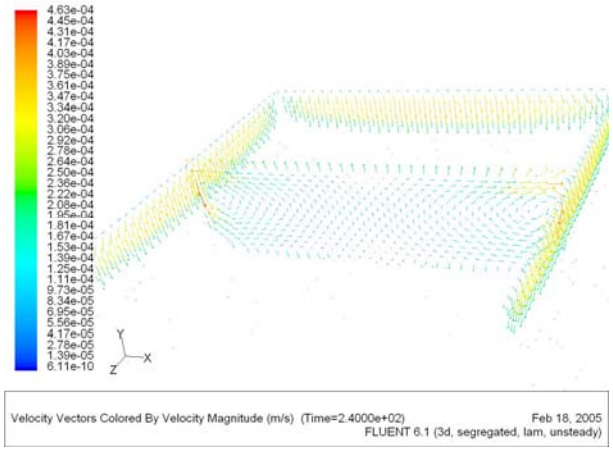

t=4 min

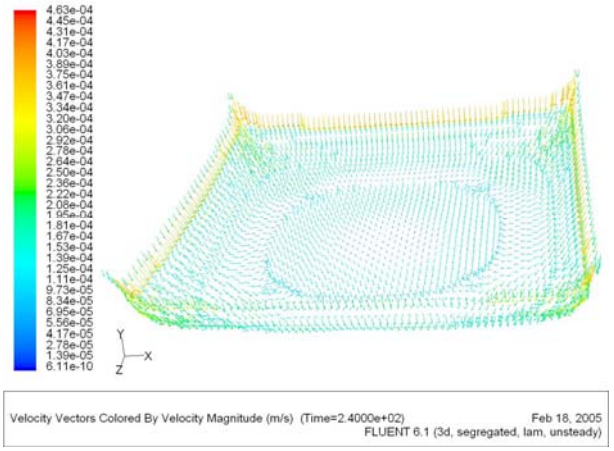

t=4 min

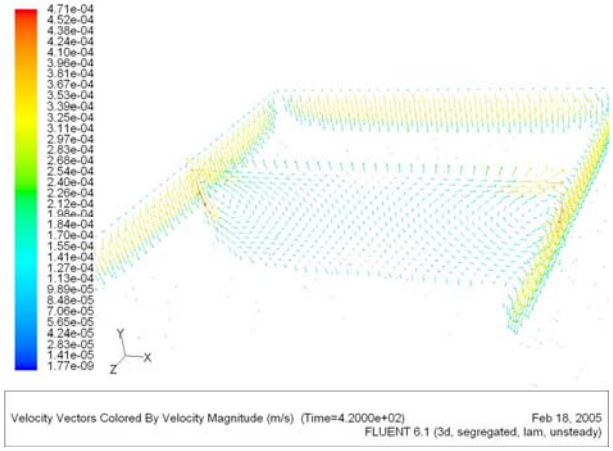

t=7 min

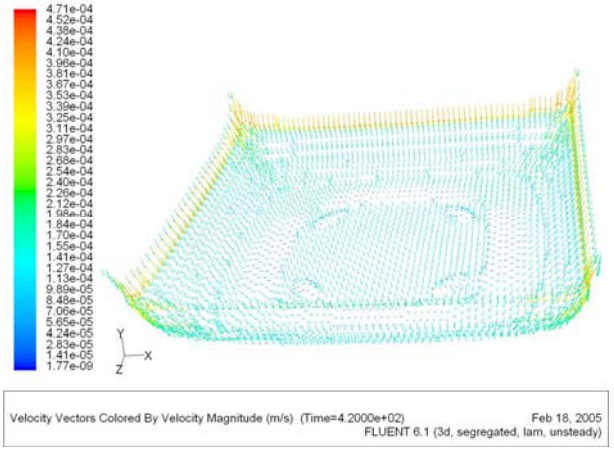

t=7 min

Figure 5.5: Velocity vectors at different times for 2x2x2 cm ice box of 110x110x110 mesh. A structured (Quad) grid type and a time step size of 1.0 second are used. (left) vectors in a central plane and (right) vectors in a melt front surface.

fields are shown in Figure 5.6. These velocity fields show that the velocity magnitude due to natural convection is still low, and consequently, the contribution of natural convection is, up to this stage, rather limited.

5.4 Melting in a 20×20 cm Ice Block

In order to validate the melting model further, melting in a two dimensional 20×20 cm block is now considered. Meshes of 300×300 and 400×400 were used. The progression of the melt front with time for the case with 400x400 mesh size is shown in Figure 5.7. Figure 5.8 shows that the melting rate for both mesh sizes is very similar and close in value. The melting rate is also compared with the melting rate for the 2×2 cm case. The two rates show good agreement.

5.5 Conclusions

Results obtained using the current melting model showed good agreement with the predictions using Solomon (1979) for a 2 by 2 cm block. The melting of a three dimensional body is limited by the available computational resources as the total number of cells used was 1,331,000 cells.

The melting in a 20 by 20 cm block was also investigated. The melting rate over the first two hours was similar to that for the 2 by 2 cm block. These results are also in qualitative agreement with experimental results previously carried out at KFUPM.

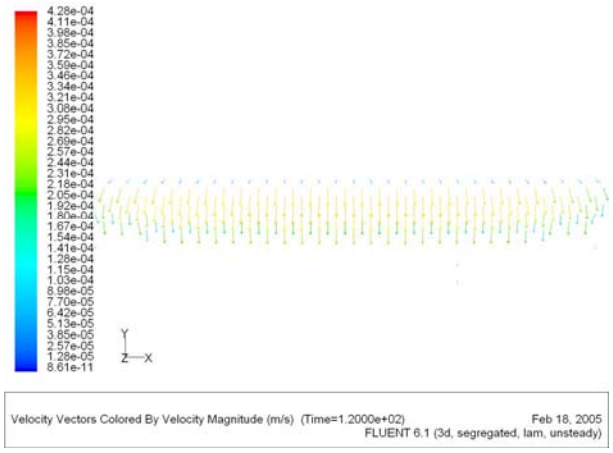

z=0 and t= 2 min.

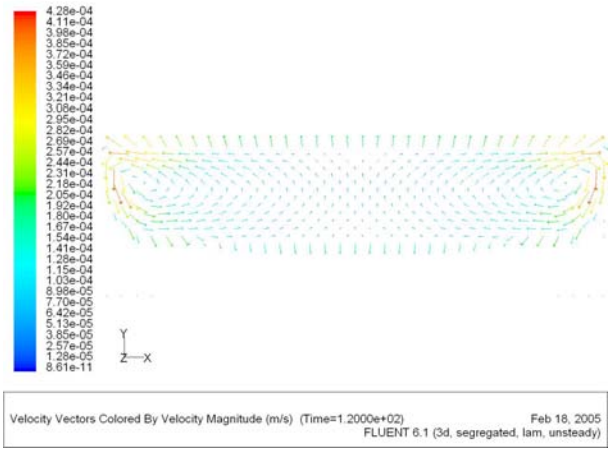

z=1 and t= 2 min.

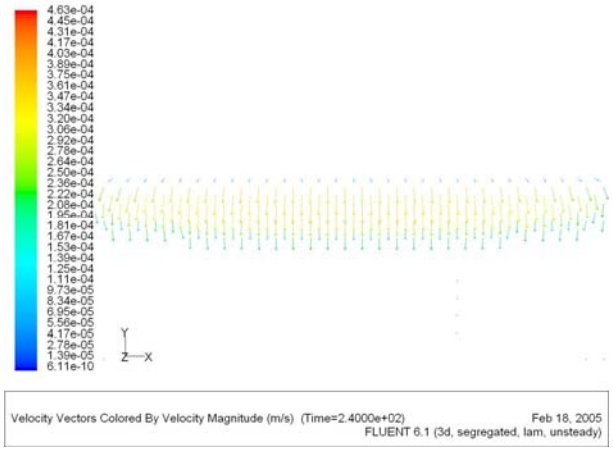

z=0 and t= 4 min.

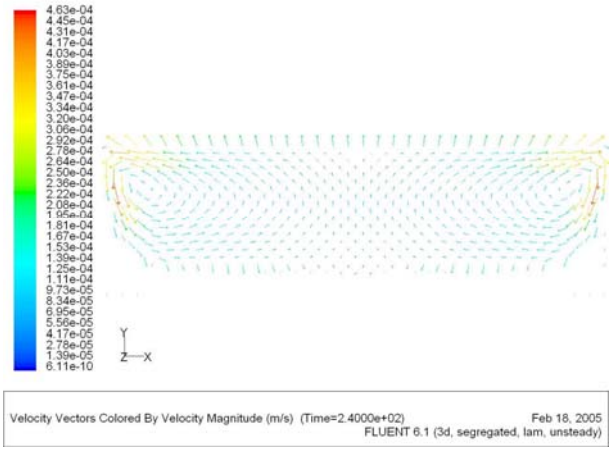

z=1 and t= 4 min.

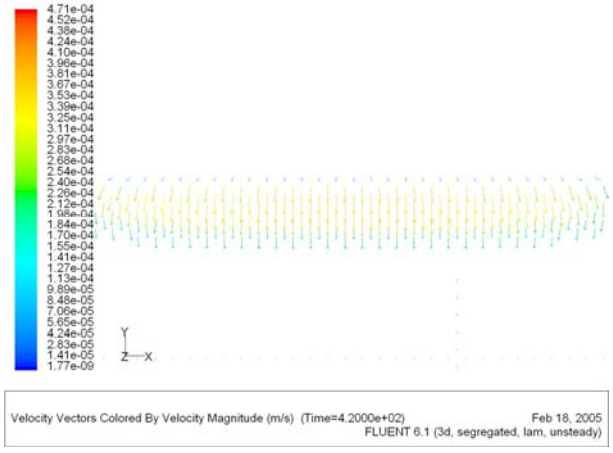

z=0 and t= 7 min.

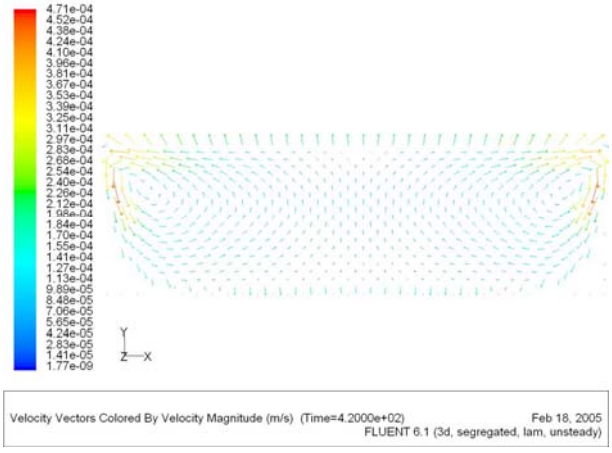

z=1 and t= 7 min.

Figure 5.6: Velocity vectors in a central plane at different times for 2x2x2 cm ice box of 110x110x110 mesh. A structured (Quad) grid type and a time step size of 1.0 second are used.

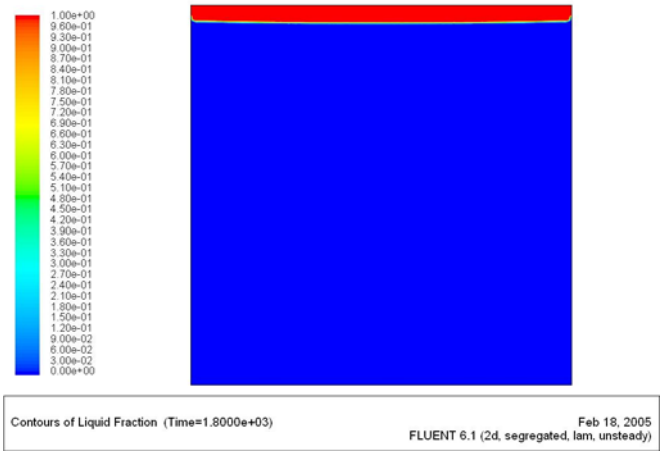

t=30 min

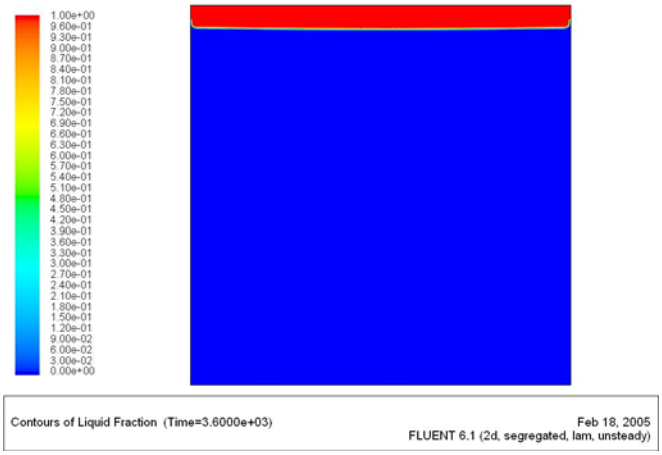

t=60 min

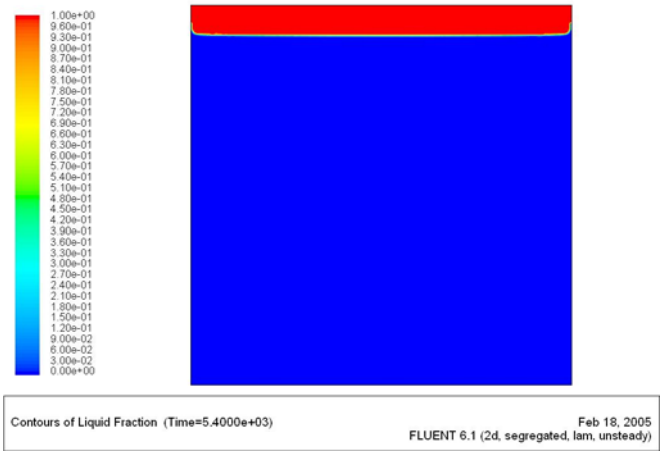

t=90 min

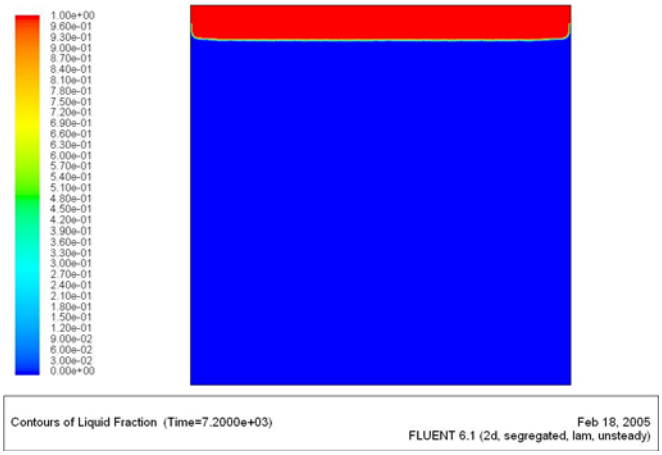

t=120 min

Figure 5.7: Melting front at different times for 20x20 cm ice box of 400x400 mesh size. A structured (Quad) grid type and a time step size of 1.0 second are used.

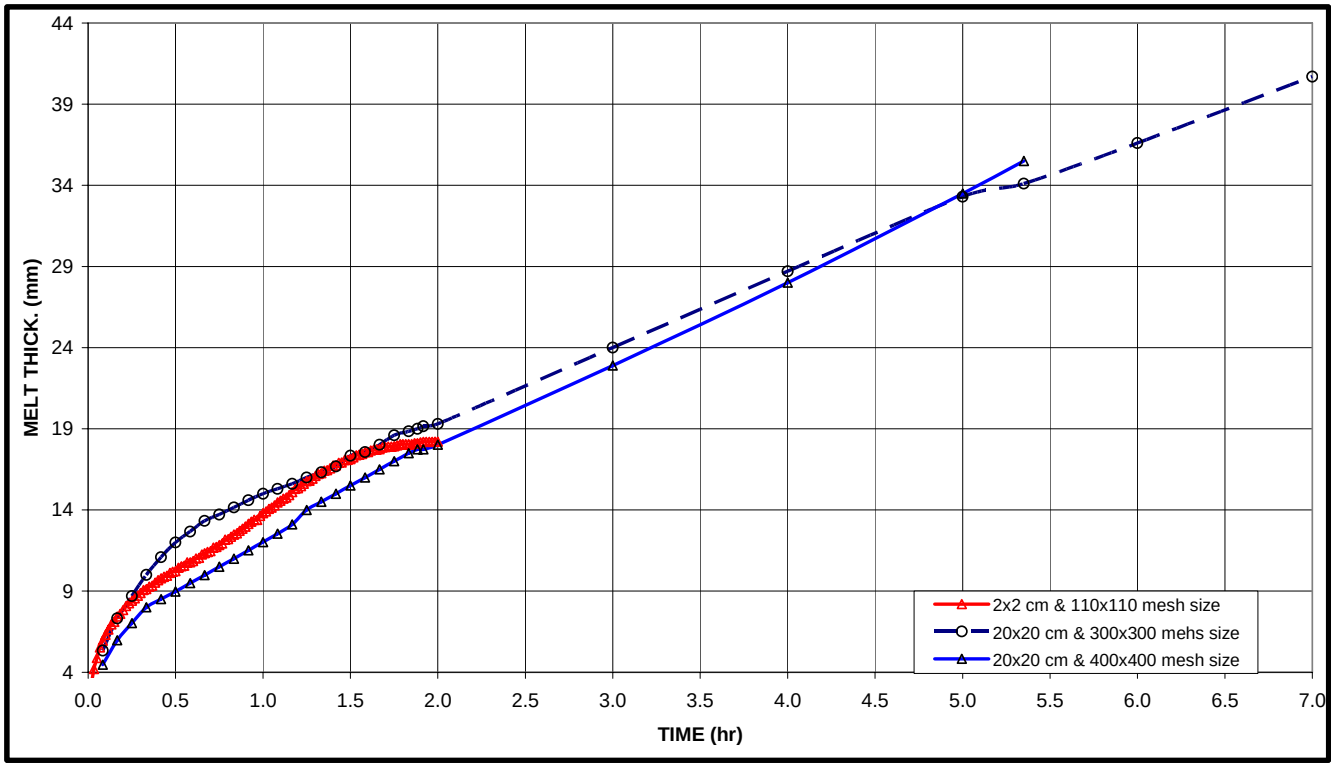

Figure 5.8: Comparison of melting rates for 2x2 cm and 20x20 cm ice block.

Chapter Six

PARAMETRIC RUNS OF MELTING IN A TWO-DIMENSIONAL ICE BOX

6.1 Introduction

In the chapter four, melting in a two-dimensional enclosure was simulated. The model was tested for independence of the grid type and size, the time step size, and the difference between solidus and liquidus temperatures. In this chapter, a number of parametric runs is carried out to investigate the effects of geometry, extent of the heated area, initial temperature and various values of wall temperatures.

6.2 Effects of Heated Area on Melting in Two-Dimensional Enclosures

In the previous runs the full top surface of the enclosure was set at a higher temperature. In certain applications, that may not be always the case. Only a part of the wall may be heated. In order to investigate the effect of the heated area on the rate of melting and the shape of the melted volume, a number of runs are carried out with a reduced heated area.

6.2.1 Melting with Half of the Top Surface Heated

In this section and the next section three cases are considered. In the first one (case 1), one half of the top surface is heated. In the second case (case 2), one half of the top surface is heated also but this hot section is placed in the center of the top face. In the third case (case 3) which will be discussed in the next section, one quarter of the top face

is heated. These three cases are shown in Figure 6.1. The boundary conditions, namely the temperatures at which the walls were kept are also shown in Figure 6.1. Figure 6.2 shows the melt front for case 1 at selected times. Figure 6.3 shows the velocity fields in the melt zones at the same selected times.

Figure 6.2 shows how the melt zone spreads not only vertically but also laterally especially away from the cold boundary set at the left wall. The melt zone becomes almost centralized 120 minutes after the start of the melting process. Figure 6.3 shows an asymmetry in the flow patterns. It should be noted that the flow patterns shown in the chapter four where the full top surface was heated were symmetrical. Figure 6.3 also shows that the flow patterns at the lower half of the melt zone 120 minutes after the start becomes rather symmetrical. However, the asymmetry continues at the top half of the melt zone due to the asymmetric boundary conditions.

Figure 6.4 shows a plot of the melt thickness versus time for this case compared with the case where the full top face was heated. It can be observed that the melting rate (mm/s) for both cases show a similar trend although the melting rate for the case where half the top surface was heated is significantly lower than when the full top surface was heated. It took 87 minutes to melt 17 mm when the full surface was heated compared to 145 minutes when only half the surface was heated. This percentage reduction in the melting rate is not the same as the percentage reduction of the heated area.

Figures 6.5-6.7 show similar plots for a case where a central half of the top surface is heated. A small change in boundary conditions between this case and the previous

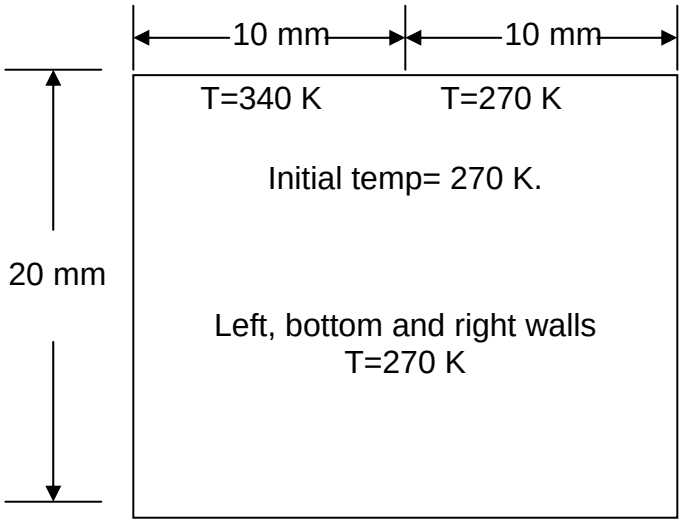

Figure 6.1a: A schematic diagram of the case where only half of the top (left side) surface is heated.

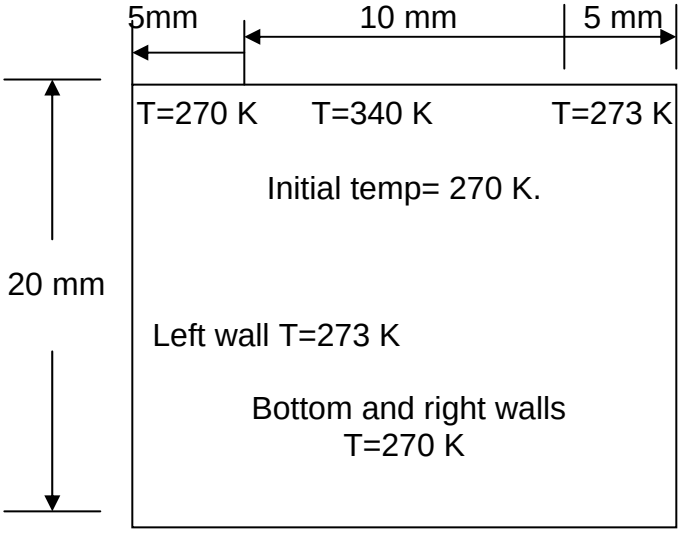

Figure 6.1b: A schematic diagram of the case where only half of the top (center) surface is heated.

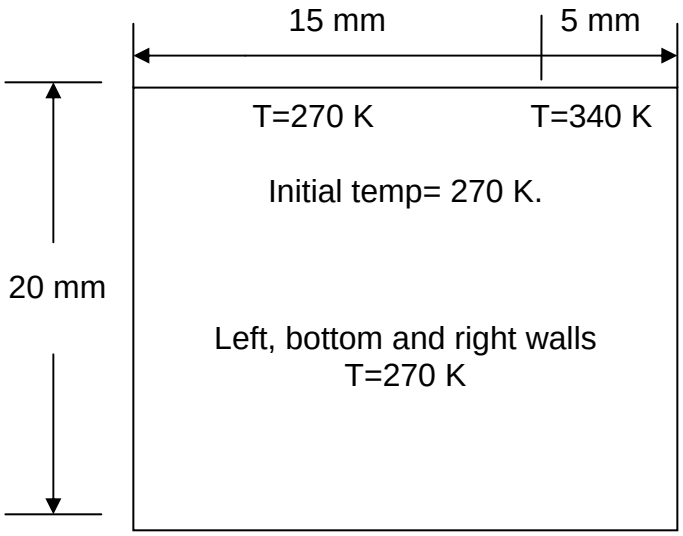

Figure 6.1c: A schematic diagram of the case where only a quarter of the top surface is heated.

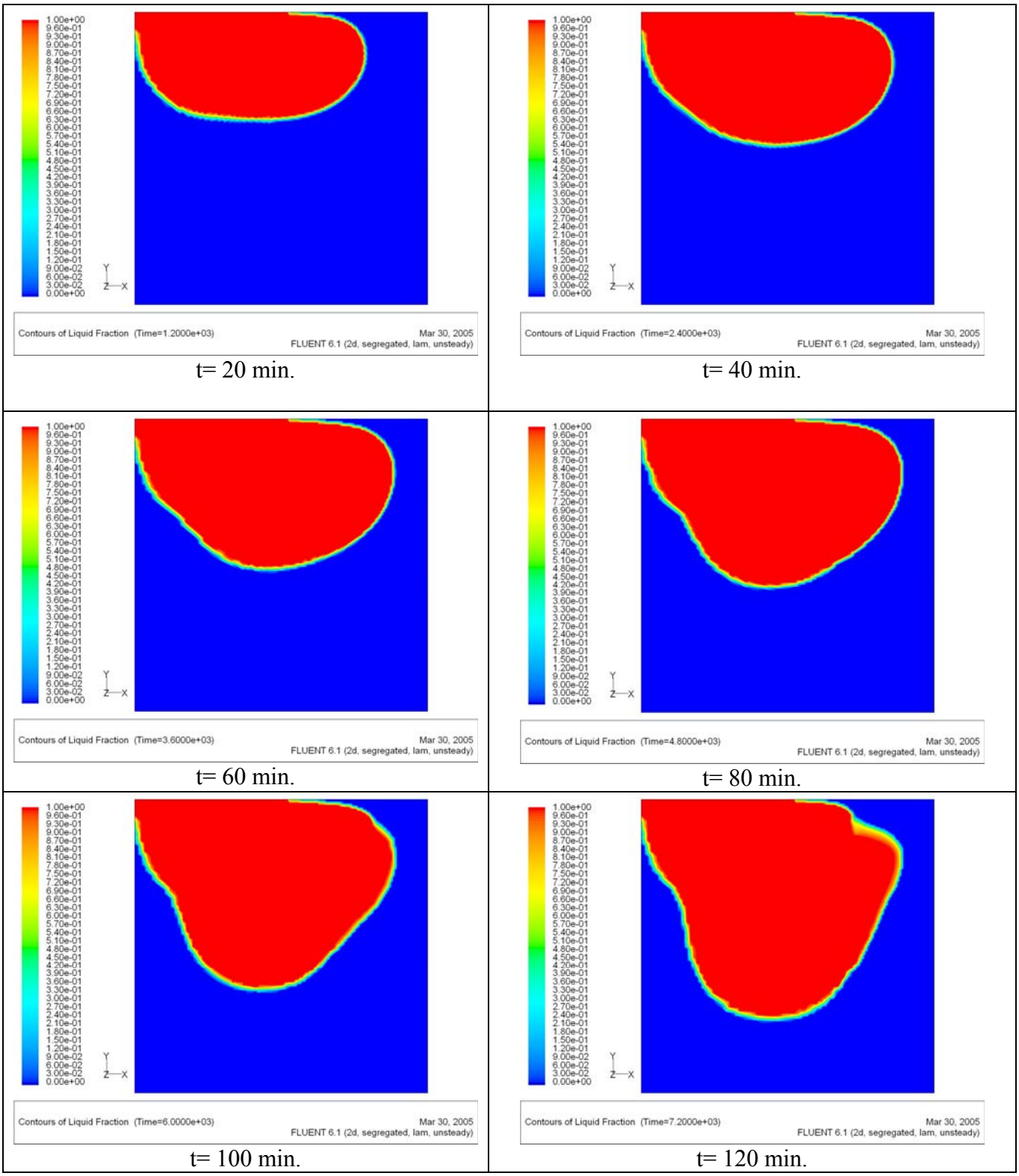

Figure 6.2a: The melt front for a 2×2 cm block with the half of the top surface heated at t= 20 min., 40min., 60 min., 80 min., 100 min. and 120 min.

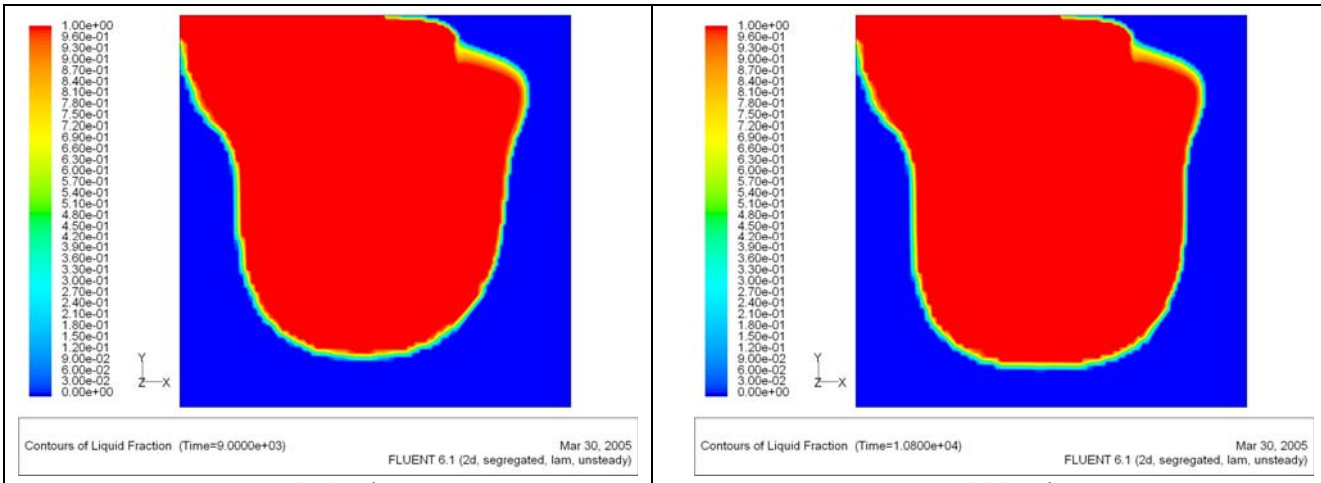

t= 150 min. t= 180 min.

Figure 6.2b: The melt front for a 2×2 cm block with the half of the top surface heated at t= 150 min and 180 min.

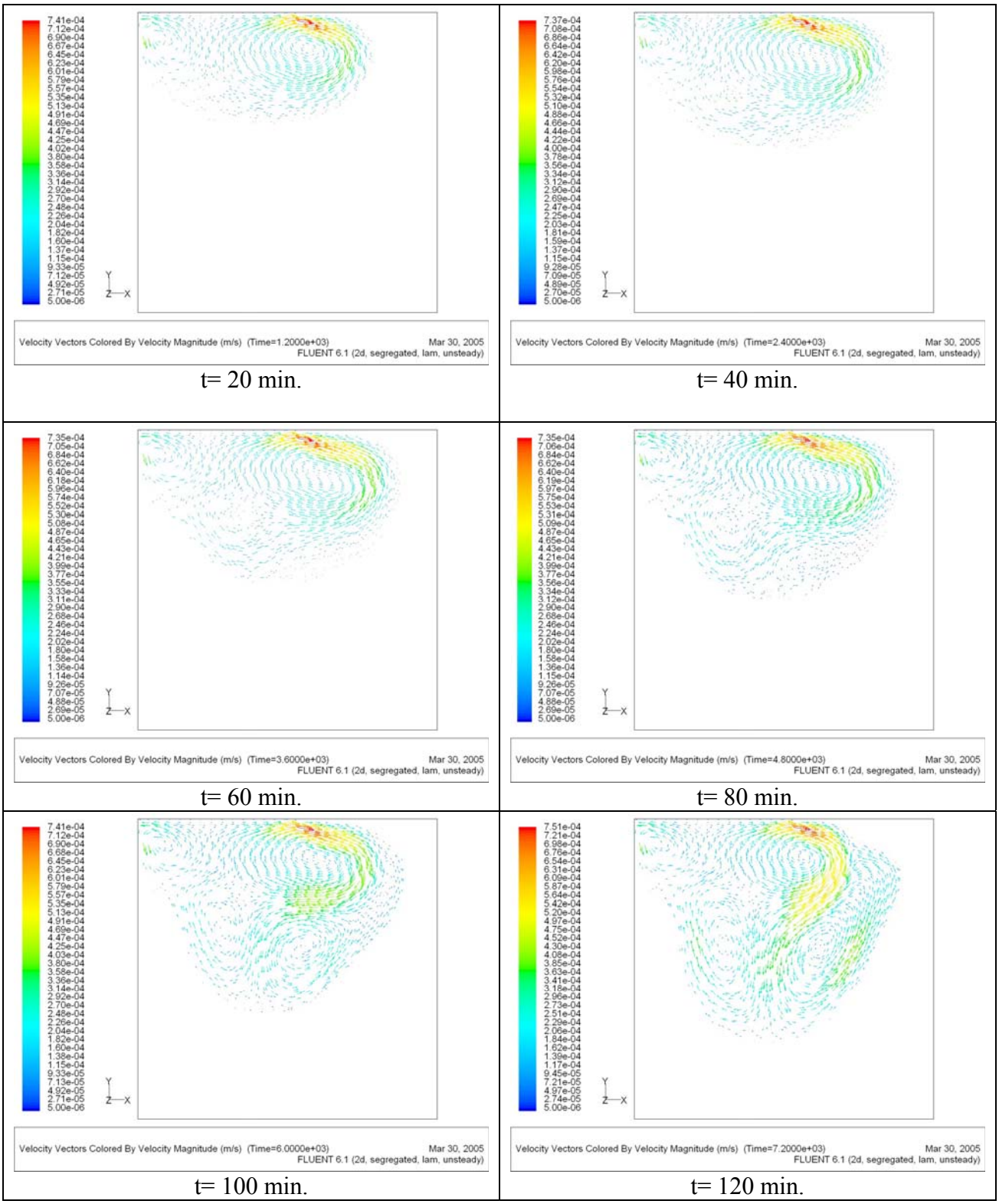

Figure 6.3a: The velocity field for a 2×2 cm block with the half of the top surface heated at t= 20 min., 40min., 60 min., 80 min., 100 min. and 120 min.

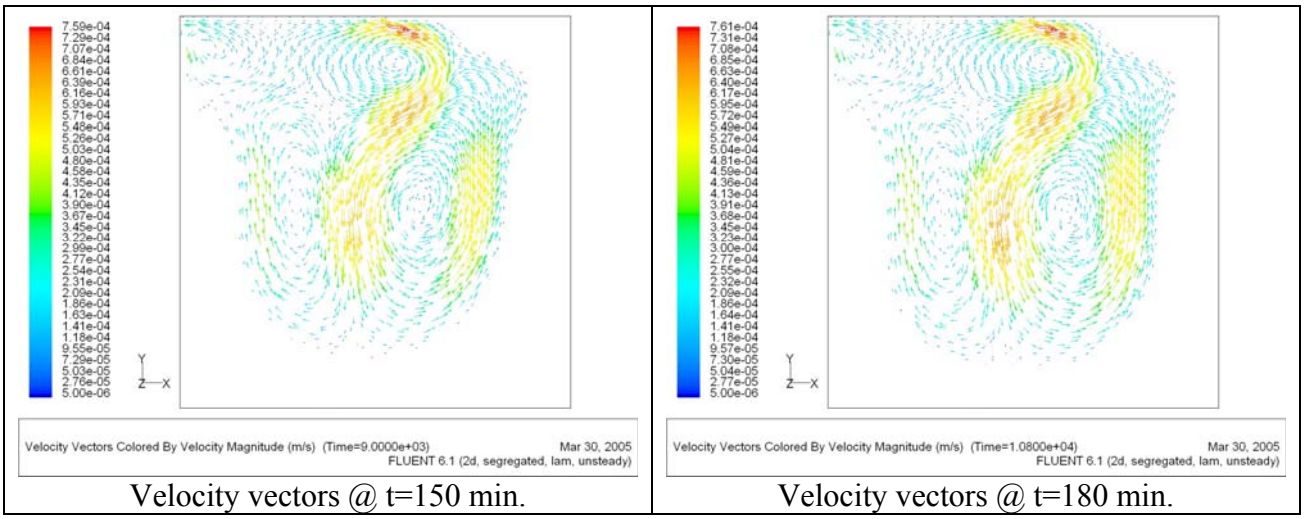

Velocity vectors @ t=150 min. | Velocity vectors @ t=180 min.

Figure 6.3b: The velocity field for a 2×2 cm block with the half of the top surface heated at t= 150 min. and 180 min.

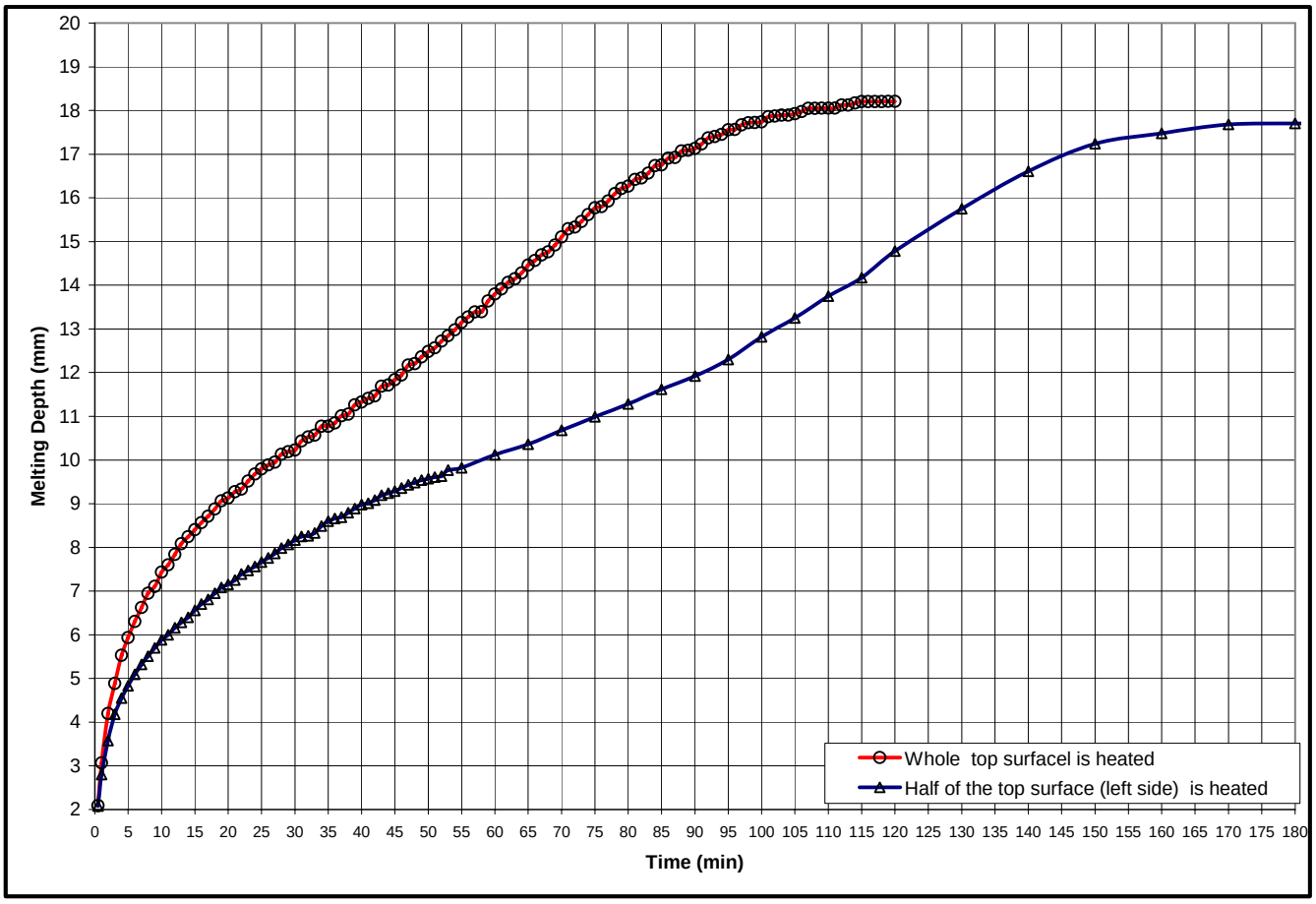

Figure 6.4: The melt thickness versus time for a 2×2 cm block for a case where half of the top surface heated and for a case where the whole top surface is heated.

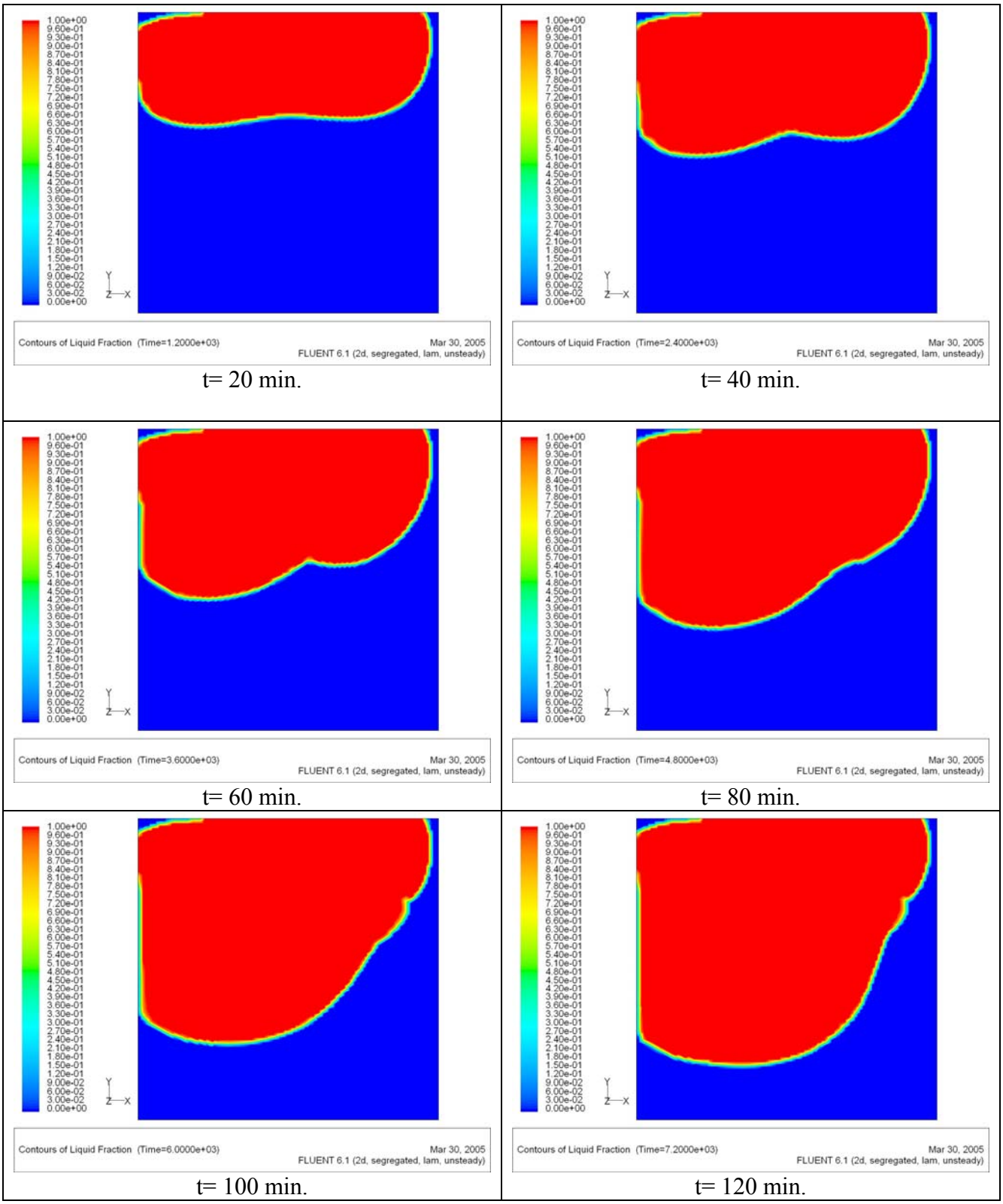

Figure 6.5a: The melt front for a 2×2 cm block with a central half of the top surface heated at t= 20 min, 40 min, 60 min, 80 min, 100 min, and 120 min.

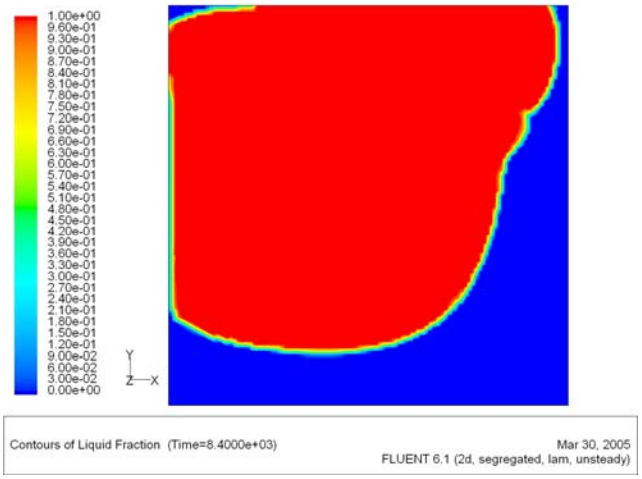

t= 140 min.

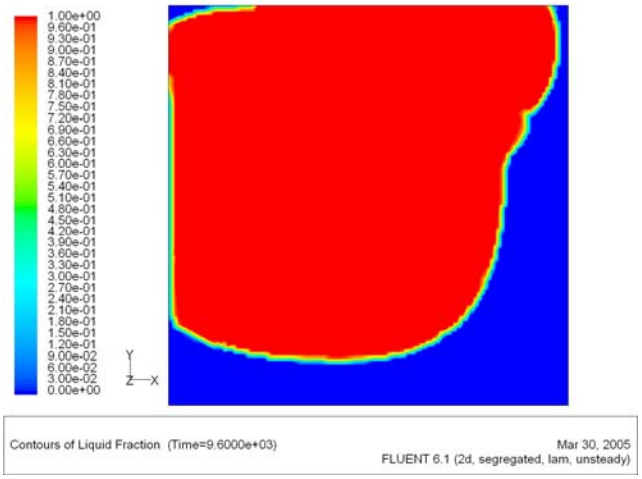

t= 160 min.

Figure 6.5b: The melt front for a 2×2 cm block with a central half of the top surface heated at t= 140min and 160 min.

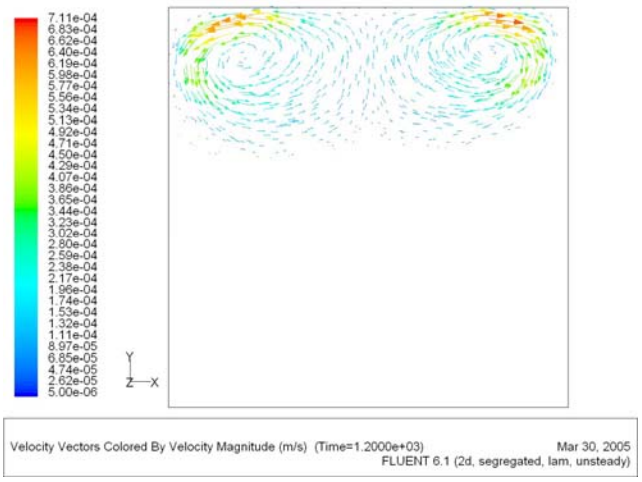

t= 20 min.

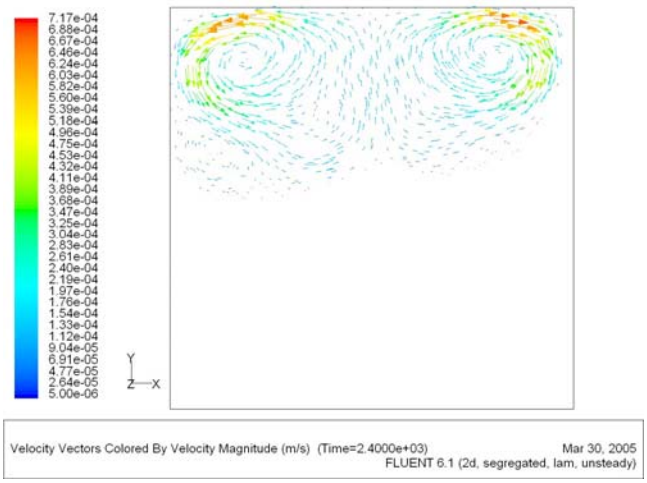

t= 40 min.

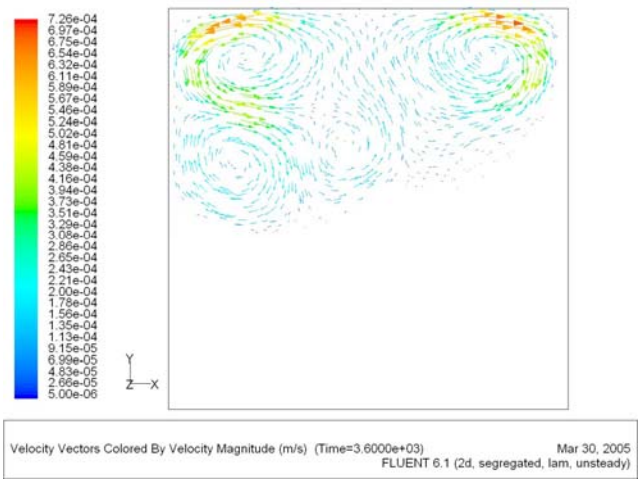

t= 60 min.

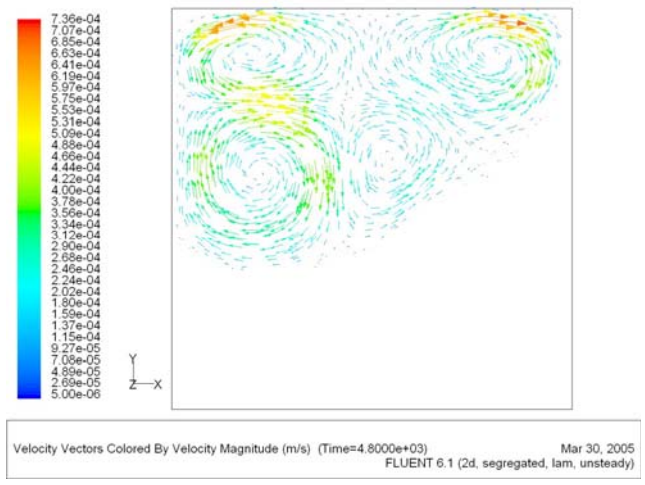

t= 80 min.

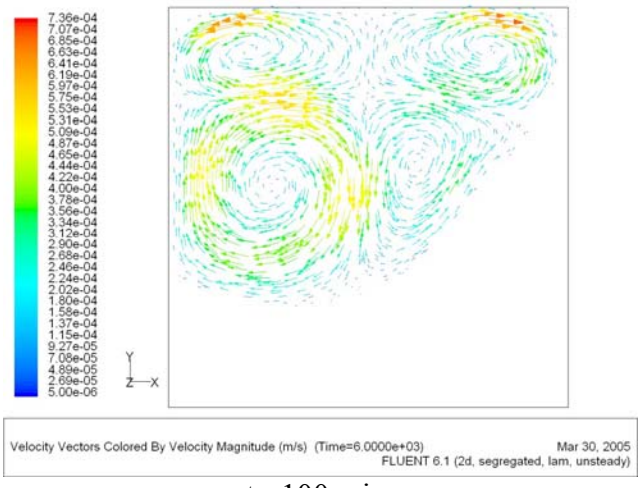

t= 100 min.

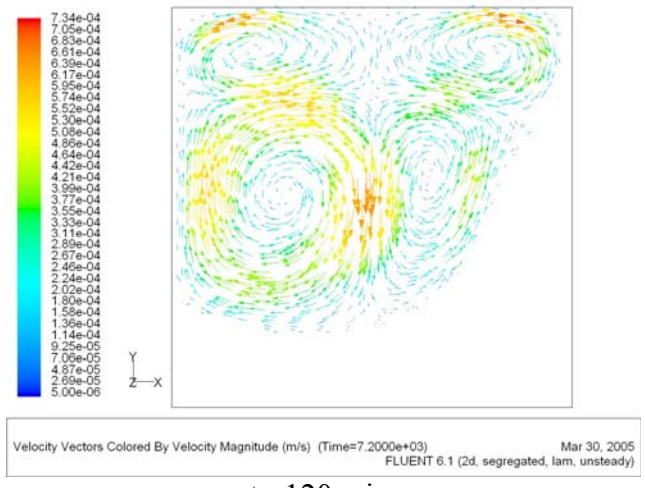

t= 120 min.

Figure 6.6a: The velocity field for a 2×2 cm block with a central half of the top surface heated at t= 20 min, 40 min, 60 min, 80 min, 100 min, and 120 min.

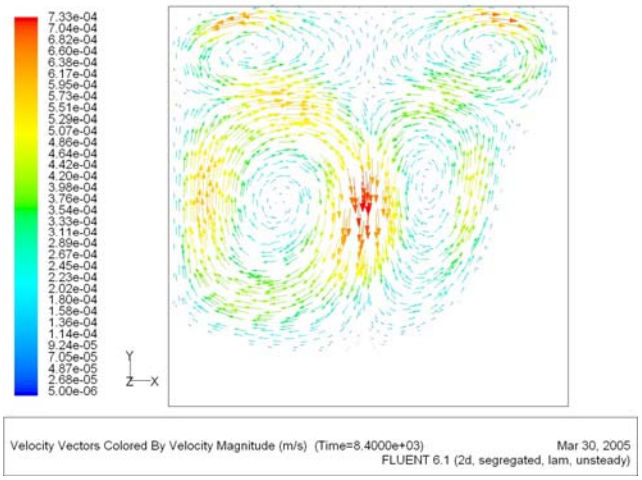

t= 140 min.

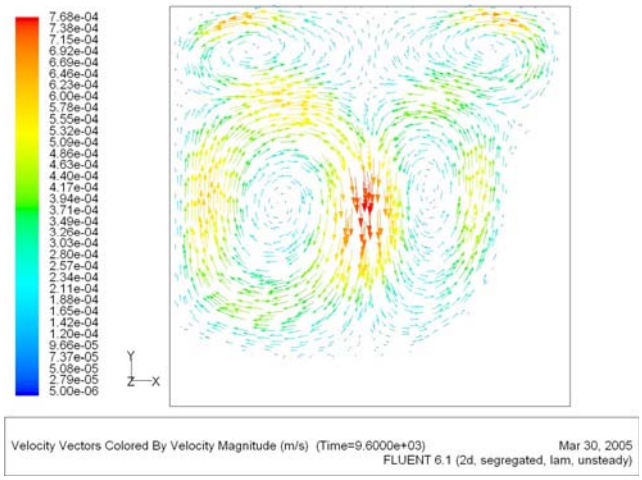

t= 160 min.

Figure 6.6b: The velocity field for a 2×2 cm block with a central half of the top surface heated at t= 140 min. and 160 min.

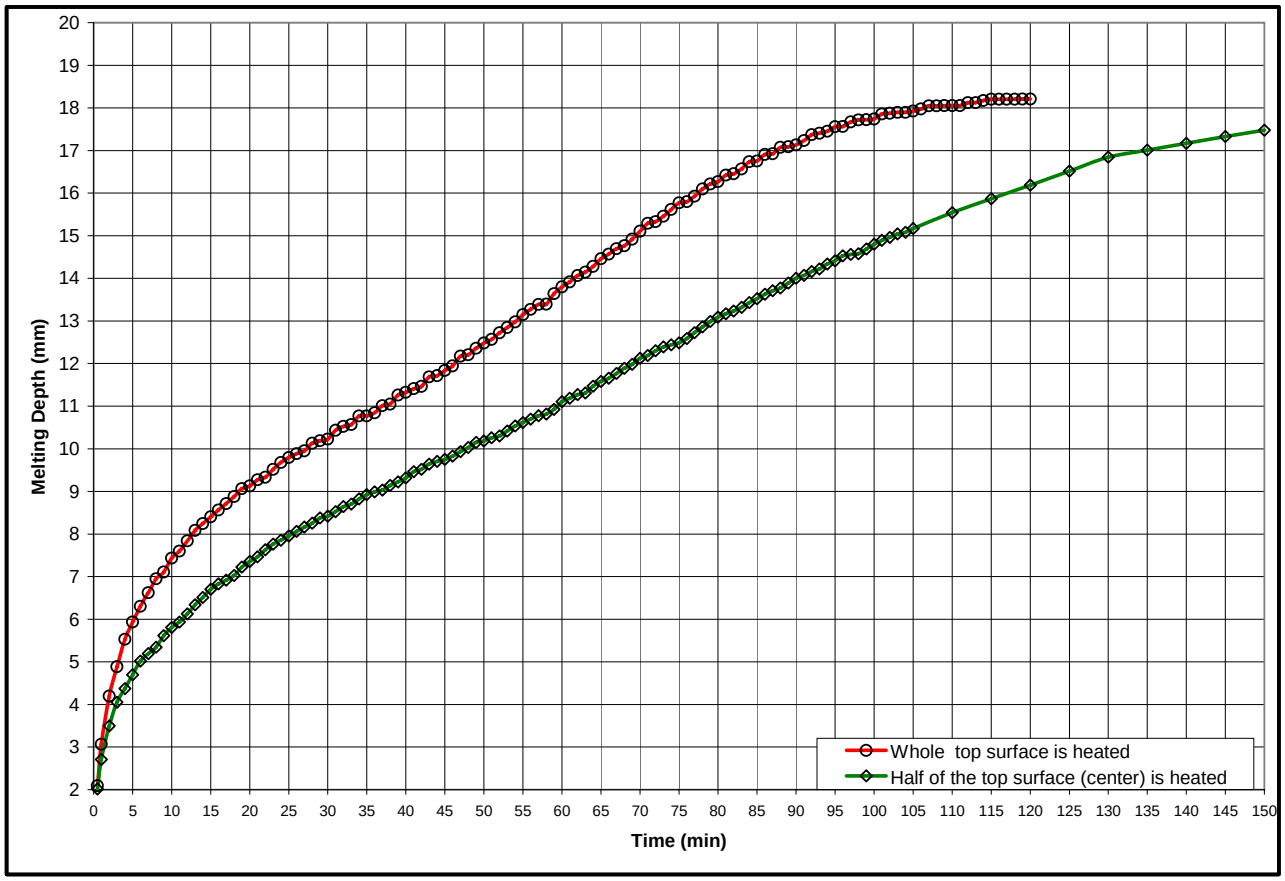

Figure 6.7: A comparison of the melt thickness versus time for cases with half the top surface heated and a case with the full top surface heated.

cases must be noted. The temperature of the left wall and the right quarter of the top surface were set in this case to 273 K and not 270 K as before. This slight difference in the boundary conditions created an asymmetry which is clearly reflected

in the melting process. The degree of asymmetry grew significantly with time as can be seen from Figure 6.5. This asymmetry is also reflected in the flow profiles shown in Figure 6.6. The melting rate for this case was marginally faster than when the left half of the top surface was heated. It took 133 minutes for the melting front to reach 17 mm. This compares with 145 minutes for the case where the top left half was heated. This is according to expectations because heat is better transferred from a central half due to its increased distance from the cold boundaries.

6.2.2 Melting with Quarter of the Top Surface Heated

Figures 6.8-6.10 show the results for a case where only one quarter of the top surface is heated. Figure 6.8 shows similar features to those discussed for the case where half the top surface was heated, especially with the shifting of the melt zone towards the center and away from the cold boundaries. Figure 6.9 shows the velocity profiles at different times of the melting process. The asymmetry during the early stages can be seen clearly.

Figure 6.10 shows a plot of the melt thickness versus time for all the above three cases in addition to that where the whole of the top surface is heated. It is clear that the melting rate for the case where only one quarter of the top surface is heated is much

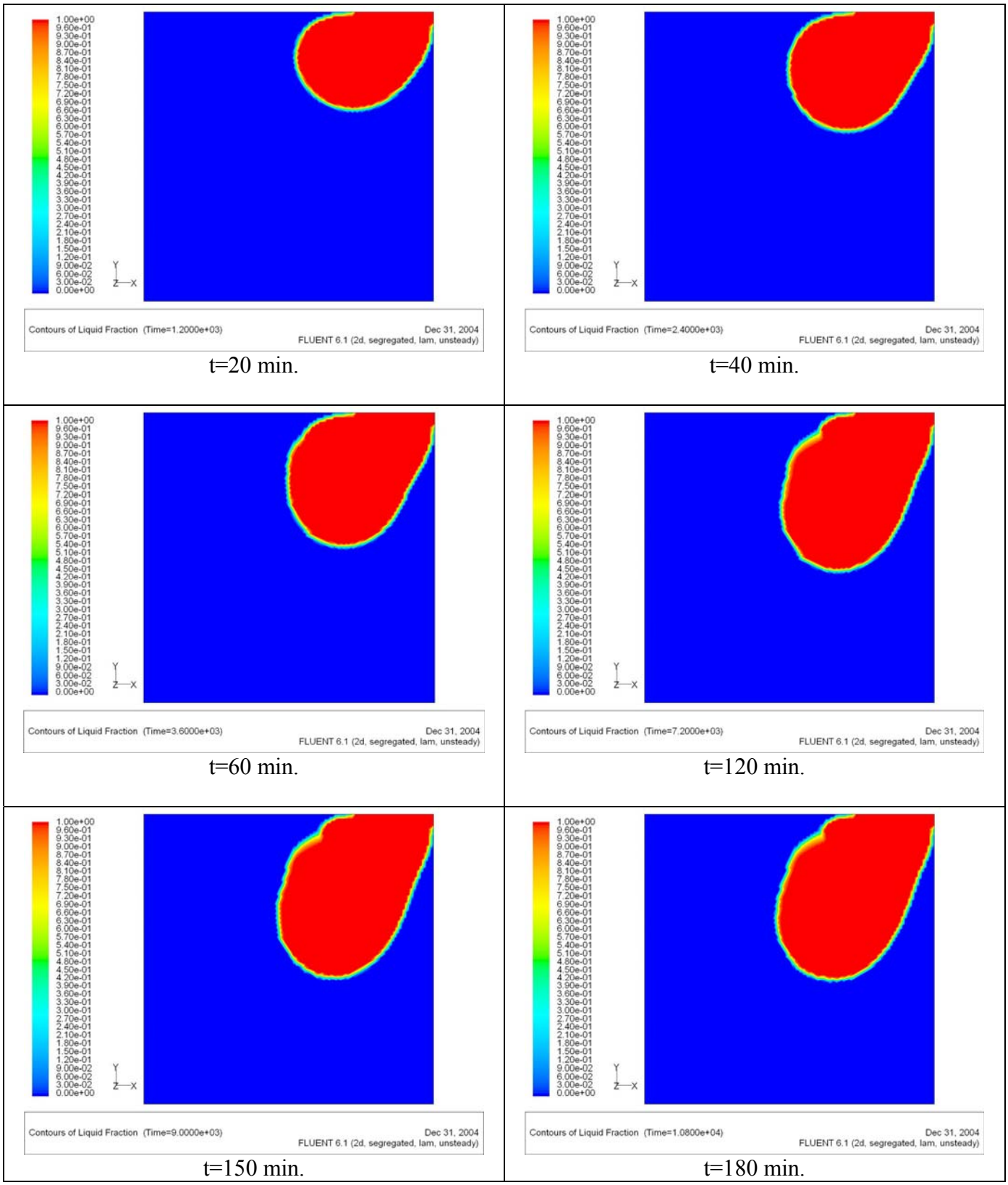

Figure 6.8: The melt front for a 2×2 cm block with a quarter of the top surface heated at melting times equal to 20, 40, 60, 120, 150 and 180 minutes.

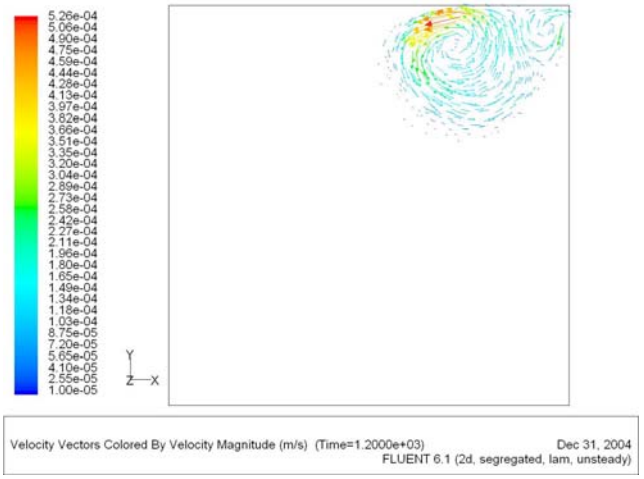

t=20 min.

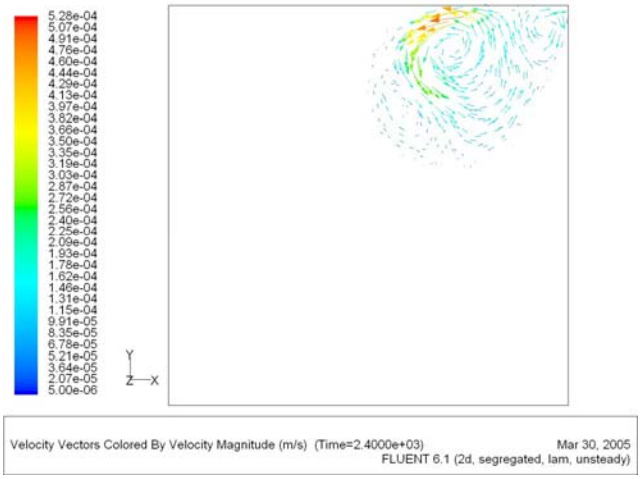

t=40 min.

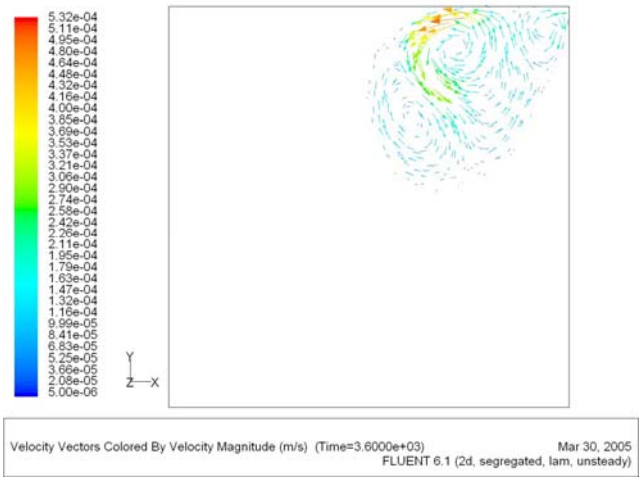

t=60 min.

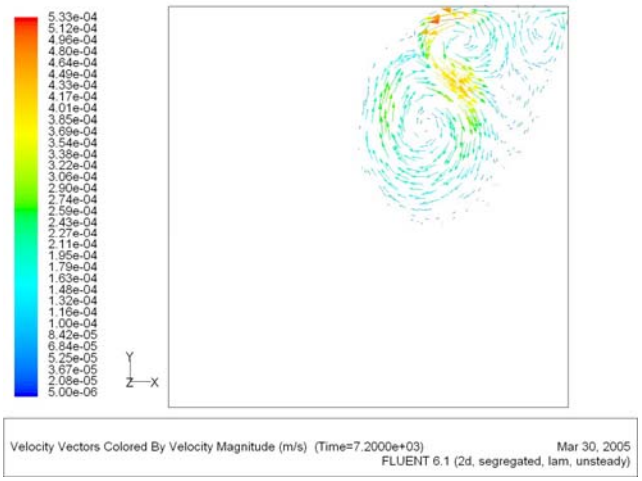

t=120 min.

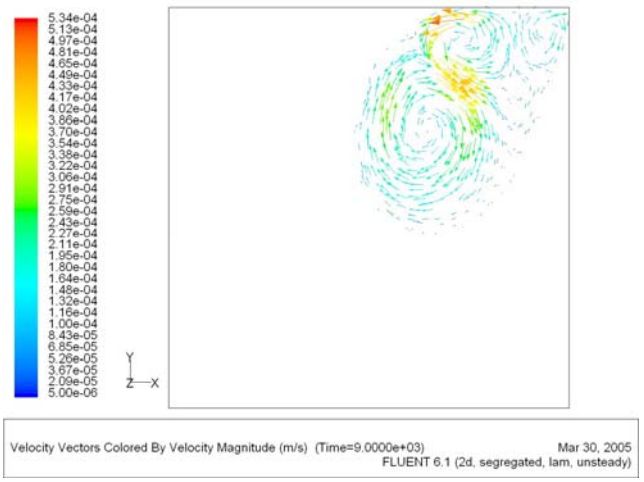

t=150 min.

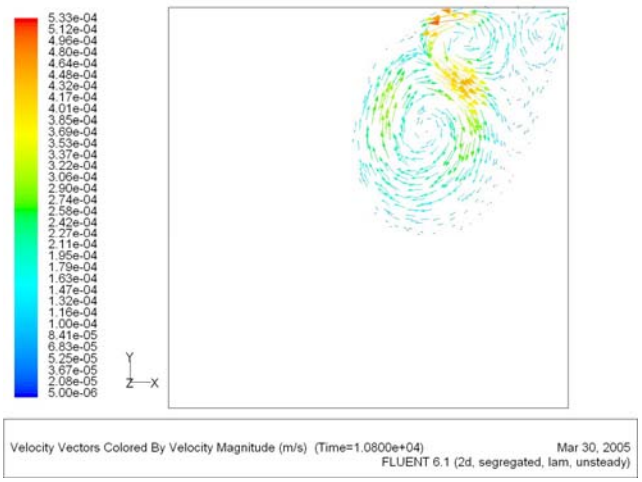

t=180 min.

Figure 6.9: The velocity filed for a 2×2 cm block with a quarter of the top surface heated at melting times equal to 20, 40, 60, 120, 150 and 180 minutes.

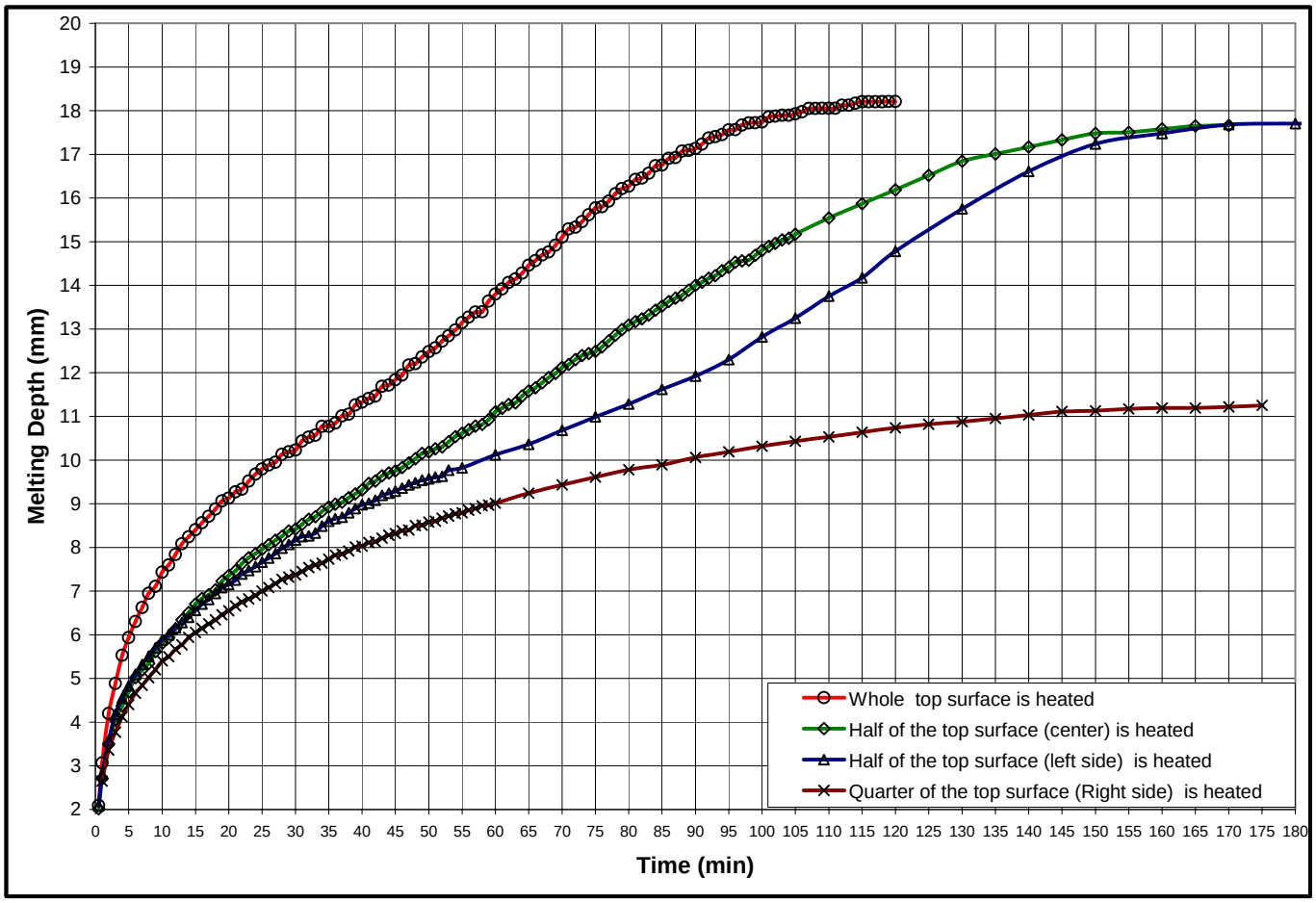

Figure 6.10: A comparison of the melt thickness versus time of a case with full top surface heated and three case with a part of the top surface only heated.

slower that the other cases with full tope surface heated and half of the top surface heated.

6.3 Melting in a Circular Enclosure

Melting is sometimes required to de-freeze pipelines, especially in countries with cold climates. To study the melting of ice in a cylindrical geometry, a two-dimensional circular model is constructed as shown in Figure 6.11. The diameter of the circle is 2 cm. An unstructured triangular mesh is used to discretize the domain. A total number of 26038 cells were used. Based on the grid independence test that was done in the previous chapter, this number of cells corresponds to a mesh size of about 0.02 cm.

Figures 6.12-6.14 show the results for a case where a quarter (top) of a circle geometry is heated. Figures 6.12-6.13 show similar features to those discussed in section 4.7 and Figures 4.14-4.15 for a square geometry with the full top surface heated.

Figure 6.12 shows the melting front at 10, 20, 30, 40, 50, 60, 70 and 80 minutes. Generally, the shape and size of the melting zone are similar to those of the square geometry. Figure 6.13 shows the velocity vectors at the same time intervals as above. The flow patterns due to natural convection are also similar to those discussed in section 4.7.

Figure 6.14 shows a comparison of the melting rate for a circle and a square geometries. It is clear that the melting rate for a circle geometry is slightly higher than that of square geometry. Although the area of a circle is less than the area of a square by

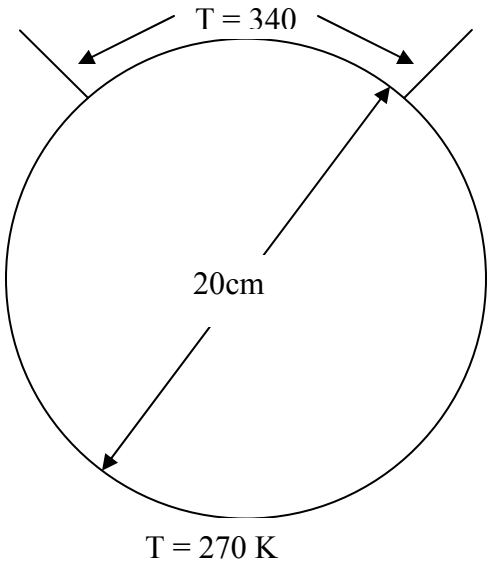

Figure 6.11: A schematic diagram for a 2 cm diameter pipe with half of the tope surface heated.

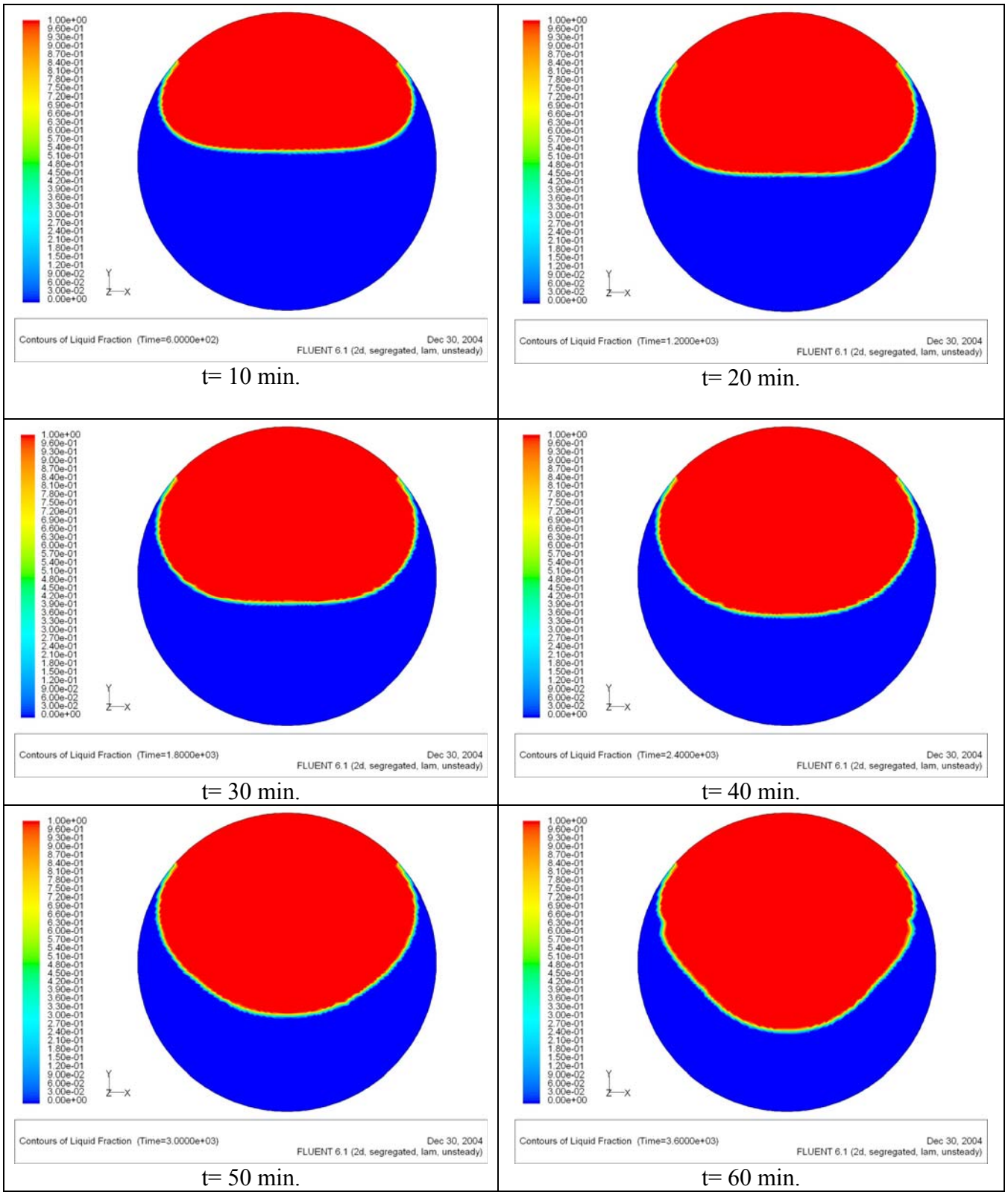

Figure 6.12a: The melt front for a 2 cm diameter pipe with the half of the top surface heated at melting times equal to 10, 20, 30, 40, 50 and 60 minutes.

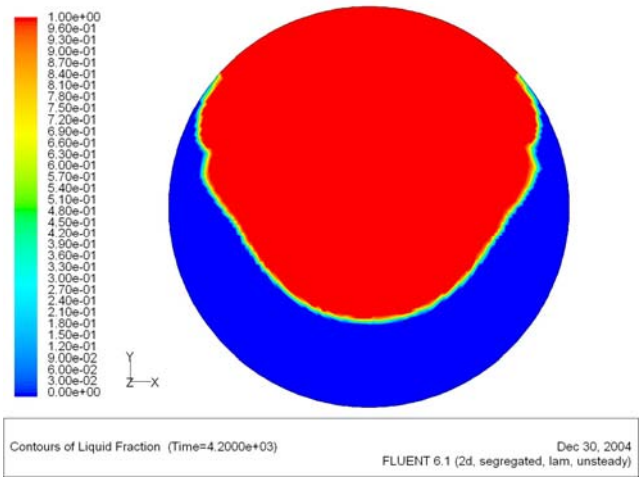

t=70 min.

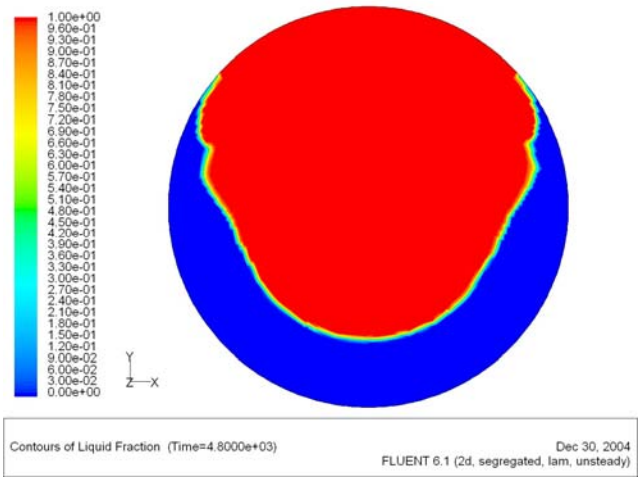

t=80 min.

Figure 6.12b: The melt front for a 2 cm diameter pipe with the half of the top surface heated at melting times equal to 70 and 80 minutes.

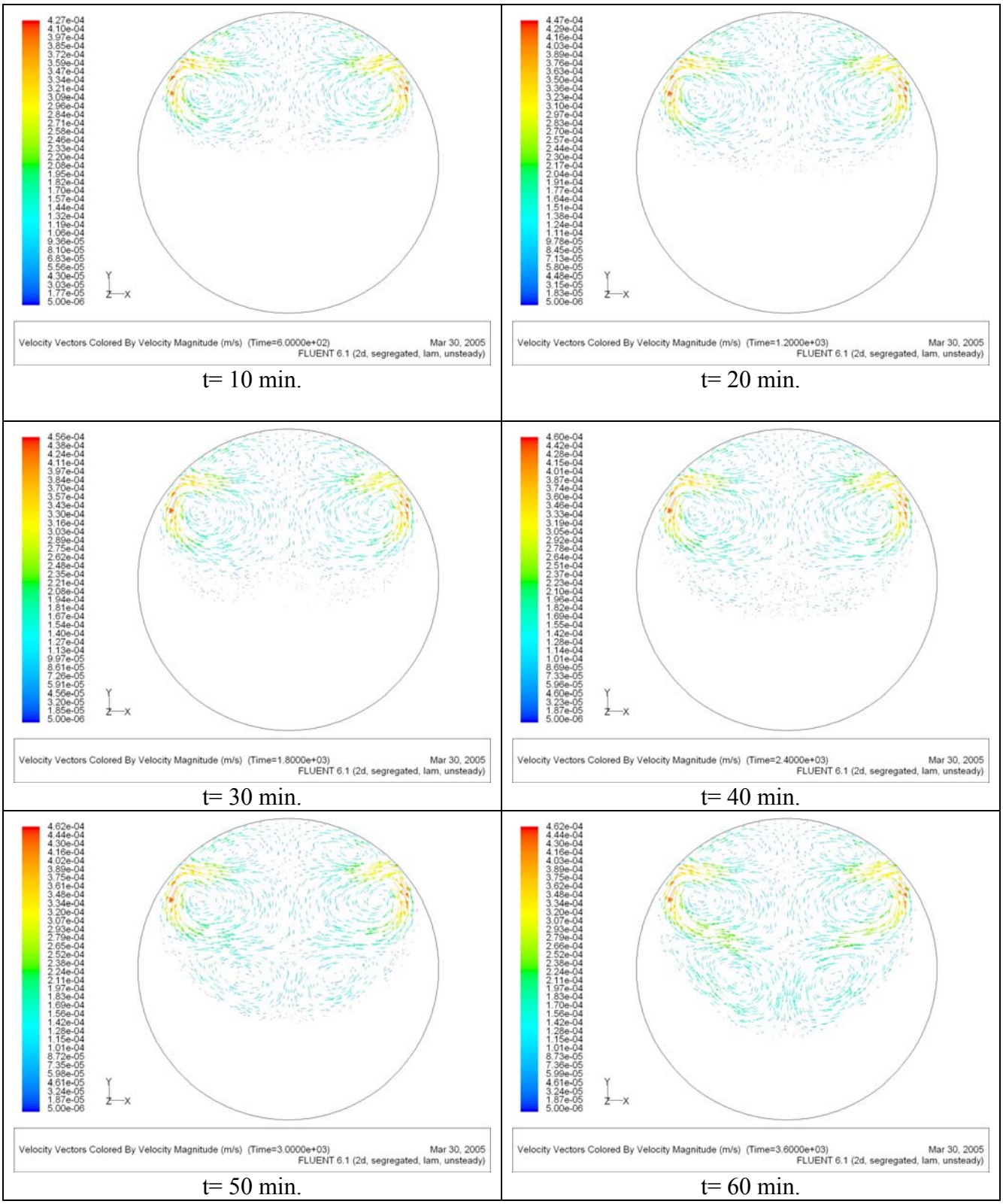

t= 10 min. t= 20 min.

t= 30 min. t= 40 min.

t= 50 min. t= 60 min.

Figure 6.13a: The velocity field for a 2 cm diameter pipe with the half of the top surface heated at melting times equal to 10, 20, 30, 40, 50 and 60 minutes.

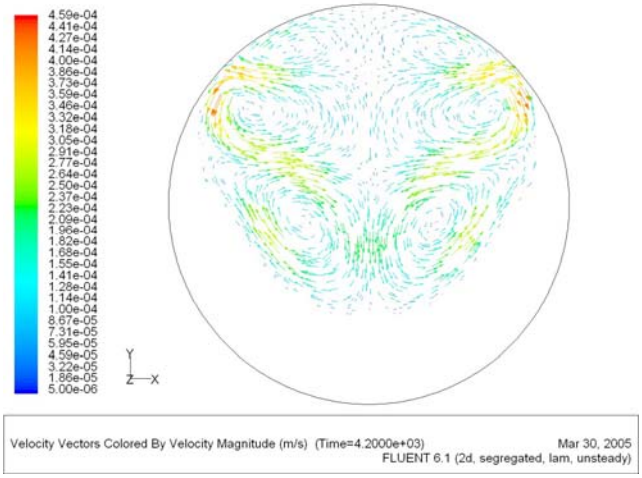

t=70 min.

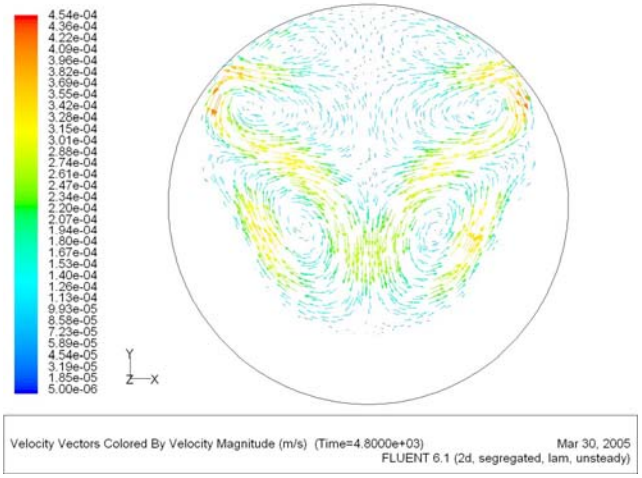

t=80 min.

Figure 6.13b: The velocity field for a 2 cm diameter pipe with the half of the top surface heated at melting times equal to 70 and 80 minutes.

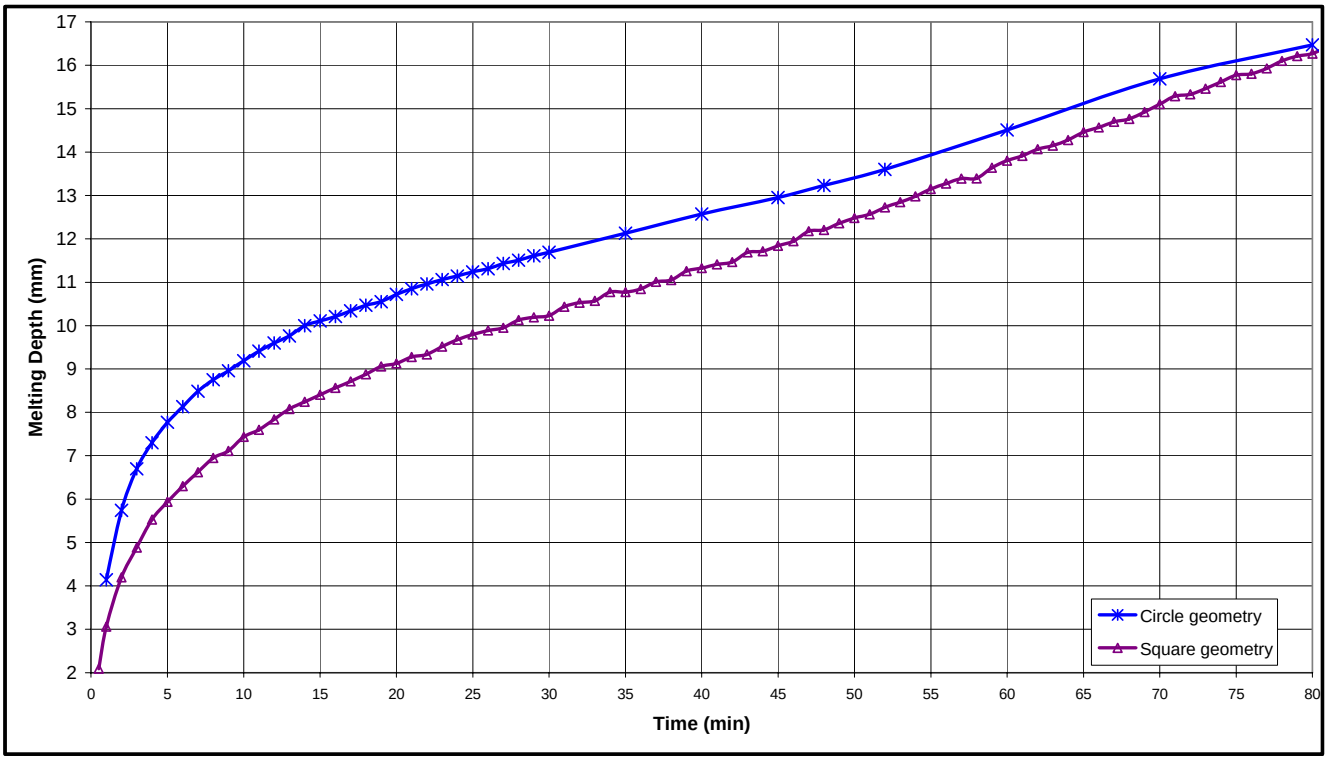

Figure 6.14: A comparison of the melting rate for a circle and a square geometries.

about 21% for a circle with a diameter equals to a square length, the area to the volume ratio or perimeter to area ratio is the same. Therefore the increase in the melting rate is mainly due to the difference in shape which contributes to more streamlined natural convection.

6.4 Effects of Initial Temperature on Melting in a 2-D Square Rectangle

The initial temperature of the ice in an enclosure is one of the parameters that may be different from a case to a case. In order to investigate the effects of the initial ice temperature on the total mixing time, simulations of melting was carried out with the initial temperature of the ice equals to 250 K. All previous simulations have been presented at an initial temperature of 270 K. Temperatures of all walls were held at 270K.

Figure 6.15 shows the effect of the initial temperature on melting rate. It is clear from the figure that as the initial temperature of ice decreases, the melting rate slightly decreases. Up to a time of 20 minutes melting, the melting rate for a case with initial temperature of 250 K and a case with initial temperature of 270 K are similar as only heat transfer by conduction took place. The difference at the 70 minutes mark is about 1.9 mm of melt thickness which is about 13%. This means that a significantly longer time is needed as the initial temperature decreases.

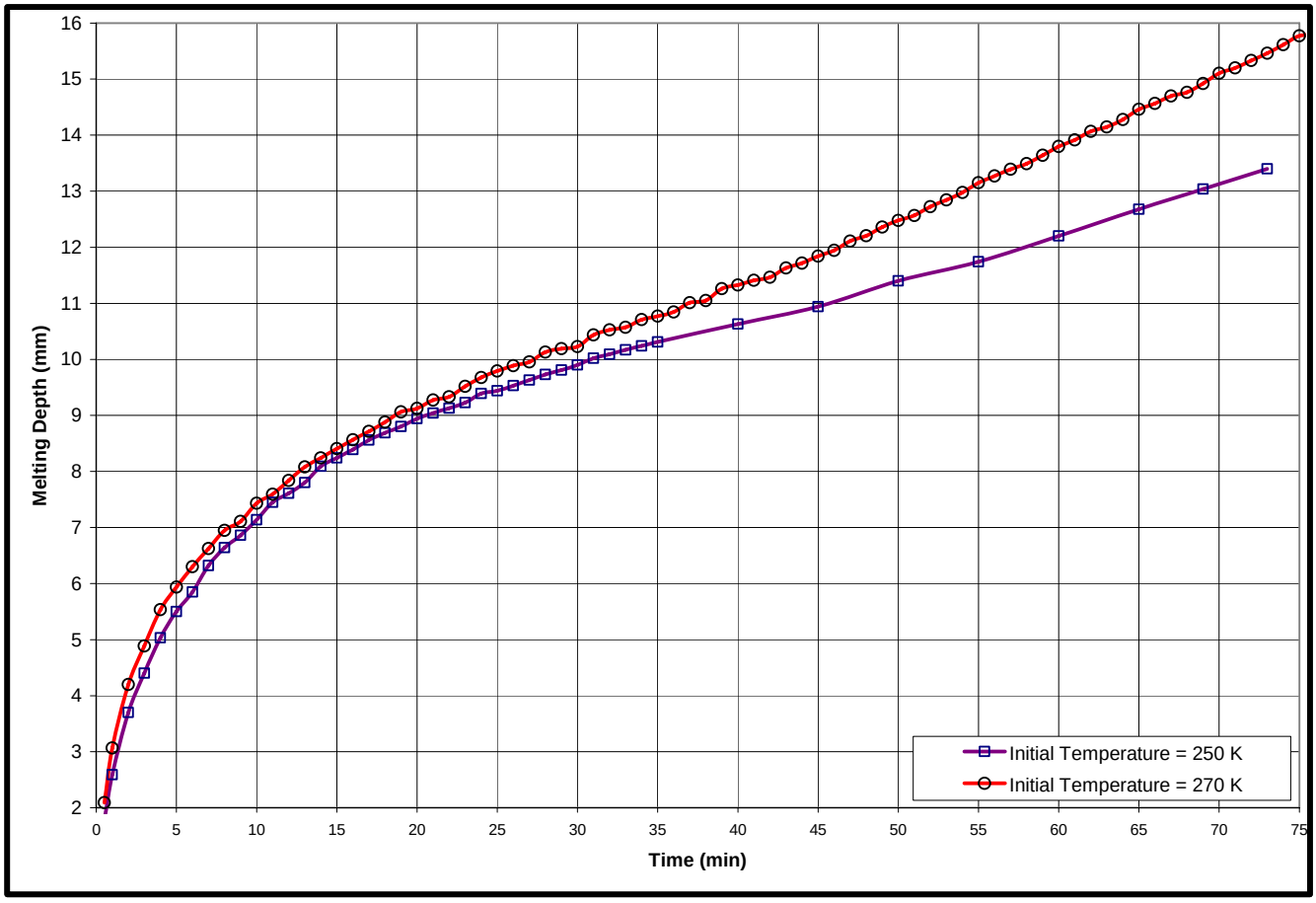

Figure 6.15: Effects of initial temperature on melting rate**.**

6.5 Effects of the Hot surface temperature on the Melting in a 2-D Square Enclosure

The effects of the hot surface temperature on the melting rate were also investigated. The hot surface temperature was 340 K in all of the previous runs. Runs with the heated surface kept at temperatures of 320 K and 360 K were carried out. The results are shown in Figure 6.16. This Figure shows that for a temperature of 320 K the melting rate is rather slow. For temperatures of 340 K or 360 K the melting rate is almost the same. This again shows that the effects of conduction heat transfer is rather limited and that the effects of natural convection depends on the hot surface temperature up a certain value after which the effects of temperature becomes insignificant.

6.6 Effects of the Boundary Temperatures on Melting rate and shape

Figures 6.17-6.18 show results for a case with a half of the top surface heated. This is similar to the case discussed in section 6.2.1 and in Figures 6.2-6.4. The only difference is that the left vertical wall is set at 273K rather than 270 K. Figures 6.17-6.18 show the melt front and the velocity fields at different stages of the melting process. The shapes of the melt zones and the flow patterns are significantly different from those in Figures 6.2-6.4. The melt zone does move towards the center of the block as before and it tends to stay close to the relatively warm boundary of 273 K (the left wall). This was also reflected in the flow patterns. However, unlike the case discussed in section 6.2.1 where the flow patterns at the lower half of the melt zone became symmetrical at the end of melting process, the flow patterns of this case do not show any indication of symmetrical

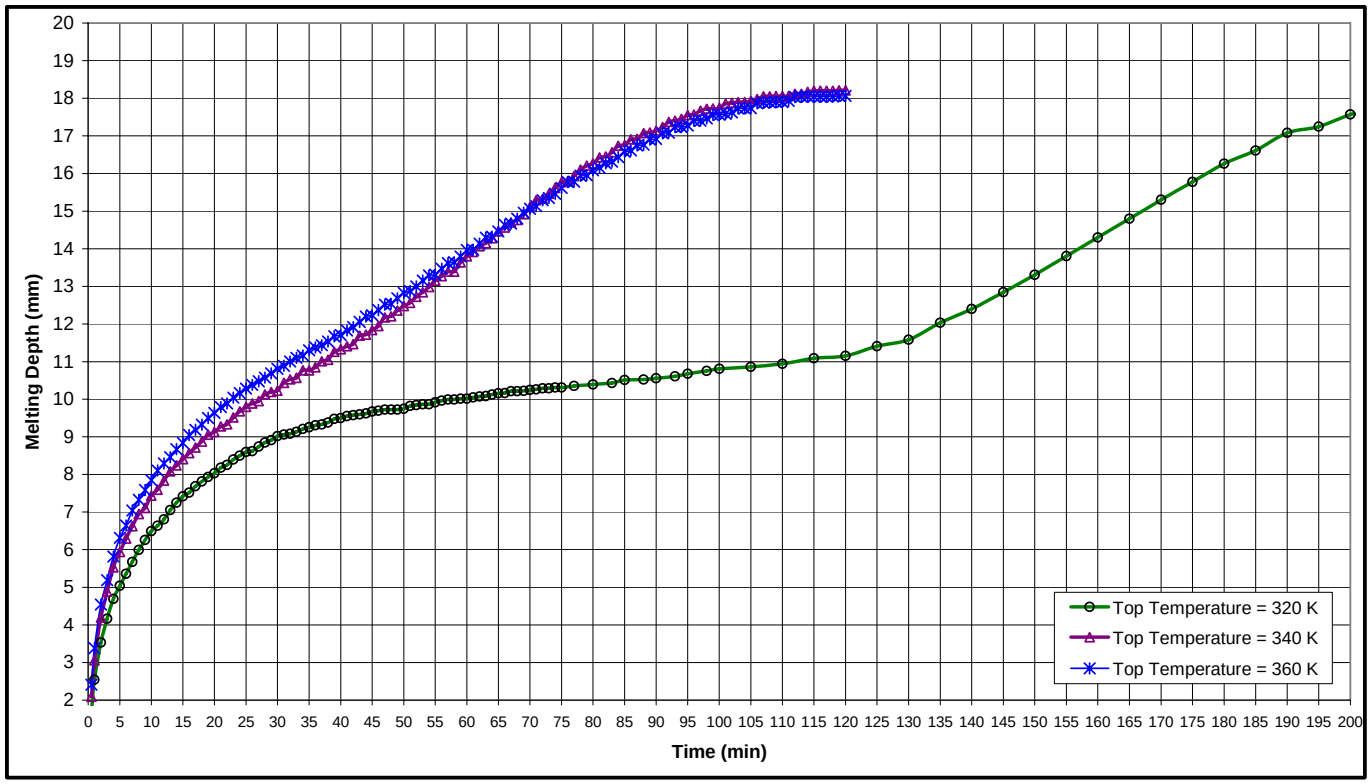

Figure 6.16: A comparison of the melt thickness versus time for cases with the top surface heated at 340 K and cases with the top surface heated at 320 K and 360 K.

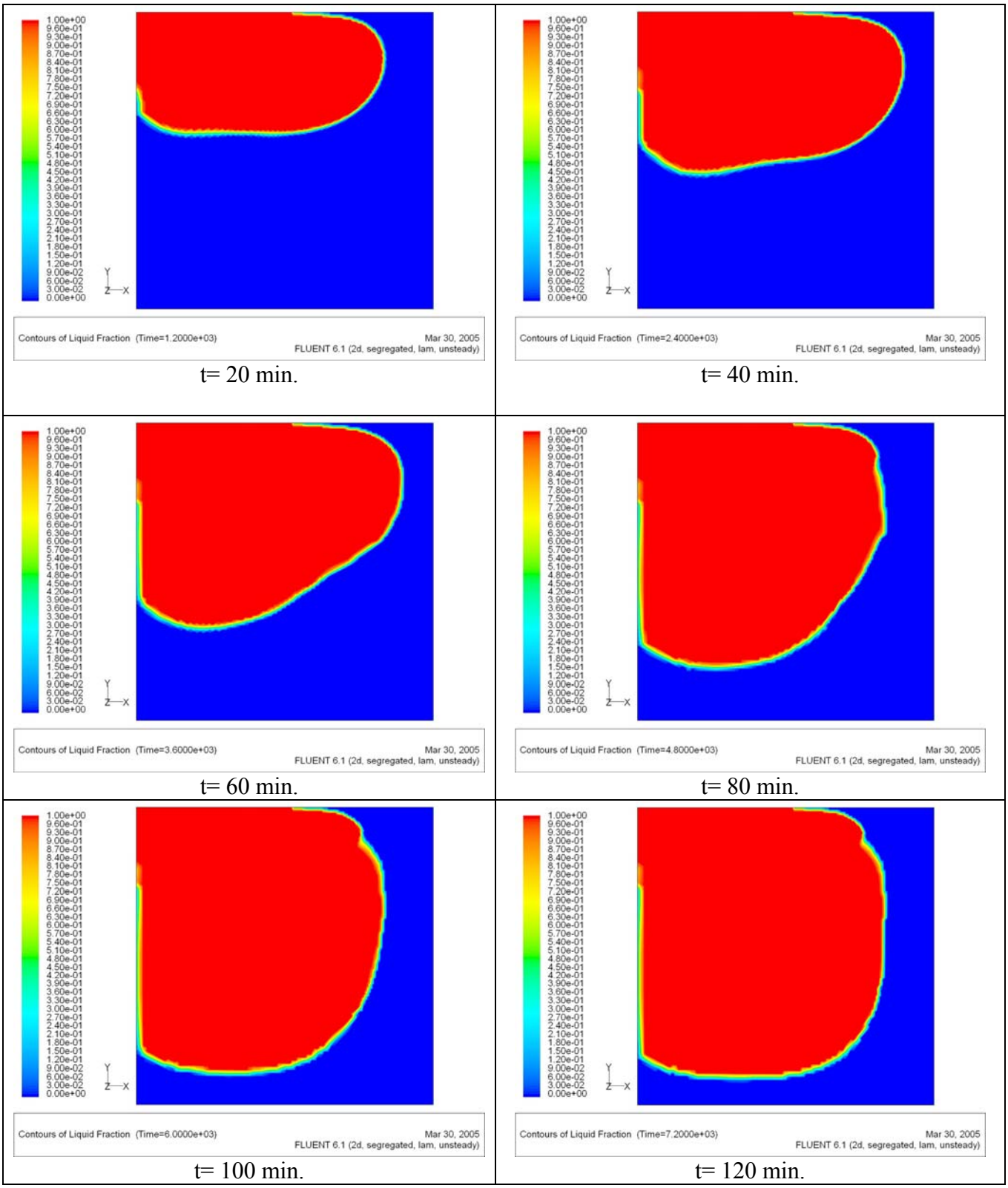

Figure 6.17: The melt front for a 2×2 cm ice block with a half of the top surface heated and different boundary conditions.

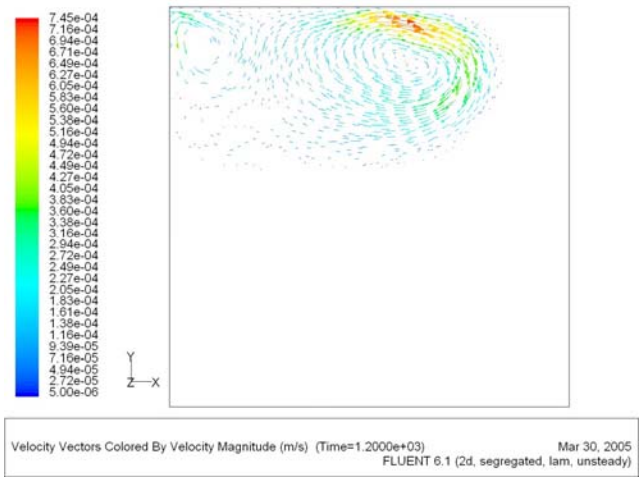

t= 20 min.

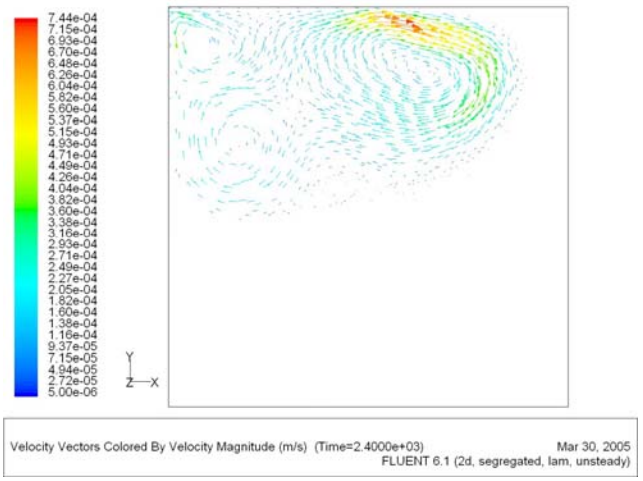

t= 40 min.

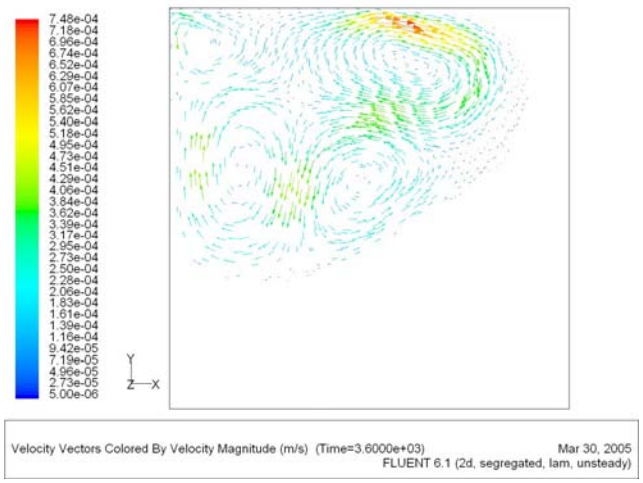

t= 60 min.

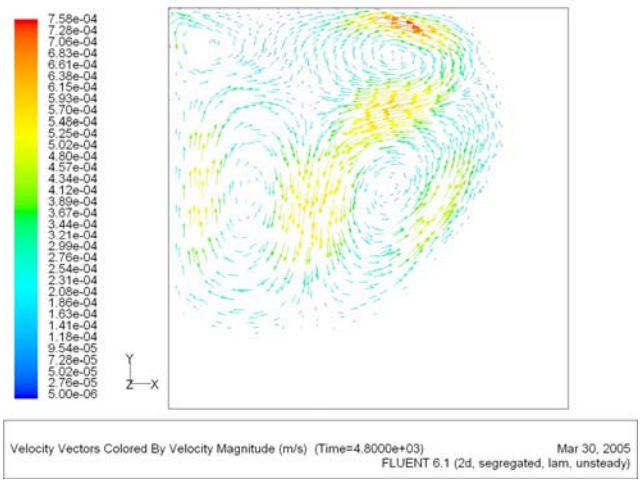

t= 80 min.

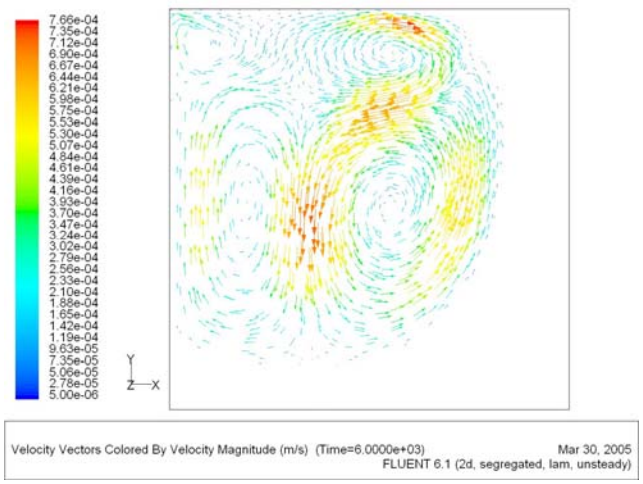

t= 100 min.

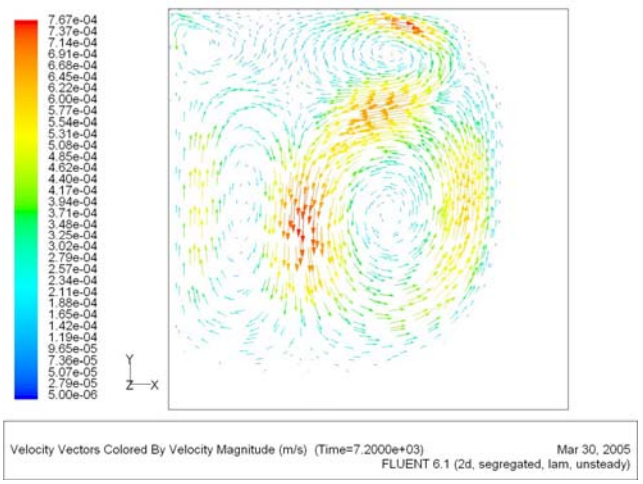

t= 120 min.

Figure 6.18: The velocity field for a 2×2 cm ice block with a quarter of the top surface heated and different boundary conditions.

at the lower half of the melt zone. The asymmetry continues at the top half of the melt zone due to the asymmetric boundary conditions.

Figures 6.19-6.20 show results for a case with a quarter of the top surface heated. This is similar to the case discussed in section 6.2.2 and in Figures 6.8-6.10. Again, the only difference is that the left vertical wall is set at 273 K rather than 270 K. Figures 6.19-6.20 show the melt front and the velocity fields at different stages of the melting process. The shapes of the melt zones and the flow patterns are significantly different from those in Figures 6.8-6.9. The melt zone does move towards the center of the block as before and it tends to stay close to the relatively warm boundary of 273 K (the left wall). This was also reflected in the flow patterns.

Figure 6.21 shows a comparison of the melt thickness versus time for these two cases and a number of the previous cases.

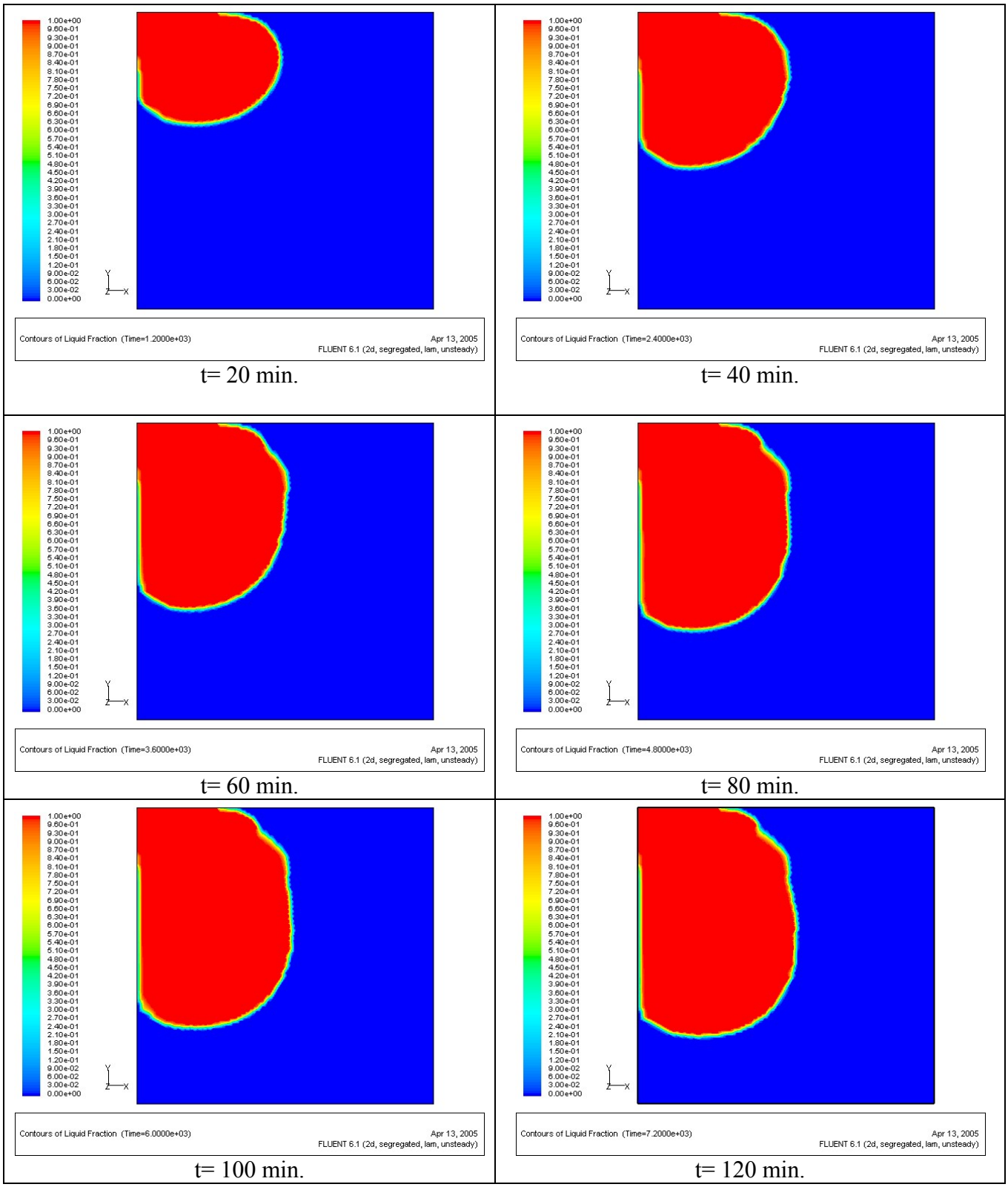

Figure 6.19: The melt front for a 2×2 cm ice block with a quarter of the top surface heated and different boundary conditions.

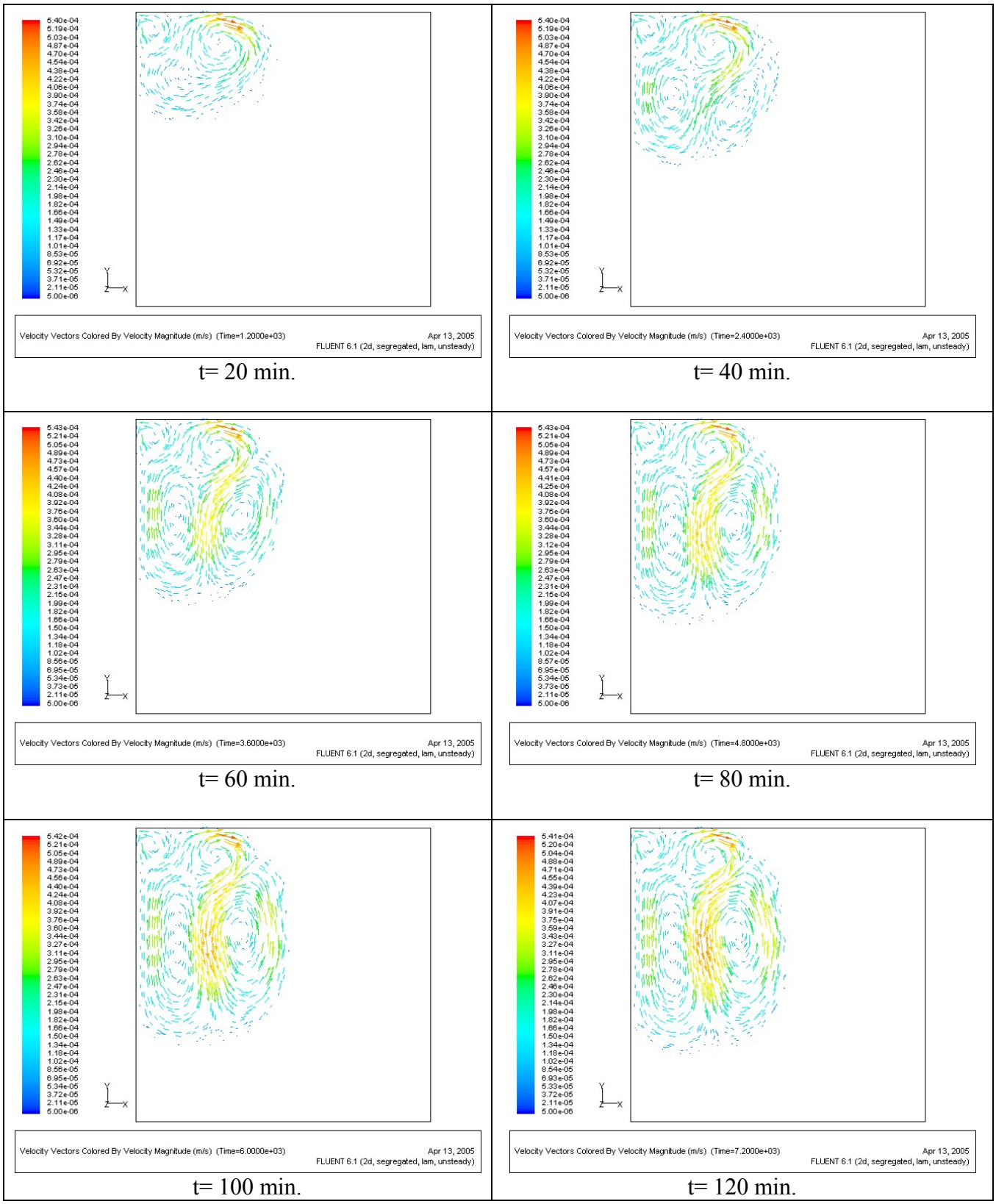

Figure 6.20: The velocity field for a 2×2 cm ice block with a quarter of the top surface heated and different boundary conditions.

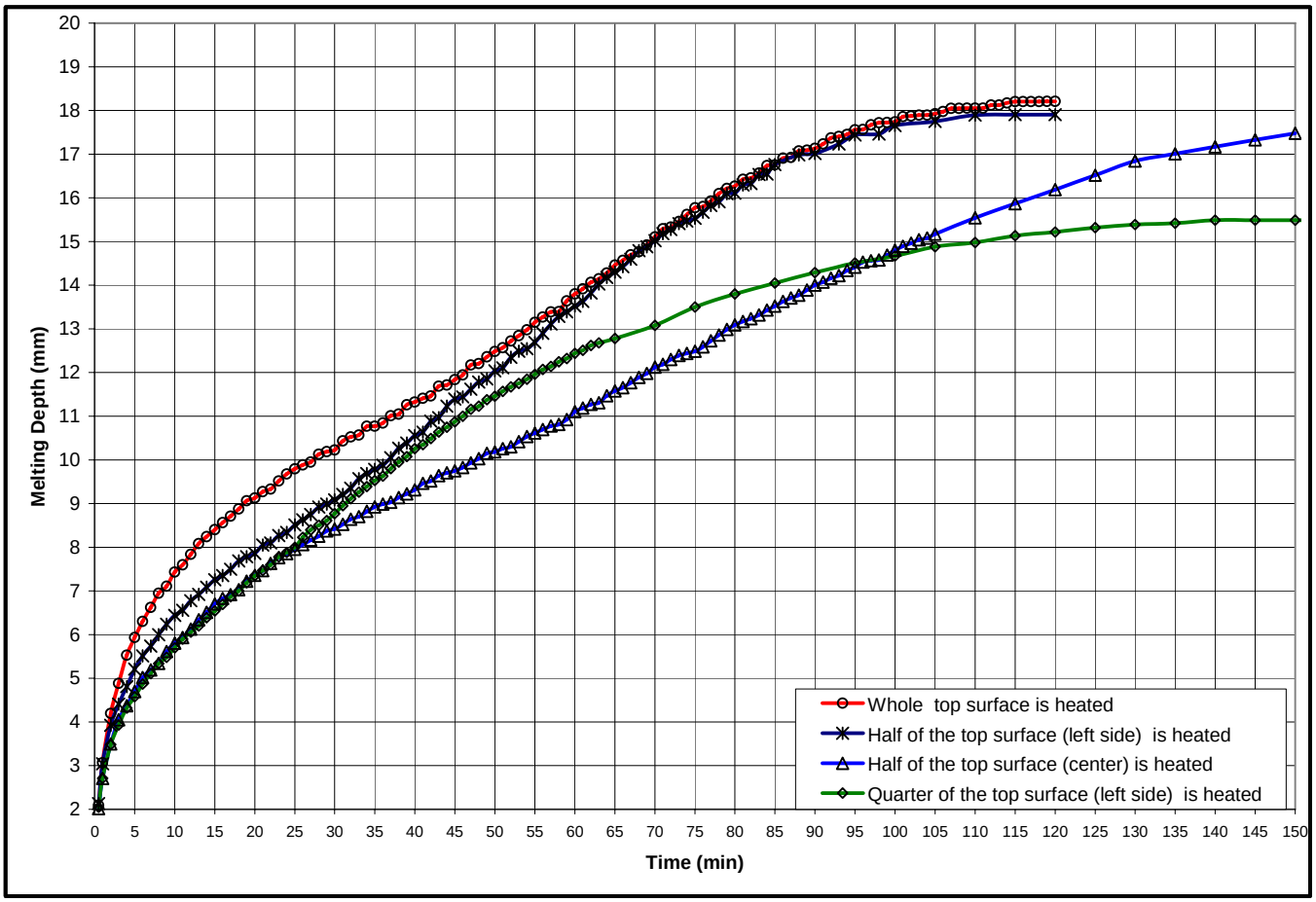

Figure 6.21: A comparison of the melt thickness versus time of a case with full top surface heated and three cases with a part of the top surface only heated and with a left wall temperature of 273K rather than 270K.

Chapter Seven

CONCLUSIONS

Melting of ice enclosures has been studied using computational fluid dynamics and a lumped heat capacity approach. This approach makes tracking of the interface un-necessary. Based on the current study the following conclusions can be made:

a. The melting rate is sensitive to the grid size and a grid size of 110 by 110 for a 2 cm by 2 cm ice block was needed for the solution to be grid size independent. This fine grid is needed to resolve the large gradients around the interface area. Such a fine grid makes it prohibitively expensive in computational terms to use this method to solve melting in large domains or in three-dimensional enclosures.

b. For reasons similar to the ones mentioned above, the melting rate was found also sensitive to the size of the time step. A size of 1 s was needed for the solution to be independent of the time step size. This again increases the computational cost for large melting problems.

c. The results showed that natural convection plays a major role in melting of ice in an enclosure heated from the top. For a 2×2 cm block, melting without natural convection was 8 times slower than melting with natural convection.

d. Simulation results were compared with predicted results using a correlation proposed Solomon (1979) and a good agreement was observed.

e. The melting rate was found to be a function of the size and location of the heated area. However, the melting rate is not directly proportional to the size of the heated area. As the size is halved, a 25% decrease in the melting rate is observed.

f. The melting rate was also found to be a function of the initial temperature of the ice. A lower temperature meant a significant longer melting time.

g. The boundary conditions dictate the shape of the melted area. Results showed clearly that melting tends to occur away from a sub-zero wall.

h. Melting in a 20×20 cm was also investigated. Results were compared to experimental model and a good qualitative agreement was observed.

i. Simulation of melting in a small three dimensional model was carried out. Due to the fine grid and the small time step needed, the computational cost of solving melting using the current method proved to be not very practical.

References

Alexiades, V. and Solomon, A.D., "Mathematical Modeling of Melting and Freezing Processes", Hemisphere, Washington, DC, 1993.

Bareiss, M. and Beer, H., "An Analytical Solution of the Heat Transfer Process During Melting of an Unfixed Solid Phase Change Material Inside a Horizontal Tube", *Int. J. Heat Mass Transfer*, Vol. 27, pp. 739-746, 1984.

Beckermann, C. and Viskanta, R., "Double-diffusive Convection During Dendritic Solidification of Binary Mixture", *PCH*, Vol. 10, pp. 195-213, 1988.

Beckermann, C. and Viskanta, R., "Natural Convection solid/Liquid Phase Change in Porous Media", *Int. J. Heat Mass Transfer*, Vol. 31, No. 1, pp. 35-46, 1988.

Brent, A.D., Voller, V.R., Reid, K.J., "Enthalpy Porosity technique for Modeling Convection-Diffusion Phase Change: Application to the Melting of a Pure Metal", *Numerical Heat Transfer* 13, pp. 297-318, 1988.

Brewster, R. A. and Gebhart B., "An Experimental Study of Natural Convection effects on Downward Freezing of Pure Water", *Int. J. Heat Mass Transfer*. Vol. 31, No. 2, pp. 331-348, 1988.

Carslaw, H.S. and Jaeger, J.C., "Conduction of Heat in Solids", Clarendon Press, Oxford, 1959.

Chellaiah, S. and Viskanta, R., "Freezing of Water-Saturated Porous Media in the Presence of Natural Convection: Experimental and Analysis", *Journal of Heat Transfer, Transactions ASME*, Vol. 111, No. 2, pp. 425-432, 1989.

Crank, J., "Free and Moving Boundary Problems", Oxford University Press (Clarendon), London and New York, 1984.

Diaz, L. A. and Viskanta, R., "Visualization of the Solid-Liquid Interface Morphology Formed by Natural Convection During Melting of a Solid from Below", *Int. Comm. Heat Mass Transfer*, Vol. 11, pp. 35-43, 1984.

Gadgil, A. and Gobin, D., "Analysis of Two-Dimensional Melting in Rectangular Enclosures in Presence of Convection", J. Heat Transfer, vol. 106, pp. 20-26, 1984.

Gau, C. and Viskanta, R., "Melting and Solidification of a Pure Metal on Vertical Wall", *J. Heat Transfer*, Vol. 108, pp. 174-181, 1986.

Gosman, A. D. and Ideriah, F.J.K., "TEACH 2E: a General Computer Program for Two Dimensional Turbulent Recirculating Flows", Report, Department of Mechanical Engineering, Imperial College, London, 1976.

Hale, N. W. and Viskanta, R., "Photographic Observation of the Solid-Liquid Interface Motion During Melting of a Solid Heated from an Isothermal Vertical Wall", *Letters in Heat and Mass Transfer*, Vol. 5, pp. 329-337, 1978.

Hale, N. W. and Viskanta, R., "Solid-Liquid Phase-Change Heat Transfer and Interface Motion in Materials Cooled or Heated from Above or Below", *Int. J. Heat Mass Transfer*. Vol. 23, pp. 283-292, 1980.

Harlow, F.H. and Welch, J.E., "Numerical Calculation of time dependent viscous incompressible flow", Phys. Fluids, Vol. 8, 1965.

Hirt, C.W. and Nicols, "Volume of Fluid (VOF) Method for the Dynamics of Free Boundaries", J. Comp. Phys., Vol. 39, 1981.

Hirt, C.W., Nicols, B.D. and Romero, "SOLA-A numerical Algorithm for Transient Fluid Flows", Los Alamos Scientific Laboratory, Report LA-5852, 1975.

Ho, C.J. and Chu, C.H., "Periodic Melting Within a Square Enclosure with an Oscillatory Temperature", *Int. J. Heat Mass Transfer*, Vol. 36, pp. 725-733, 1993.

Ho, C. J. and Viskanta, R. "Heat Transfer During Melting From an Isothermal Vertical Wall", *J. Heat Transfer*, Vol. 106, pp. 12-19, 1984.

Inaba, H., Nagaya, M., Fukuda, T. and Sugawara, M., "A Study on Transient Characteristics of Melting Phase Change Material in Inclined Rectangular Heat Storage Enclosures", *Trans. JSME*, Vol. 55B, pp. 200-205, 1989.

Kowalewski, T. A. and Rebow M., " An Experimental Benchmark for Freezing Water in the Cubic Cavity", in CHT'97: Advances in Computational Heat Transfer", G. De Vahl Davis and E. Leonardi, eds., Begell House, pp. 149-156, 1998

Kahraman, R., Zughbi, H.D., Al-Nassar, Y., Hastaoglu, M. A. and Sobh, N. "A Simplified Numerical Model For Melting of Ice with Natural Convection", *Int. Comm. Heat Mass Transfer* Vol. 25, No. 3, pp. 359-368, 1998

Kahraman, R., Zughbi, H. D. and Al-Nassar, Y. "A Numerical Simulation of Melting of Ice Heated from Above", *Mathematical and Computational Applications,* Vol. 3 No. 3, pp. 127-138, 1998

Kowalewski, T. A. and Rebow, M., "An Experimental Benchmark for Freezing water in the Cubic Cavity", *Advances in Computational Heat Transfer*, Turkey, May 1997.

Kowalewski, T. A., "Experimental Validation of Numerical Codes in Thermally driven Flows", *Advances in Computational Heat Transfer*, Turkey, May 1997.

Liu, A., Voth, T.E. and Bergman, T.L., "Pure Material Melting and Solidification With Liquid Phase Boundary and Surface Tension Forces", *Int. J. Heat Mass Transfer*, Vol. 36, pp. 411-422, 1993.

Marshall, R.H., "Natural Convection Effects in rectangular Enclosures Containing a Phase Change Material", in *Thermal Storage and Heat Transfer in Solar Energy Systems*, edited by F. Kreith *et al*., ASME, New York, pp. 61-69, 1978.

Moor, F. E. and Bayazitoglu, Y., "Melting within a Spherical Enclosure", *J. Heat Transfer*, Vo. 104, pp. 19-23, 1984.

Ozisik, M.N., "*Heat Conduction"*, Wiley Inter-science, Toronto, 1980.

Patankar, S.V., "Numerical Heat Transfer and Fluid Flow", Hemisphere, Washington, DC, 1980.

Saitoh, T. and Moon, J.H., "An Experimental Study for Combined Close-Contact and Free Convection Melting in a Spherical Capsule", *Proc. 6th Int. Symp. Transp. Pheno. Therm. Engng*., pp 1-6, 1993.

Saitoh, T. and Moon, J.H., "Experimental Performance of Latent Heat Thermal Energy Storage Unit Packed With Spherical Capsules", *Proc. of the 5th Int. Energy Conf*., pp. 1-8, 1993.

Salcudean, M., and Abdullah, Z., "On the Numerical Modeling of Heat Transfer During Solidification Processes", *Int. J. Numer. Methods Engng.*, Vol. 28, pp. 445-473, 1988.

Shih, T.M. and Ohadi, M.M., "Literature Survey on Numerical Heat Transfer (1990-1991)". *Numerical Heat Transfer, Part A* Vol. 23, pp. 129-169, 1993.

Shih, T-M, Ohadi, M.M. and Lie W, "Literature Survey on Numerical Heat Transfer", *Num. Heat Transfer, Part A*, Vol. 29, pp. 441-481, 1996.

Solomon, A. D., "*Melt time and heat flux for a simple PCM body*", Solar Energy, 22, pp. 251-257 (1979)

Sugawara, M., Inaba, H. and Seki, N., "Effect of Maximum Density of Water on Freezing of a Water-Saturated Horizontal Porous Layer", *ASME Journal of Heat Transfer*, Vol. 110, pp. 155-159-173, 1988.

Van Buren, P. D. and Viskanta, R., Interferometric Measurement of Heat Transfer During Melting from a Vertical Surface, *Int. J. Heat Mass Transfer*, Vol. 23, pp. 568-571, 1980.

Voller, V.R., Cross, M. and Markatos, N.C., "An Enthalpy Method for Convection/Diffusion Phase Change", *Int. J. Num. Meth. Engng*., vol. 24, pp. 271-284, 1987.

Voller, V.R., Cross, M., "An Explicit Numerical Method to track a Moving Phase Change Front", *Int. J. Heat Mass Transfer*, vol. 26, No. 1, pp. 147-150, 1983.

Voller, V.R., Markatos, N. C. and Cross, M., "solidification in Convection and Diffusion", in N.C. Markatos et al. (eds), Numerical simulations of Fluid Flow and Heat/Mass transfer Processes, Springer-Verlag, Berlin, pp. 425-432, 1986.

Voller, V.R., Markatos, N. C. and Cross, M., "Techniques for accounting for the moving interface in convection/diffusion phase change", In Numerical Methods in Thermal Problems (Edited by R. W. Lewis and K. Morgan), Vol. 4, pp. 595-609. Pineridge Press, Swansea 1985.

Voller, V.R., and Prakash, C., "A Fixed grid Numerical Modeling Methodology for Convection-Diffusion Mushy Region Phase Change Problems", *Int. J. Heat and Mass Transfer* 30, pp. 1709-1719, 1987.

Voller, V.R., Swaminathan, C.R., and Thomsa, B.G., "Fixed Grid Techniques for Phase Change Problems: a Review", *Int. J. Numer. Meth. Eng.* 30, pp. 875-898, 1990.

Weaver, J. A. and Viskanta, R., "Freezing of Liquid-Saturated Porous Media", *ASME Journal of Heat Transfer*, Vol. 108, pp. 654-659, 1986.

Webb, B. W. and Viskanta, R., 'Natural-convection-dominated melting heat transfer in an inclined rectangular enclosure', *Int. J. Heat Mass Transfer*, Vol. 29, No. 2, pp. 183-192, 1986.

Webb, B.W., Moellemi, M.K. and Viskanta, R., "Experiments on Melting of Unfixed Ice in a horizontal Cylindrical Capsule", *ASME Journal of Heat Transfer*, Vol. 109, pp. 454-459, 1987.

Wolff, F. and Viskanta, R., "Melting of a Pure Metal from a Vertical Wall", *Exper. Heat Transfer*, Vol. 1, pp. 17-30, 1987.

Yeoh, G.H., Natural Convection in a Solidifying Liquid, Ph.D. Thesis, University of New South Wales, Australia, 1992.

Zughbi, H. D., Kahraman, R., Al-Nassar, Y., and Hastaoglu, M. A., "Simulation of Melting in a three-Dimensional Body", International Symposium on Advances in Computational Heat Transfer, Cesme, Turkey, May 26-30, 1997.

VITA

Name: Abdul Muttaleb Ali Naser Al-Salman

Date of Birth: 04/10/1967

Nationality: Saudi Arabia

Educational Qualification: B.Sc. Chemical Engineering (1993)
King Fahd University of Petroleum & Minerals
Dhahran, 31261, Kingdom of Saudi Arabia

E-mail: abdulmuttaleb.salman@aramco.com